Characterization of Tertiary Membrane Fouling in Cold Climates

by

Chen Tao

A thesis
presented to the University of Waterloo
in fulfillment of the
thesis requirement for the degree of
Doctor of Philosophy
in
Civil Engineering - Water

Waterloo, Ontario, Canada, 2021

Examining Committee Membership

The following served on the Examining Committee for this thesis. The decision of the Examining Committee is by a majority vote.

External Examiner: Dr. Katsuki Kimura
Professor
Division of Environmental Engineering
Hokkaido University

Supervisor: Dr. Wayne Parker
Professor
Department of Civil and Environmental Engineering
University of Waterloo

Internal Member: Dr. Peter Huck
Professor
Department of Civil and Environmental Engineering
University of Waterloo

Internal Member: Dr. Monica Emelko
Professor
Department of Civil and Environmental Engineering
University of Waterloo

Internal-External Member: Dr. Christine Moresoli
Professor
Department of Chemical Engineering
University of Waterloo

Author's declaration

This thesis consists of material all of which I authored or co-authored: see Statement of Contributions included in the thesis. This is a true copy of the thesis, including any required final revisions, as accepted by my examiners.

I understand that my thesis may be made electronically available to the public.

Statement of contributions

Chapter 3 and Chapter 4 have been published in peer-reviewed journals. The contributions were stated as:

Chen Tao: Methodology, Investigation, Data curation, Writing - Original Draft.

Dr. Wayne Parker: Supervision, Writing - review & editing.

Dr. Pierre Bérubé: Supervision, Writing - review & editing

Abstract

Cold climates have limited the application of membrane technologies in tertiary treatment by affecting both secondary biological and tertiary membrane processes. There is a need to develop a fundamental understanding of fouling mechanisms and to identify solutions to fouling of tertiary membranes under cold climates. A combination of bioprocess modelling and advanced SMP characterization illustrated the effect of secondary temperature (8, 14 and 20 ℃) and HRT (10, 15 and 20 h) on biomass process rates and SMP production. Liquid chromatography-organic carbon detection (LC-OCD) results revealed a significant increase in total SMP concentration as secondary temperature decreased with the fractions of polysaccharide and protein being more sensitive to temperature. In contrast, reducing HRT did not significantly affect total SMP concentration in effluents whereas SMP composition varied. Both biomass decay (BAP) and substrate utilization (UAP) yields increased as secondary temperature decreased while only UAP yields decreased as HRT decreased. A strong correlation was observed between secondary temperature and BAP/UAP yields whereas the generation of BAP was more temperature sensitive than UAP.

The development of resistances due to fouling as a function of secondary temperature and HRT was assessed. Reducing secondary temperature resulted in a substantial increase in total membrane resistances over multiple filtration cycles which was contributed by increased hydraulically reversible and irreversible resistances. A two-stage pattern in fouling rates development was observed indicating potential fouling mechanisms of cake and pore blocking. Shortening HRT led to increased hydraulically reversible and irreversible resistances whereas the degree and pattern of the change were affected by temperature. When filtration tests were conducted at the secondary operating temperature, the hydraulically irreversible permeability further decreased relative to filtration at 20 ℃. Water viscosity and intrinsic membrane resistance were observed to be responsible for 20–29% of the total decrease in hydraulically irreversible permeability. These declines established the upper limit to which fouling mitigation strategies could enhance hydraulically irreversible permeabilities. The hydraulically irreversible permeability decline beyond that associated with changes in viscosity and intrinsic membrane resistance was attributed to narrowed membrane pores that retained additional SMP fractions and modified membrane-foulant interactions.

Correlation analysis revealed that the fouling of tertiary membranes was governed by high and low molecular weight (MW) organics which were generated to a greater extent at low secondary

temperature and short HRT conditions. Multiple linear correlation analysis results indicate that filtration temperature presented the highest contribution to tertiary membrane fouling followed by secondary temperature and HRT.

The effect of coagulation with alum (0–1.0 mM) on fouling of tertiary membranes was studied at secondary temperatures of 8 and 20 ℃. The removal efficiency of high MW organics by coagulation was consistently higher than that of low MW organics. The coagulated effluent concentrations were higher for the SBR effluent generated at 8 ℃ than those generated at 20 ℃. The results of filtration tests revealed that pre-coagulation can effectively reduce total membrane resistances; however, at the preferred dosages, the values of hydraulically reversible and irreversible membrane resistances were higher for the SBR operated at 8 ℃ due to higher concentrations of SMP fractions remaining in the coagulated effluent.

The present study provides basic knowledge and insights into factors that should be considered when developing strategies for mitigating fouling of tertiary membranes under low temperature and high flow conditions. The approach of process modelling and differentiating the effects of secondary HRT, temperature and filtration temperature developed in the present study provides insights into fouling development of tertiary membranes and the results can be employed to understand the limits of tertiary fouling control under challenging conditions. The potential of pre-coagulation in membrane fouling alleviation and effluent quality improvement can be limited at low temperatures and high flows. Further investigation should be conducted to explore the potential of other pretreatments or adjustments of secondary operating conditions (such as solids retention time (SRT)) to achieve more effective fouling control under cold climates.

Acknowledgements

First and foremost, I would like to express my gratitude to my supervisor Dr. Wayne Parker. Your guidance and support through the course of my PhD studies has made this work possible. I also really appreciate the direction, prompt feedback and the amount of work efforts that you provided. Dr. Parker has taught me by example, on critical thinking, problem solving, professionalism and much more. Thank you, for offering me this wonderful opportunity to work on this research project and to learn so much from you.

To my PhD committee, Dr. Katsuki Kimura (Division of Environmental Engineering, Hokkaido University), Dr. Christine Moresoli (Department of Chemical Engineering, University of Waterloo), Dr. Peter Huck (Department of Civil and Environmental Engineering, University of Waterloo), and Dr. Monica Emelko (Department of Civil and Environmental Engineering, University of Waterloo), I am extremely grateful for your insightful feedback and guidance during my PhD studies.

I would like to thank Dr. Pierre Bérubé (Department of Civil Engineering, The University of British Columbia) for his guidance on manuscript preparation. Dr. Bérubé's contribution to this project was crucial. My warm thanks to Dr. Nick Adams, Virgjil Turtulli and Dr. Qirong Dong for sharing their knowledge and experience, and Dr. Sigrid Peldszus, Lin Shen and Kirti S. Nemani for their assistance with the LC-OCD measurements. Special thanks to Mark Merlau and Mark Sobon for their assistance in the lab. This project could not be completed without you.

I extend my appreciation to Kitchener Wastewater Treatment Plant for providing activated sludge and Suez for providing the membrane equipment. And to our research group members for their support and accompany.

Funding for this project was provided by National Sciences & Engineering Research Council of Canada (NSERC), the China Scholarships Council program, and the Regional Municipality of York.

Finally, I would like to thank my family and friends. I would not be where I am today without their unconditional support and encouragement. In particular, I would like to thank my parents for supporting me with my education in Canada. I also thank my husband Michael Wang for his love and support.

Dedication

I dedicate this work to my parents and husband.

Table of Contents

List of Figures

List of Tables

List of Abbreviations

ASM	activated sludge model
BAP	biomass-associated product
bs OM	biodegradable soluble organic matter
bp OM	biodegradable particulate organic matter
COD	chemical oxygen demand
C SBR	control SBR
DOC	dissolved organic carbon
EEM	excitation emission matrix
EfOM	effluent organic matter
Em	Emission
EPS	extracellular polymeric substances
Ex	Excitation
F_{rev}	hydraulically reversible fouling rate
F_{irr}	hydraulically irreversible fouling rate
F/M	food/microorganism
HRT	hydraulic retention time
K_b	complete blocking
K_c	cake fouling
K_i	pore blocking
K_s	standard blocking
LC-OCD	liquid chromatography-organic carbon detection
LMH	liters per square meter per hour
LMW	low molecular weight
MBBR	moving bed biofilm reactor
MBR	membrane bioreactor
MW	molecular weight
MLSS	mixed liquor suspended solids
MLVSS	mixed liquor volatile suspended solids
nbs OM	non-biodegradable soluble organic matter
nbp OM	non- biodegradable particulate organic matter
NOM	natural organic matter

OCD	organic carbon detection
OM	organic matter
OND	organic nitrogen detection
PAC	polyaluminum chloride
$R_{t,i}$	total resistance
R_m	intrinsic resistance
$R_{rev,i}$	hydraulically reversible resistance
$R_{irr,i}$	hydraulically irreversible resistance
SBR	sequencing batch reactor
SMP	soluble microbial products
SNOD	SMP-based dissolved organic nitrogen
SRT	solids retention time
SSR	sum of squared residuals
SVI	sludge volume index
sCOD	soluble chemical oxygen demand
tCOD	total soluble chemical oxygen demand
T SBR	test SBR
TKN	total Kjeldahl nitrogen
TMP	trans-membrane pressure
UAP	utilization-associated product
UF	ultrafiltration
UVD	ultraviolet detector
VFA	volatile fatty acid
WRRF	wastewater resource recovery facility
WWTP	wastewater treatment plant

Chapter 1
Introduction

1.1 Background

The purpose of tertiary treatment is to provide final cleaning of effluents to improve quality before reusing, recycling or discharging (Vera et al., 2015). With more stringent water supply limitations and discharge regulations, ultrafiltration (UF) has gained considerable acceptance for the tertiary treatment of municipal wastewater (Yang et al., 2021). However, membrane fouling is commonly recognized as a major obstacle achieving further adoption of UF in tertiary treatment. Effluent organic matter (EfOM), which mainly originates from biological processes employed for secondary treatment, has been identified as a dominant foulant in low-pressure membrane processes (Guo et al., 2014). The membrane fouling caused by EfOM results in the need to operate at higher applied pressures and with larger membrane surfaces, and more frequent cleaning to offset the loss in permeability, resulting in higher operating costs and energy consumption.

EfOM is a highly heterogeneous mixture of residual influent substrate, soluble microbial products (SMP), and nonbiodegradable or slowly biodegradable organic materials (Barker & Stuckey, 1999). EfOM has been reported to account for as much as 86.5% of total chemical oxygen demand (COD) and total organic carbon (Wang & Chen, 2018) in the secondary effluent. Among EfOM fractions, the SMP, which is biologically derived from substrate metabolism during biomass growth (UAP) and cell lysis during biomass decay (BAP) (Namkung & Rittmann, 1986), has been found to contribute the majority of soluble organic matter in wastewater effluents and to be the dominant foulant responsible for membrane fouling (Soh et al., 2020). Therefore, any important factor that affects the quality of effluents and subsequent tertiary fouling extent is the presence of SMP that are produced during biological treatment processes.

The concentration and composition of SMP in secondary effluent are impacted by the operating conditions of biological treatment (Shi et al., 2018). The composition and concentration of SMP have been reported to vary depending on factors such as solids retention time (Fu et al., 2017), carbon to nitrogen ratio (Ly et al., 2018) and organic loading rate (Maqbool et al., 2017). In winter seasons of cold weather countries, such as Canada, extreme operating conditions such as low temperature and short HRT caused by earlier snowmelt are expected to result in greater production of SMP and therefore lead to higher fouling potentials (Abu-Obaid et al., 2020). Moreover, the operating temperature of UF filtration can enhance the fouling potential due to increased water viscosity and reduced membrane pore size (Alresheedi & Basu, 2019; Cui et al., 2017). However, there has been

little characterization of the fouling of tertiary membranes under the low temperature and high flow conditions and the fouling mechanism are not well addressed. Hence, understanding the effects of operating conditions on SMP production and developing correlations between SMP fractions and tertiary fouling are of importance for sustainable application of ultrafiltration in municipal wastewater treatment.

Advances in coagulation/flocculation strategies as pretreatments for ultrafiltration have received considerable attention. Coagulation can mitigate fouling by removing SMPs or changing their physical-chemical characteristics (Chen et al., 2020; Peleato et al., 2017). In the prior studies the DOC concentration of the UF influent ranged from 4.5–8 mg/L (Chen et al., 2021; Liu et al., 2019). However, DOC concentrations in the secondary effluents have been found to be higher under low temperature (Drews, 2010) and high flow (Johir et al., 2012) conditions due to increased SMP generation by biomass. Hence, the preferred dosage of coagulants and the mechanisms of membrane fouling alleviation can be expected to change. This was deemed to be particularly relevant to the present study.

There is little information in the literature that addresses fouling of tertiary membranes under either cold weather or high flow operations. However, as will be subsequently demonstrated, the membrane bioreactor (MBR) literature reveals that membrane fouling has the potential to increase under low temperature conditions. It should be noted that with MBRs, the membranes interact with a range of potential foulants that span from truly soluble species (i.e. SMP) to suspended solids (i.e. floc). In tertiary configurations, the membranes are less exposed to settleable components (i.e. floc). It is anticipated that there will be less cake formation on tertiary membranes than that would be observed with MBR membranes. However, the lack of a cake layer may increase the accumulation of soluble foulants in the membrane pores due to the absence of the "shielding" of pores that can be provided by cake. The potential for fundamentally different fouling mechanisms and the need to provide fouling mitigation strategies for tertiary configurations provides the motivation for the present work.

1.2 Research objectives and scope

The global goal of the present study was to obtain insights into fouling of tertiary membranes under selected challenging conditions, including low temperature and high flows. Ultimately, the present study will assist in minimizing the costs and resources required to enhance the tertiary membrane performance. This was accomplished by completing the following subgoals:

(1) Characterize and model SMP production as a function of temperature when treating municipal wastewater,

(2) Assess the impacts of low temperature operation on hydraulically irreversible membrane permeability of tertiary membranes,

(3) Evaluate the impact of secondary operating temperature and filtration temperature on fouling of tertiary membranes,

(4) Investigate the effect of secondary treatment HRT on SMP production and fouling of tertiary membranes at different temperatures,

(5) Explore the impact of pre-coagulation on fouling of tertiary membranes at low temperatures.

1.3 Research approach and thesis organization

This thesis is organized into eight chapters, including an Introduction (Chapter 1), Literature Review (Chapter 2), five results chapters (Chapter 3–7) prepared in journal article format, and Conclusions (Chapter 8).

In Chapter 1, the research motivation, objectives, scope and thesis structure are presented.

In Chapter 2, results of a comprehensive literature review of the fundamentals of SMP and the effect of secondary treatment operating conditions on SMP production are presented. The membrane fouling when treating secondary effluent is reviewed and summarized. In addition, the pretreatment of secondary effluent as a fouling mitigation strategy is reviewed.

In Chapter 3, the quantitative relationship between SMP generation, including UAP and BAP, and the operating temperature of SBRs treating real municipal wastewater was investigated. LC- OCD analysis and conventional parameter wastewater quality characterization were coupled with activated sludge modelling to interpret the generation of SMP fractions that are relevant to membrane fouling. Chapter 3 has been published as: Tao, C., Parker, W., & Bérubé, P. (2021). Characterization and modelling of soluble microbial products in activated sludge systems treating municipal wastewater with special emphasis on temperature effect. Science of the Total Environment, 779, 146471.

In Chapter 4, the contributors to hydraulically irreversible permeability of tertiary membranes at cold temperatures were identified and quantified. A comprehensive test plan that allowed for separate assessment of the impacts of temperature on the secondary and tertiary systems was developed. Chapter 4 has been published as: Tao, C., Parker, W., & Bérubé, P. (2022). Assessing the role of cold temperatures on irreversible membrane permeability of tertiary ultrafiltration treating municipal wastewater. Separation and Purification Technology, 278, 119556.

In Chapter 5, the effects of temperature, including secondary treatment operating temperature and filtration temperature, on fouling of tertiary membranes were investigated. Filtration tests were

conducted at bench scale at 20 ℃ to investigate the effect of SBR temperature on tertiary fouling and subsequently at the source SBR temperatures to characterize the effect of filtration temperature on tertiary fouling.

In Chapter 6, the interaction of secondary operating temperature and HRT on fouling of tertiary membranes was evaluated. The SBRs treated real municipal wastewater over a range of temperatures and HRTs to generate feed water for the tertiary filtration tests. Filtration tests were conducted at bench scale at 20 ℃ to investigate the effect of SBR temperature and HRT on tertiary fouling and subsequently at the source SBR temperatures to characterize the effect of filtration temperature on tertiary fouling.

In Chapter 7, the impact of pre-coagulation of the effluent of secondary systems that were operated at different SBR temperatures on tertiary fouling was assessed. The preferred dosage of coagulation at different SBR temperatures was compared.

In Chapter 8, major conclusions and contributions from the present study were summarized. Several recommendations were also made for future research.

Chapter 2

Literature Review

2.1 Introduction

In the review of the literature on tertiary fouling under low temperature and high flow conditions, the following issues were identified in Figure 2-1: (1) the fundamentals of SMP including its definition, composition, and characterization techniques; (2) the effect of challenging operating conditions in secondary treatment on SMP including temperature and HRT effect; (3) membrane fouling when treating secondary effluent with the effects of SMP characteristics and filtration conditions; and (4) tertiary fouling control strategies through pre-treatment of secondary effluent. Because the tertiary ultrafiltration membrane process has received little attention under extreme conditions, a considerable portion of review was based on studies of membrane bioreactors (MBRs).

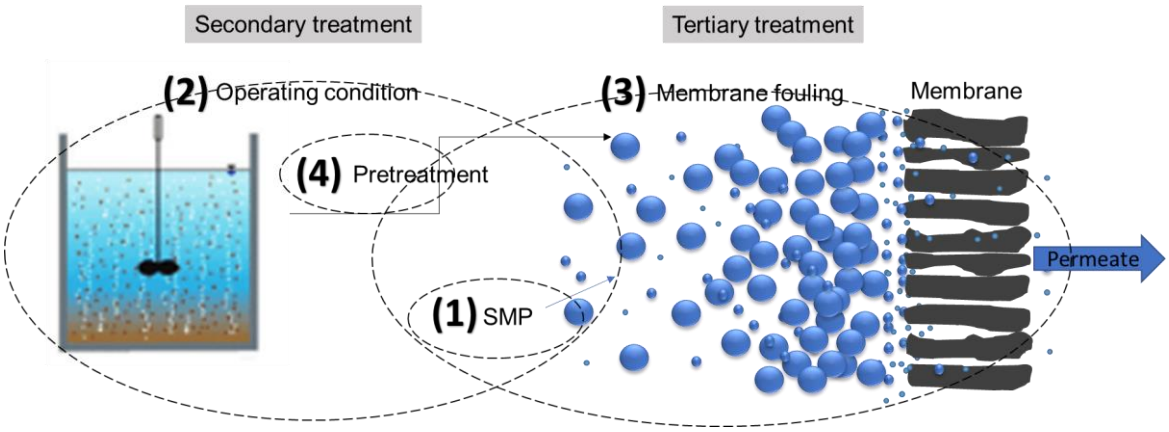

Figure 2-1. Concept map of literature review.

2.2 Soluble microbial products in wastewater

2.2.1 Introduction to soluble microbial products

Membrane fouling by SMP remains one of the limitations for the widespread application of membrane technology incorporated with biological treatment (e.g. MBR, tertiary membrane). Over the past decade, numerous studies have been devoted to characterization of membrane foulants, and SMP appears to exhibit a significant role (Ferrer-Polonio et al., 2018).

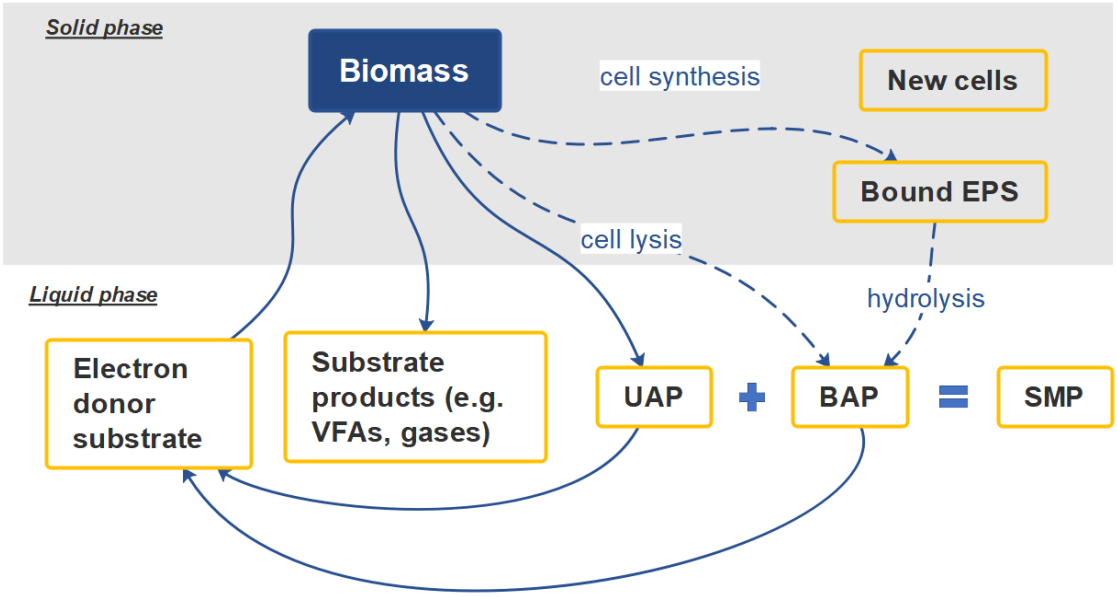

Figure 2-2. Diagram of the metabolism of SMP formation in a heterotrophic biological wastewater treatment system (adapted from Aquino and Stuckey, 2008).

EfOM from activated sludge systems is a combination of influent recalcitrant organic matter, SMPs, and trace harmful chemicals (Shon et al., 2006). Recalcitrant organic matter is resistant to biodegradation and thus is challenging to be removed by typical wastewater treatment. SMPs originate from biological treatment process of wastewater treatment plants (WWTPs) (Jarusutthirak & Amy, 2007). Trace harmful chemicals are microcontaminants associated with wastewater effluent and may cause adverse impacts to human and aquatic health, such as disinfection by-products (DBP) and pharmaceuticals. Of particular interest are SMPs that are found to be the majority of soluble organic matter in wastewater effluent (Soh et al., 2020). For the purpose of wastewater reclamation and reuse, it is imperative to study the properties of SMP in biologically treated wastewater effluent in detail in order to reduce their adverse effects.

SMP has been defined as a group of organics that are released into solution from substrate metabolism and biomass decay (Barker & Stuckey, 1999). Based upon the generation process, SMP can be divided into biomass-associated products (BAP) and utilization-associated products (UAP). Figure 2-2 illustrates the pathways of BAP and UAP formation. BAP are produced through cell lysis and bound EPS hydrolysis which contain cell wall fragments. UAP are produced from substrate utilization and are then excreted to the bulk phase. Both BAP and UAP can be recycled as electron-donor substrates (Shi et al., 2018).

BAP and UAP can present distinct chemical and degradation kinetics. The major components and properties of BAP and UAP were summarized and compared in Figure 2-3. BAP and UAP mainly consist of polysaccharide, protein and humic substances (Barker & Stuckey, 1999). BAP molecules tend to be larger and have a greater molecular weight as compared to UAP substances (Shi et al., 2018). However, UAP with smaller molecules and lower molecular weight are more readily biodegradable (Ni et al., 2012). Hence, it can be anticipated that BAP might present higher potential for SMP-based fouling because of their greater accumulation and larger size (Jiang et al., 2010).

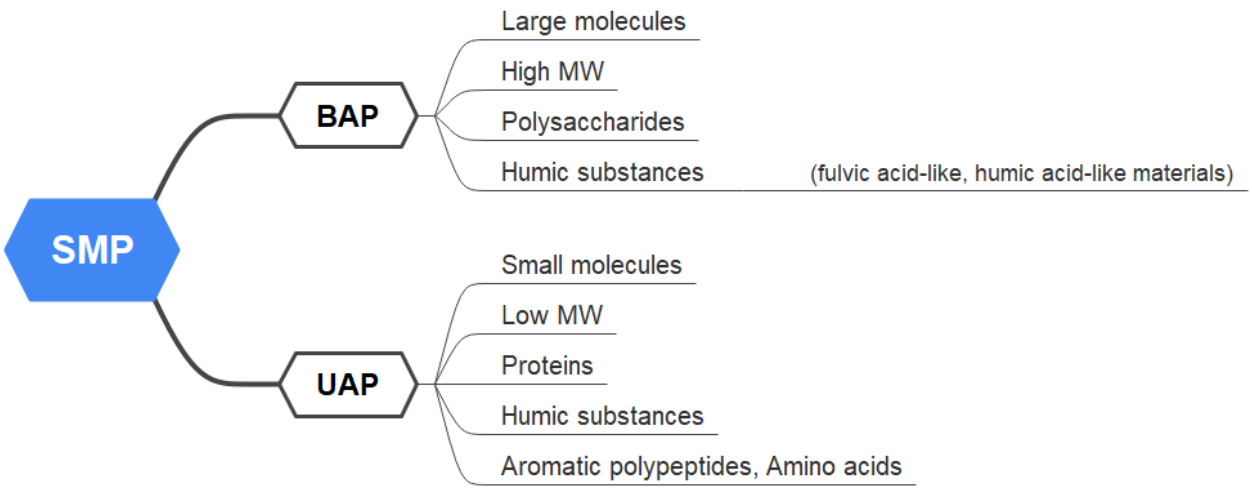

Figure 2-3. Characteristics of BAP and UAP (adapted from Shi et al., 2018).

2.2.2 SMP characterization techniques

Generally, common generic parameters are measured in order to assess the performance of biological wastewater treatment process. These include analyses such as chemical oxygen demand (COD), biochemical oxygen demand (BOD), total dissolved organic carbon (DOC) and SUVA (Pramanik et al., 2016). However, the conventional characteristics do not provide insights into the mechanism of bioprocess and fouling potential of specific components. Therefore, there is a need to identify the specific fractions present in SMP.

As illustrated in Figure 2-4, SMP can be characterized by their concentration (Menniti & Morgenroth, 2010), molecular weight (Teng et al., 2020), fluorescence (Ly et al., 2018), aromaticity (Weishaar et al., 2003), hydrophobicity (Bessiere et al., 2009), biodegradability and biotoxicity (Wang, 2018). Among them, liquid chromatography-organic carbon detection (LC-OCD) and

excitation-emission matrix (EEM) are the most widely employed to identify the properties of SMP that are associated with membrane fouling.

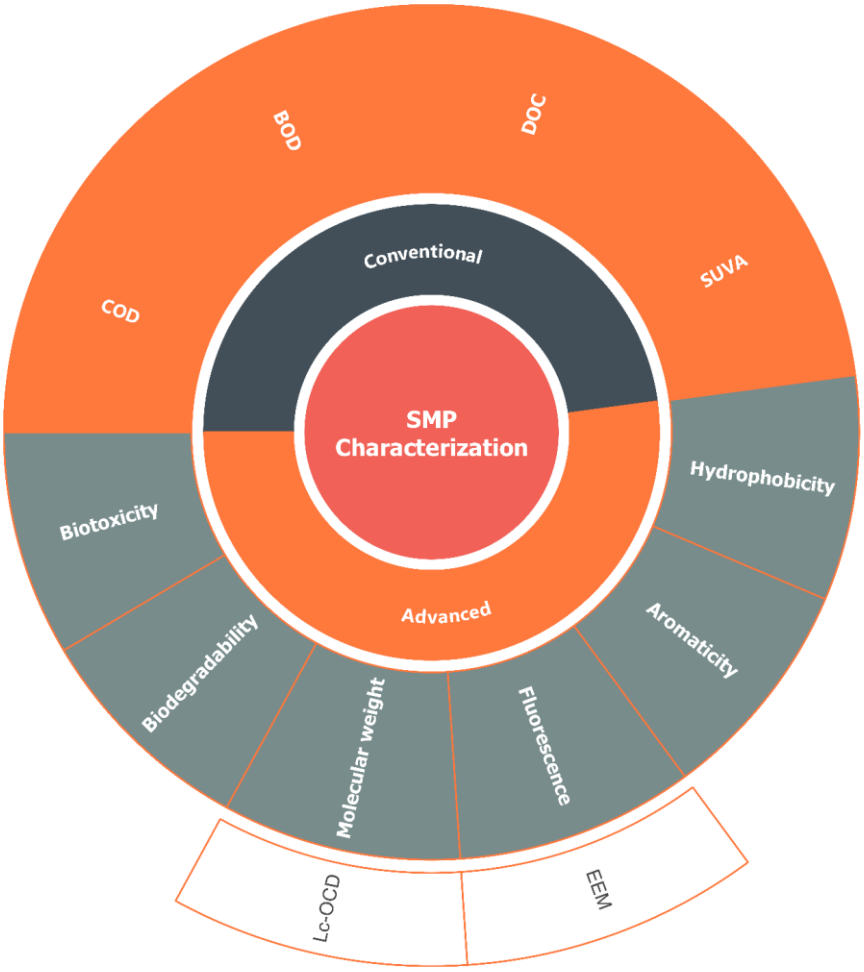

Figure 2-4. SMP characterization methods.

LC-OCD was developed to separate dissolved organic matter into various fractions based on molecular size (Huber et al., 2011). LC-OCD can isolate and quantify five organic fractions, including biopolymers (BP), humic substances (HS), building blocks (BB), low molecular-weight (LMW) acids and LMW neutrals (Huber et al., 2011). Furthermore, the concentration of polysaccharide and protein can be estimated by coupling with the results from organic nitrogen detector (OND) and UV (at 254 nm) detector (UVD). LC-OCD has been initially used to identify natural organic matter (NOM) in studies related to drinking water (Chen et al., 2014; Kimura et al.,

2018; Kimura & Oki, 2017; Peiris et al., 2013). In recent years, the capability of LC-OCD analysis to identify SMP in wastewater treatment and their fouling potential has also been confirmed (Bang et al., 2019; Cai et al., 2020; Hao et al., 2020; Riley et al., 2018; Wang et al., 2017).

EEM has been applied to identify SMP by comparing their fluorescence fingerprints (Drews, 2010). EEM produces fluorescence spectra over a range of excitation (Ex) and emission (Em) wavelengths and can identify various SMP fractions, including aromatic protein, soluble microbial product like, humic acid-like and fulvic acid-like substances (Chen et al., 2003). Regarding wastewater treatment, EEM has been used in recent years to characterize the effect of COD/N ratio on SMP generation in secondary effluent (Ly et al., 2018), identify reversible and irreversible foulants in MBRs (Poojamnong et al., 2020), evaluate the effect of UV/TiO_2 pretreatment (Yang et al., 2019) and ferrate pretreatment (Liu et al., 2018) on fouling alleviation, and analyze membrane fouling behaviors of SMP during the lifecycle of *Escherichia coli* (Yang et al., 2021). Compared to other available SMP characterization techniques, EEM can offer rapid and consistent analyses with high instrumental sensitivity (Peiris et al., 2010).

2.3 Effect of secondary treatment operating conditions on SMP

2.3.1 Effect of temperature on SMP production

Temperature can influence the production of SMPs by affecting the metabolic activity and biomass decay of microorganisms (Choi et al., 2013). Compared with other parameters including substrate concentration, aeration rate and ammonia concentration, temperature has been found to present the greatest impact on SMP generation (Xu et al., 2011). Thus, it has become increasingly apparent that a better understanding of the effect of temperature on SMP production is needed.

The variation of SMP generation in wastewater treatment with temperature and HRT reported in the literatures has been summarized in Figure 2-5. The effect of temperature was initially discussed. It was found the SMP concentrations were negatively correlated with temperature ranged from 8 to 30 ℃ in the reviewed literatures (Hu et al., 2019; Ma et al., 2013; Sun et al., 2014; Wang et al., 2010). It was interesting to note that the polysaccharides and proteins as major components of SMP presented different trends with temperatures. In a MBR treating municipal wastewater, the concentration of polysaccharide increased from 10 to 60 mg/L as temperature declined from 26 to 8 ℃; however, the corresponding change for proteins were from 10 to 20 mg/L (Wang et al., 2010). In another study of MBR, the concentration of polysaccharide increased from 0.60 to 5.75 mg/g MLSS whereas the concentration of protein increased from 0.75 to 3.0 mg/g MLSS from 19.7 to 8.7 ℃ (Ma et al., 2013). Hence, the production of polysaccharides seems more sensitive to temperature than proteins.

However, Sun et al. (2014) reported that polysaccharides and proteins concentrations both increased from 5 to 15 mg/L in a full-scale MBR when temperature decreased from 27 to 13 ℃. The different response of polysaccharides and proteins can be due to variations in influent characteristics (Wang & Chen, 2018). Moreover, the effect of temperature on SMP-based dissolved organic nitrogen (SDON) was evaluated in an activated sludge reactors (Hu et al., 2019), with the highest SDON values observed at 8 ℃ (1.01-1.30 mg/L) followed by 15 ℃ (1.00-1.21 mg/L) and 25 ℃ (0.91-0.97 mg/L). Hence, reduction in temperature can induce increased concentrations of SMP, and polysaccharides were more sensitive to temperature than proteins. However, the results were mostly based on MBRs research and further studies need to be conducted to address the relationship between SMP and fouling of tertiary treatment with the effect of secondary operating parameters.

Apart from concentration, temperature can affect the composition of each SMP fraction. It has been demonstrated that the concentration of lipopolysaccharides, a fraction of polysaccharide originating from the cell walls of Gram-negative bacteria, rose at low temperatures (10 ℃) resulting in higher fouling potential in MBRs (Kakuda et al., 2020). The severe membrane fouling caused by lipopolysaccharides was reported to relate to their high affinity to membrane polymers and their unique molecular weight distribution (Kimura et al., 2019). This influence of temperature on the other composition of SMP needs to be further investigated in tertiary treatment with membranes.

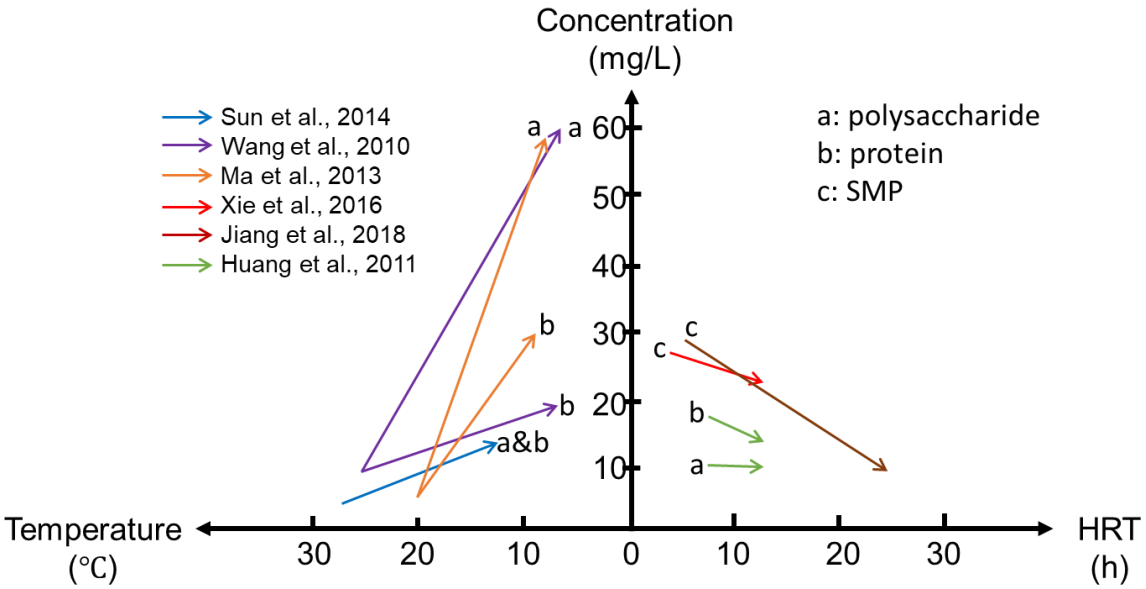

Figure 2-5. Trends in SMP concentration before and after secondary temperatures and HRTs' change.

2.3.2 Effect of HRT on SMP production

In temperate regions wastewater resource recovery facilities (WRRFs) often need to operate during periods of elevated flow that results from events such as snow melt, and HRT decreases accordingly during these periods. HRT is another operating parameter affecting the production of SMP since HRT can govern food to microorganisms (F/M) ratio of the bioreactor and MLSS concentration (Meng et al., 2009). Hence it is of interest to understand how HRT affects SMP generation.

The impact of HRT on SMP concentrations in activated sludge systems is summarized in Figure 2-5. Similar to temperature, the concentration of SMP was negatively correlated with HRT (Huang et al., 2011; Jiang et al., 2018; Xie et al., 2016). The total concentration of SMP in an MBR was reported to increase from 13 to 18 mg/L as HRT decreased from 12 to 8 h (Huang et al., 2011). With a similar HRT range studied by Huang et al. (2011), the SMP concentrations was found to incresae from 22 to 27 mg/L in a full-scale wastewtaer treatment plant (Xie et al., 2016). The SMP concentrations as a function of HRT were also observed in a hybrid moving bed biofilm reactor (MBBR)-MBR system with 16.6–29.7 mg/L at HRT of 6 h followed by 4.9–10 mg/L and 4.9–6.3 mg/L at HRT of 18 and 24 h, respectively (Jiang et al., 2018). In an MBBR-MBR treating landfill leachate, the SMP concentration increased from 145 to 157 mg/L as HRT decreased from 48 to 36 h (Duyar et al., 2021). The greater SMP concentration observed in the landfill leachate treatment may have been due to its higher organic loading. Hence it was concluded that reducing HRT would induce higher SMP generation . However, less attention has paid to effect of HRT on individual SMP fraction. The interactive influence of HRT and secondary temperature also needs to be further investigated. -

2.4 Membrane fouling when treating secondary effluent

2.4.1 Impact of SMP on membrane fouling

SMPs during ultrafiltration treatment are attracting more and more attention as they were considered as the major foulants that will cause organic fouling during wastewater reclamation (Filloux et al., 2012). The major fouling mechanisms associated with SMP have been summarized as follows: (1) SMP can be adsorbed in membrane pores and narrow the passageways available to water; (2) SMP can block access to membrane pores by forming cake/gel layers on membrane surface; and (3) with the presence of particles SMP can bind particles together and form a low permeability layer on the membrane surface (Guo et al., 2012). It was noted that the fouling mechanisms of SMP significantly depend on their molecular size with the portion of larger size forming cake layer and smaller size blocking membrane pores. The impact of SMP fractions on membrane fouling with different

molecular weight/size was subsequently discussed. Figure 2-6 presents typical organic constituents and their size ranges to facilitate comparison.

Polysaccharides are the dominant fractions of SMP and are defined as macromolecules with MW range of 10^4–10^7 Da. Polysaccharides have been confirmed to exhibit a key role in membrane fouling as their molecular size are close to or larger than that of membrane pore size (~0.02 μm) as illustrated in Figure 2-6. In recent studies of MBR treating municipal wastewater, the relationship between polysaccharide and membrane resistances (Kakuda et al., 2020; Liu et al., 2018), TMP (Iorhemen et al., 2019), fouling index (UMFI) (Poojamnong et al., 2020) , and the contribution of polysaccharide to irreversible fouling (Kimura et al., 2015) have been demonstrated. These studies revealed that the polysaccharides were considered as the dominant foulants in MBRs and might be more responsible for fouling compared with protein. Fewer studies evaluated the role of polysaccharide in tertiary membrane fouling. Ly et al. (2018) studies the effect of COD/N ratio on SMP in effluent from SBRs and subsequent membrane fouling and they concluded that polysaccharide contributed more to reversible fouling when N is deficient (COD/N ratio of ~100/2). However, the nature of polysaccharides and their fouling propensity were found to change under different operating conditions as previously discussed in Section 2.3 and therefore it is still a challenge to correlate polysaccharides to membrane fouling.

The fraction of protein, with similar molecular size/weight to polysaccharides (Figure 2-6), has also been reported as one of the major foulants for low-pressure UF (Steinhauer et al., 2015). Most of the above literature associated with polysaccharide also confirmed the fouling potential of protein. However, several attempts have reported that the protein fraction in SMP resulted in less fouling than that of polysaccharides in wastewater treatment (Ly et al., 2018; Rosenberger et al., 2006). The different fouling propensity of polysaccharides and proteins might be due to their different hydrophobicity (Shi et al., 2018). Polysaccharides exhibit hydrophilic properties whereas protein are usually hydrophobic in nature (Iorhemen et al., 2016). Hydrophilic organics can cause severe membrane fouling in hydrophobic membranes by pore blocking and/or hydrogen bonds (Kimura et al., 2014; Yamamura et al., 2014). Thus, it was expected that proteins may present less fouling potential in the tertiary membranes.

Apart from polysaccharides and proteins, the fraction of humic substances that consist of intermediate molecular weight and size (10^3–10^6 Da) was also widely studied. Since the molecules of humic substances can pass the membranes more easily as shown in Figure 2-6, it was widely accepted that humic substances contribute less to membrane fouling in MBRs treating municipal wastewater (Iversen et al., 2009; Shi et al., 2018; Tian et al., 2012). However, it has also been found that the

fraction of humic substances can foul membranes to some extent when treating wastewater. It has been reported that humic substances, large MW proteins and hydrophilic polysaccharides were all dominant foulants in the full-scale MBR (Sun et al., 2014). Guo et al. (2014) compared the fouling propensity of humic substances in EfOM and NOM and found that humic substances were the major foulants in UF treating surface water whereas polysaccharides and humic substances were speculated as the main foulants for UF treating wastewater. These distinctions of fouling potential of humic substances might be due to the differences in operating conditions, determination devices and statistically analysis for fouling evaluation.

Understanding on fouling potential of each SMP fraction is the theoretical basis and one of the focuses for identifying fouling behavior and selecting fouling control strategies. However, the results significantly depend on the extraction methods and measurement approaches. The shift of SMP fractions under low temperature and high flow conditions and their effects on tertiary membrane fouling will be explored in the present study.

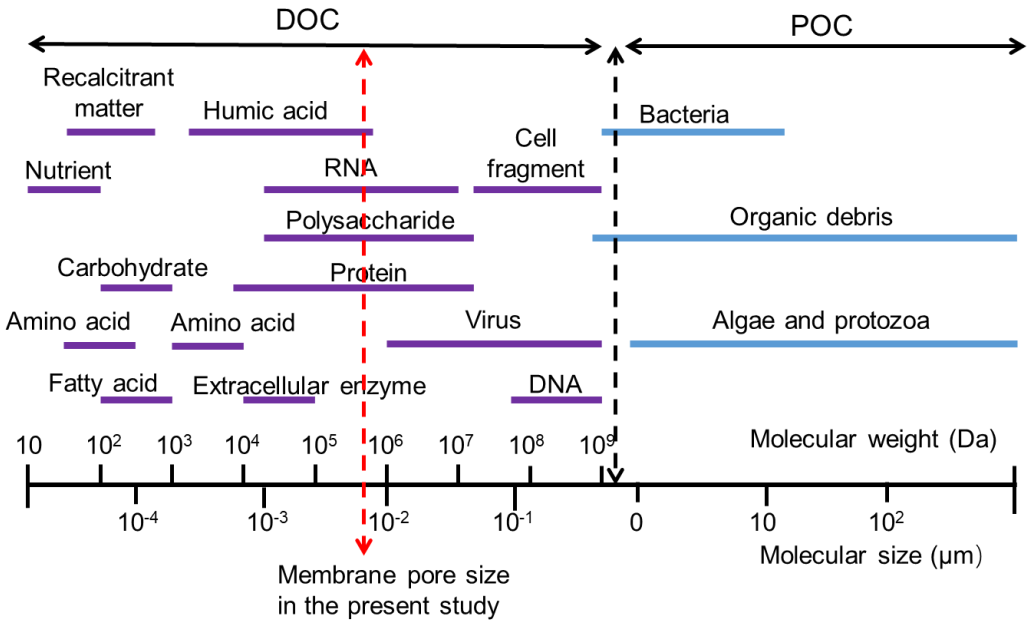

Figure 2-6. Typical organic constituents and their size ranges (adapted from Shon et al., 2006).

2.4.2 Impact of filtration temperature on membrane fouling

Temperature not only has an effect on the bioconversion process but is also shown to influence membrane performance. In membrane filtration process, temperature can affect the formation and

morphology of the fouling layer. It was reported that low temperatures (under 20 ℃) may cause the cake to shrink and resulted in a denser cake layer with higher specific cake resistance (Boerlage et al., 2003). However contradictory results have been observed at a higher temperature range, with the mean cake layer thickness obtained at 37, 45 and 55 ℃ decreasing from 296.5 to 168.9 μm. This was attributed to higher shear forces and changes in microbial community at high temperature (Gao et al., 2012). It could be concluded that the cake layer can become denser and exhibit higher resistance under both relatively low and high temperature conditions.

Temperature can affect the fluid dynamics in membrane processes. At low temperature, increased liquor viscosity can reduce the stress generated by coarse bubbles (van den Brink et al., 2011). Low temperature decreases the particle back transport velocity due to reduced Brownian diffusion which is linearly related to temperature. However, the reduced stress and lower particle back transport velocity at low temperatures is difficult to measure in filterability set-ups that are commonly employed in lab testing. Hence, a mathematical model was used by Belfort et al. (1994) to study the fluid dynamics. It was reported that the back-transport of particle sizes larger than 1 μm was dominated by hydrodynamic forces, and it strongly depended on the shear rate and the particle size, whereas for particle sizes smaller than 0.1 μm, molecular diffusion was the dominant mechanism (Belfort et al., 1994). As previously discussed, temperature can influence the size of particles generated in secondary treatment process, therefore their impact on fouling could be accentuated by the effect of temperature on fluid dynamics.

2.5 Pre-treatment of secondary effluent

In recent years, many pretreatment processes prior to UF membrane have been implemented to mitigate membrane fouling. Strategies that have been employed included adsorption (Huang et al., 2017), coagulation/flocculation (Liu et al., 2021; Aly et al., 2021), and oxidation (Yu et al., 2019). Among them, coagulation/flocculation has been most widely used as a pretreatment to mitigate fouling by removing SMP or changing their physical-chemical characteristics (Chen et al., 2020; Peleato et al., 2017). The effects of coagulant type, dosage and coagulation mode on fouling mitigation were summarized subsequently.

The selection of coagulant is a key variable for coagulation performance. Yu et al. (2013) compared alum and $FeCl_3$ pre-treatment on UF membrane fouling by characterizing the UF performance, flocs, and cake layer. It was observed that TMP increased at a higher rate in the $FeCl_3$-UF than the alum-UF. The greater thickness and lower porosity of the cake layer in the $FeCl_3$-UF system was considered as the likely cause of higher resistance. Under the same condition, alum

showed better performance than $FeCl_3$. Zhao et al. (2010) reported that aluminum species could determine the characteristics of coagulant flocs and further affect the efficiency of fouling control. The performance of three species of aluminum coagulants on membrane fouling control were also studied by Feng et al. (2015). Among mononuclear Al species (Al_a), medium polymeric species (Al_b) and colloidal species (Al_c), Al_b was found to be most effective in reducing membrane fouling, and the flocs formed by Al_b were smaller with higher strength and a more compact structure. Similar results were obtained with Al species when employed for fouling mitigation by Wang et al. (2017).

Considerable efforts have been made to evaluate alternative coagulants and combinations of coagulants. Alum could be added simultaneously with hypochlorite to reduce biofouling (Yu et al., 2016). In order to achieve both oxidation and coagulation, the mixture of ferric iron and ferrate (Yu et al., 2016), and ferrous iron with K_2MnO_4 (Yu et al., 2015) were tested and showed good treatment performance. Additionally, organic coagulants, such as polyacrylamide polymer, have also been found to be good alternatives when conducting flocculation and coagulation as fouling control strategy (Yu et al., 2013; Liu et al., 2017). However, while coagulation has been shown to be effective as a pretreatment for drinking water, few studies have reported their feasibility for wastewater pretreatment especially under cold climates.

The dosage of coagulants can also play a significant role in fouling mitigation. Lee et al. (2009) reported the optimal dosage could minimize fouling and cake layer resistances, however, it also significantly depended on influent composition. For in-line coagulation in tertiary membrane filtration, pilot experiments revealed that adding 1, 5 and 10 mg/L Fe^{3+} exhibited similar performance to prevent irreversible fouling (Naim et al., 2014). Shen et al. (2017) tested different dosage ratio of polyaluminum chloride (PAC) to poly dimethyldiallylammonium (PDMDAAC) chloride on treatment performance and membrane fouling, and the best performance was observed at PAC and PDMDAAC of 1.0 mg/L and 0.1 mg/L, respectively. The characteristics of coagulated particles, such as size and surface charges, were affected by the doses of coagulants. Therefore, optimizing the coagulant dose is important when coagulation is employed as pretreatment for membrane treatment.

The operation mode of coagulation in tertiary membrane filtration has also received attention. Ding et al. (2017) compared *in-situ* coagulation with pre-coagulation for a gravity-driven MBR. They found *in-situ* coagulation increased permeability more than two-fold compared with pre-coagulation, while both processes reduced reversible resistance and cake layer resistance. Further, the addition mode significantly affects the coagulation efficiency. Two-stage addition of alum was evaluated by Liu et al. (2011) and it was found that membrane fouling was effectively mitigated and this was attributed to a 50% increase in the average floc size with two-stage addition mode. Therefore, it was

concluded that it is important to optimize the coagulation process to achieve the highest performance of fouling mitigation.

2.6 Research gaps and needs

- Understanding on characteristics and fouling potential of SMP is the theoretical basis and one of the focuses for assessing fouling behaviour and selecting fouling control strategies. However, the exact mechanisms of SMP including BAP/UAP generation when treating real municipal wastewaters under cold temperatures remain unrevealed. The linkage between secondary biological processes and SMP formation need to be studied.
- Reductions in tertiary membrane permeability at low temperatures may be attributed to increased concentrations of foulants in secondary treatment effluents as well as increased water viscosity and changed membrane properties. There is limited knowledge on the extent to which temperature influences the relative contribution of these factors to hydraulically irreversible fouling in tertiary applications. Further exploration on differentiating these factors will help improve the understanding of temperature effect.
- MBR-focused research has suggested several potential mechanisms for increased fouling under low temperatures, however, the extrapolation of these results to tertiary treatment is challenging due to differences in the exposure of membranes to the various foulants. A comprehensive evaluation of the temperature effect on SMP generation with a linkage to fouling of tertiary membranes need to be conducted.
- It is anticipated that climate change will increase the frequency of extreme weather events and cause earlier snowmelts that may extend the periods of low temperature and high flow. However, the impacts of the interaction between low temperature and high flow on fouling of tertiary membranes have received little attention. Therefore, a thorough investigation is necessary to identify the impact of secondary system HRT on fouling of tertiary membranes over a range of temperatures.
- The drinking water treatment literature reveals a number of strategies for mitigating ultrafiltration membrane fouling. However, there has been little testing of these strategies in tertiary wastewater applications. It is expected that the preferred dosage of coagulants and the mechanisms of membrane fouling alleviation may change under low temperature and high flow condition. Therefore, fouling mitigation mechanisms should be further studied under different secondary operating conditions. This will greatly increase the understanding of fouling mitigation and be useful for developing strategies to better optimize operation.

Chapter 3

Characterization and modelling of soluble microbial products in activated sludge systems treating municipal wastewater with special emphasis on temperature effect

GRAPHICAL ABSTRACT

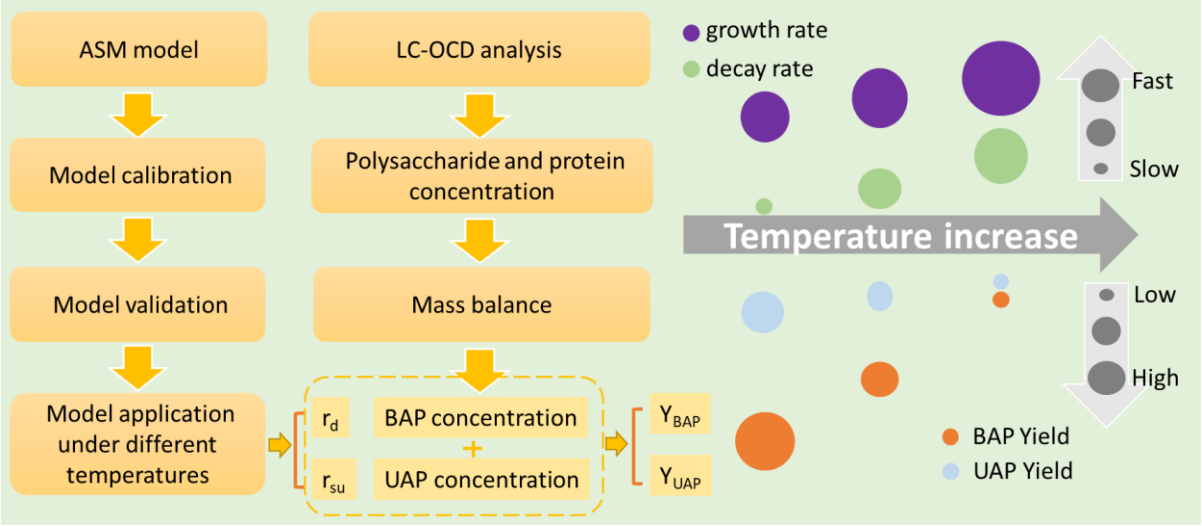

3.1 Introduction

Membrane technologies, which can effectively remove particulate and colloidal matter, macromolecules and pathogens, are now being successfully used to meet the requirements of increasingly stricter effluent quality. However, membrane fouling impedes widespread adoption of this technology in tertiary treatment due to the deposition and adsorption of effluent organic matter (EfOM), which is considered as the most important foulant in biologically treated wastewater effluents (Soh et al., 2020). The reduction in membrane productivity and increase in operational costs can be more severe in Northern regions such as Canada and Northern Europe that regularly experience long-term cold temperatures (Cui et al., 2017). A negative impact of seasonal changes on full-scale tertiary membrane fouling has been documented and was attributed to increased EfOM

under low temperatures and high flows (Abu-Obaid et al., 2020). Therefore, for the purpose of improving effluent quality in cold regions, it is imperative to study the characteristics of EfOM to better understand the fouling mechanisms with the goal of minimizing the propensity for fouling.

The EfOM present in biologically treated wastewater has been reported to consist of a complex mixture of soluble microbial products (SMPs), natural organic matter (NOM), and trace chemicals (Jarusutthirak & Amy, 2007). SMPs have been reported to constitute a dominant part of EfOM in secondary effluents and are biologically derived from substrate metabolism (utilization-associated products, UAP) and biomass decay (biomass-associated products, BAP) (Barker & Stuckey, 1999). NOM originates from natural aquatic systems and consists of a group of heterogeneous macromolecules (Matilainen et al., 2011). EfOM can also include trace levels of pharmaceuticals/personal care products residues (Michael-Kordatou et al., 2015). Previous experimental results have demonstrated that only a small portion of the EfOM arises from the original influent substrate and the majority of the soluble organic matter is of microbial origin (Tian et al., 2011). Therefore, the presence and complexity of biologically related SMP is of a particular interest in terms of EfOM characterization and their effect on membrane fouling.

Several studies have focused on characterization and fractionation of SMP as potential components causing reversible and/or irreversible fouling. Biopolymers, as high molecular weight (MW) compounds (>10,000 Da), mainly consisting of proteins and polysaccharides, have been documented to be the dominant components of SMP, and have been observed to be major contributors to total fouling of membranes by secondary effluents (Rosenberger et al., 2006). Additionally, biopolymers were reported to play a more significant role in low pressure membrane fouling than intermediate MW (1000-10,000 Da) and low MW (<1000 Da) compounds (Filloux et al., 2012). Therefore, it was deemed important to differentiate the SMP components especially under different operating conditions to better explore their fouling properties.

A joint characterization of SMP in terms of chemical composition and bacterial metabolism would allow for an assessment of how the biological process operating conditions can influence their presence in treated effluents. Advanced analytical tools such as liquid chromatography with organic carbon detection (LC-OCD) are gaining prominence with respect to characterization and quantification of SMP fractions including polysaccharides, proteins and humic substances (Huber et al., 2011). However, it has proven challenging to differentiate SMP into BAP and UAP experimentally due to their heterogeneous properties. A combination of experimental and modelling

approaches has been proposed to quantitatively determine UAP and BAP treating synthetic wastewater (Ni et al., 2012), however, there has been little characterization of UAP and BAP in systems treating real wastewaters.

Factors affecting the chemical composition of SMP in biological wastewater treatment have been evaluated experimentally by others. The composition and concentration of SMP have been reported to vary depending on factors such as solids retention time, carbon to nitrogen ratio and organic loading rate (Jarusutthirak & Amy, 2007; Ly et al., 2018; Maqbool et al., 2017). However, little is known about how low temperature operation affects the biological mechanism of SMP generation with real wastewater. It is hypothesized that SMP generation will be temperature dependent because substrate utilization and biomass decay that lead to UAP and BAP depend on operating temperature (Hu et al., 2019). A comprehensive evaluation of the effect of low temperature operation on UAP and BAP generation in systems treating real wastewaters with a linkage to substrate utilization and biomass decay has not been reported.

In this context, the present research sought to develop quantitative relationships between UAP/BAP generation and the operating temperature of a biological treatment process treating real municipal wastewater. LC-OCD analysis and conventional parameter wastewater quality characterization were coupled with activated sludge modelling to interpret the generation of SMP fractions that are relevant to membrane fouling. This is the first study to report the linkages between biological processes and SMP formation in the treatment of real wastewaters. The establishment of these linkages over a range of operating temperatures observed in practice is a significant contribution of the study. The relationships developed in this study will allow practitioners to predict membrane fouling potential as a function of activated sludge operating condition.

3.2 Materials and methods

3.2.1 Experimental set-up and operation

Two identical lab-scale sequencing batch reactors (SBR) were operated with a 4 h cycle duration to approximate continuous flow conditions (Figure 3-1). One SBR was operated at 20 ℃ as a control while the other SBR (test) was initially operated at 14 ℃ in the first phase for over six months and subsequently 8 ℃ in the second phase for over three months. The temperatures are representative of summer and winter operating conditions in Ontario, Canada. The SBRs were fed with real municipal wastewater collected every two days from the City of Waterloo sewer system and sieved with a 2 mm

mesh to remove large particles. The raw wastewater was chilled at 4 ℃ during storage to ensure the stability of organic matter. The hydraulic retention time (HRT) of the SBRs was 20 h, and the solids retention time (SRT) was maintained at 25 days. Both SBRs reached pseudo steady state before sampling during the first and second phase.

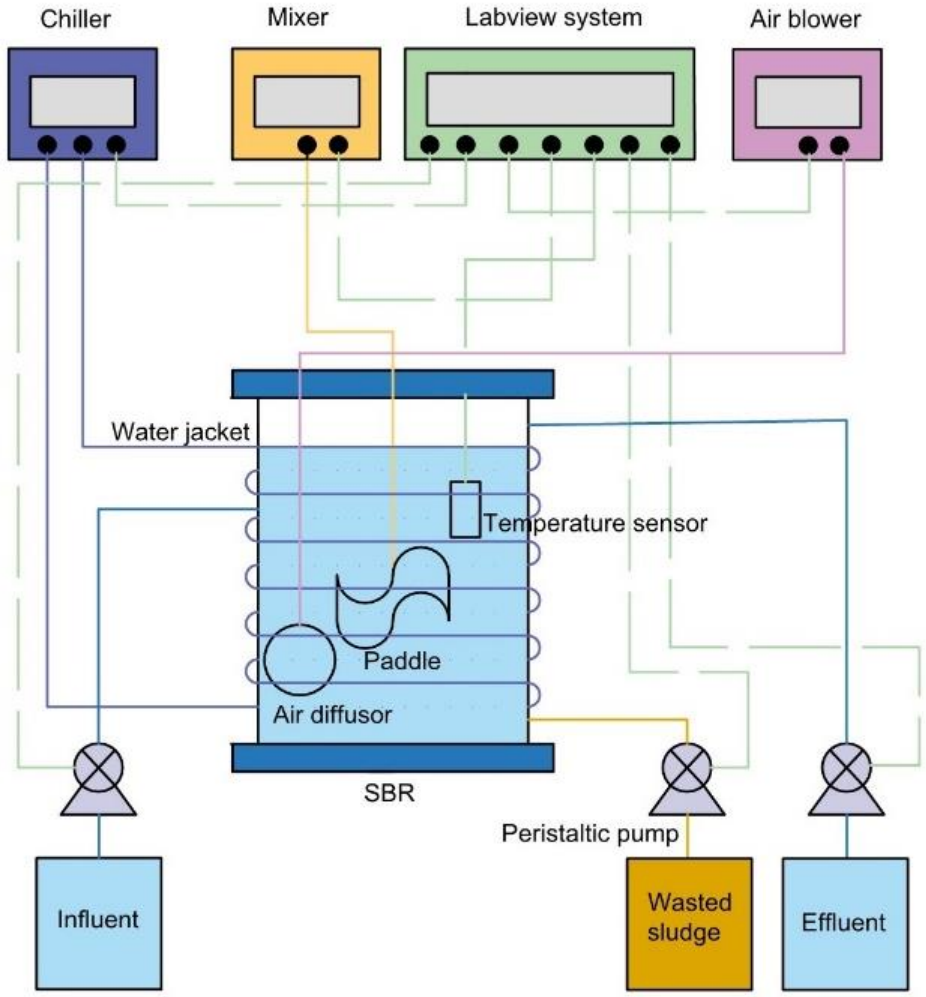

Figure 3-1. Schematic of laboratory-scale SBR.

Each reactor consisted of a 12 L polymethyl methacrylate container with a working volume of 10 L. A mechanical mixer with a shaft paddle operating at 150 rpm was employed to mix the SBR contents. A constant airflow for aeration was provided through an air diffuser located at the bottom of

the reactor. A water jacket, controlled by a chiller (Polyscience, USA), was used to maintain the water temperature inside the test SBR while the control reactor was operated at room temperature (20°C). The water temperature was regularly monitored by a thermometer. The SBR time sequence process was controlled using LabView® software (version 2017, National Instruments Corporation, USA).

Samples of the SBR mixed liquor were collected once per week for analysis of total suspended solids (MLSS), volatile suspended solids (MLVSS), and sludge volume index (SVI). Samples of raw wastewater and effluents were characterized once per week with respect to water quality parameters that were anticipated to be affected by temperature, including pH, turbidity, soluble COD (sCOD), total COD (tCOD), dissolved organic carbon (DOC), UV_{254}, ammonia, nitrate and nitrite nitrogen concentrations. In addition, LC-OCD analysis was conducted once per week for samples of raw wastewater and effluents.

3.2.2 Analytical methods

MLVSS, MLSS and SVI were analyzed in accordance with Standard Methods (APHA, 2005). tCOD, sCOD, DOC, UV254 and turbidity were measured as indicators of organic matter. Soluble components were obtained by filtering through 0.45 μm nylon filters. tCOD and sCOD were analyzed according to Standard Methods (APHA, 2005). Filtered samples were analyzed for DOC using a Shimadzu analyzer (TOC-L, Shimadzu, Japan) and for UV absorbance at 254 nm (UV_{254}) by a spectrophotometer (8453, Agilent, USA). The turbidity of samples was analyzed with a HACH 2100N Turbidimeter. Nitrogen species concentrations were analyzed to indicate the state of nitrification in the SBRs. The filtered samples were analyzed calorimetrically for Total Kjeldahl nitrogen (TKN), ammonia (NH_4^+-N), nitrate (NO_3^--N) and nitrite (NO_2^--N) (APHA, 2005).

LC-OCD analysis was used to provide insight into the composition of SMP in the raw wastewater and SBR effluents. The samples were filtered with 0.45 μm nylon filters before analysis. The LC-OCD system was equipped with an HPLC pump (S-100, Knauer, Germany) that was operated at a flow rate of 1.1 mL/min to an autosampler and a chromatographic cation exchange column (TSK HW 50S, Toso, Japan). The LC-OCD employed three detectors including fixed wavelength UV (UVD), organic carbon (OCD) and organic nitrogen (OND) detection in series. The UVD measured the spectral absorption coefficient at 254 nm. The OCD oxidized organic matter in a UV reactor and the organic carbon was quantified from the produced CO_2. The OND oxidized organic nitrogen and measured the produced nitrate using a UVD operated at 220 nm. Based upon the multiple signals, the

LC-OCD analysis reports dissolved organic matter as biopolymers, humic substances, building blocks, LMW acids and LMW neutrals (Huber et al., 2011).

3.2.3 Statistical analysis

All statistical analyses were performed using the Origin Pro 2020 software package. Student t-tests were employed to compare the characteristics of effluents and mixed liquor of control SBR between the two steady-state phases. One-way ANOVA was used to determine if there was a statistically significant difference between the SBR effluents and mixed liquors that were generated at 8, 14 and 20 ℃. Where appropriate the mean values observed at each operating condition were compared via Tukey test. Data sets were considered statistically different at a 95% confidence interval ($P<0.05$).

3.3 Results and discussion

This study sought to establish relationships between the generation of SMPs that influence membrane fouling and bioprocess operations. The performance of the SBRs with respect to conventional wastewater quality parameters was initially assessed to establish the bioprocess conditions that were present at the different operating temperatures. The SMP composition, as determined by LC-OCD analysis was then examined to characterize how temperature impacted these responses. The concentrations of SMP fractions (UAP and BAP) were estimated from the LC-OCD data. Process modelling was conducted to establish the rates of substrate utilization and endogenous decay at the different temperatures. The yields of UAP and BAP were then calculated as the ratio of the observed UAP and BAP production to the rates of substrate utilization and endogenous decay respectively. The impact of temperature on UAP and BAP yields was then examined.

3.3.1 Conventional wastewater quality performance

The biological performance of the SBRs was assessed at each operating temperature by examining a range of conventional wastewater quality parameters (Table 3-1). Since a real wastewater was employed in the study, the characteristics of the control SBR (20 ℃) effluents observed in the two phases were initially compared using student t-tests to assess the stability over long-term operation. The results demonstrated that all of the measured parameters were not significantly different between the phases. Hence, the data from the control SBR in both steady-state phases was combined for subsequent comparisons with the test SBR. The characteristics of the SBR effluents at the three temperatures were initially compared using a one-way ANOVA and then subsequently with Tukey tests. A P-value below 0.05 was employed to delineate whether the means were statistically different.

Table 3-1. Conventional characteristics of SBR effluents.

Parameter	Phase 1			Phase 2		
	Raw wastewater	C SBR (20 ℃)	T SBR (14 ℃)	Raw wastewater	C SBR (20 ℃)	T SBR (8 ℃)
	(average ± standard deviation)					
Turbidity (NTU)	270±32	1.8±0.4	3.2±1.2	297±39	1.3±0.3	6.6±1.4
sCOD (mg/L)	150±8	38±5	47±9	156±13	37±5	46±7
tCOD (mg/L)	506±28	43±8	63±9	480±30	43±8	63±9
DOC (mg/L)	50+9	8.9±0.7	12±1	53±6	9.3±0.9	13±1
NO_3^--N (mg/L)	0.44±0.09	53±5	48±3	0.49±0.05	58±6	47±5
NO_2^--N (mg/L)	*	*	*	*	*	*
NH_4^+-N (mg/L)	54±4	*	*	59±5	*	*

*Below detection limits (2 mg/L for ammonia-N; 0.6 mg/L for nitrite-N).

The overall performance of the bioreactors with respect to carbon removal was assessed by examining tCOD in the raw and treated wastewaters. The average removals of tCOD were 91%, 88% and 87% for 20, 14 and 8 ℃ SBR, respectively but were observed not to be significantly different. This indicated little influence of operating temperature on overall carbon removal, which formed the basis for the subsequently described bioprocess modelling.

The soluble carbon-related metrics including sCOD and DOC were evaluated to assess the overall effect of temperature on effluent quality. From Table 3-1 it can be observed that the concentration of sCOD was approximately 10 mg/L higher in the test SBR effluent than the control SBR in both phases. A 43% increase in DOC concentration was also observed with the decrease in temperature from 20 ℃ to 14 ℃ but there was no additional increase at 8 ℃. Therefore, the temperature of 14 ℃ resulted in greater effluent sCOD and DOC compared to 20 ℃ which might indicate increased generation of SMP at 14 ℃. However, no additional change of sCOD and DOC was induced by further temperature decrease from 14 ℃ to 8 ℃. The increased concentrations in soluble components (sCOD, DOC) suggest reduced biological reaction rates at low temperatures (Lishman et al., 2000). Further analysis that was conducted to investigate the effect of temperature on SMP components is described subsequently.

Nitrogen species concentrations were measured to evaluate the state of nitrification in the SBRs and thereby provide an indicator of the microbial community present under the differing operating conditions. From Table 3-1 it can be observed that complete nitrification was achieved at all temperatures as indicated by low effluent NH_4^+-N concentrations (<2 mg/L) and negligible NO_2^--N accumulation (<0.6 mg/L). The effluent NO_3^--N concentrations at 8℃ (46±4 mg/L) and 14℃ (47±3.7mg/L) were significantly lower than those at 20 ℃. The lower NO_3^--N levels were attributed to a reduction in endogenous decay of biomass at low temperatures (Nachaiyasit & Stuckey, 1997). A reduction in endogenous decay in nitrifiers and heterotrophs would suggest that there was a reduction in the generation of BAP through endogenous decay at lower temperatures.

The particulate metrics including turbidity and particulate COD were examined as they can provide an indirect measure of activated sludge flocculation properties. It was observed that there was a significant effect of temperature on the turbidity of the effluents with a 313% increase in this response as temperature reduced from 20 ℃ to 8 ℃. Particulate COD was determined as the difference between tCOD and sCOD and was observed to increase by 220% as the temperature reduced from 20 ℃ to 8 ℃, which was consistent with the turbidity results. The increased particulate organic matter indicated a negative impact of low temperature on flocculation with less activated sludge floc being captured. Previous research has demonstrated that extracellular polymeric substances (EPS) bound to sludge flocs increased under low temperature operation (8 ℃) which was attributed to a change in the microbial population towards more EPS-producing bacteria (Wang & Zhang, 2010). The increased effluent turbidity and particulate COD concentrations at the low temperature conditions in the present study may have been due to increased EPS generation that was not retained in the floc in the SBRs.

3.3.2 SMP characterization

SMP has been reported to be a complex mixture of proteins, polysaccharides, humic substances, DNA and lipids, with proteins and polysaccharides as the dominant components (Soh et al., 2020). LC-OCD was employed to quantify the presence of SMP fractions and Figure 3-2 presents typical LC-OCD chromatograms of the raw wastewater and SBR effluents at the different temperatures. From Figure 3-2 it can be observed that high MW biopolymers, intermediate MW humic substances and low MW building blocks, acids and neutrals were the DOC fractions reported by the LC-OCD analysis. As SMP is primarily composed of DOC with a MW greater than 10 kDa (Tian, et al., 2011), the subsequent discussion focuses on the intermediate-high MW fractions.

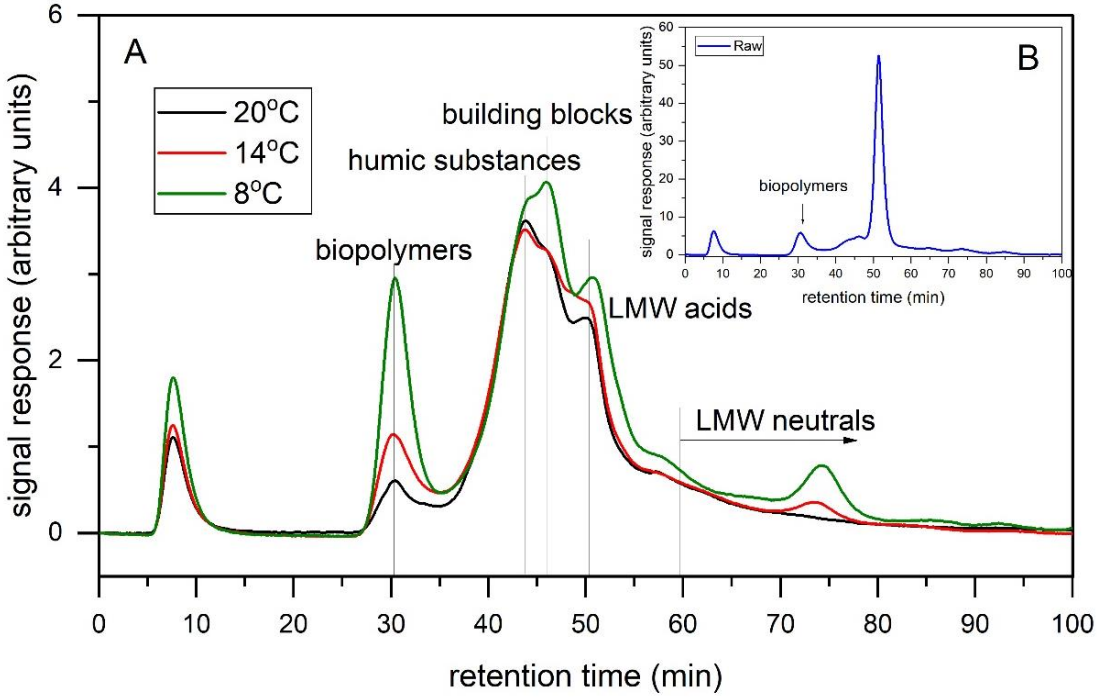

Figure 3-2. LC-OCD chromatograms of (A) SBR effluents at different temperatures and (B) raw wastewater.

From Figure 3-2 it can be observed that the concentration of biopolymer fraction was the highest in raw wastewater and increased in effluents as temperature decreased from 20 ℃ to 8 ℃. The biopolymers measured in raw wastewaters were previously reported to be bioavailable (Barker & Stuckey, 1999) and hence it was assumed that they would be consumed as substrate by the biomass given the long SRT of the systems. Hence the biopolymers present in the effluents were assumed to be primarily associated with biomass metabolism products. In contrast, the humic substance concentrations were similar in the raw wastewater and effluents. Humic substances are typically considered to be biologically recalcitrant and will pass through bioprocesses (Lin et al., 2014) and the results indicate minimal generation of humic substances in the SBRs. The results further confirmed that biopolymers consisting of polysaccharide and protein were the dominant fractions in the SMP.

Prior studies demonstrated that the UAP and BAP fractions of SMP have different composition with respect to proteins and carbohydrates and for this reason the concentrations of proteins and polysaccharides in the SBR effluents were initially investigated (Tian et al., 2011). The biopolymer

concentrations reported by the LC-OCD analysis were divided into polysaccharide and protein components assuming all of the DON in the biopolymers was bound in proteinaceous matter and employing a typical C:N mass ratio of 3 for proteins (Huber et al., 2011). Table 3-2 presents the effluent concentrations of polysaccharide and protein at the three operating temperatures. As presented, the temperature impacted polysaccharide and protein concentrations to different extents. Both biopolymer concentrations increased as temperature decreased, but the increase in polysaccharide concentrations was more sensitive to temperature than that of proteins. This led to a substantial difference between protein and polysaccharide concentrations at 8 ℃ (581±42 μg/L and 1245±100 μg/L, respectively). This pattern was consistent with previous research with membrane bioreactors (MBRs). Ma et al. (2013) and van den Brink et al. (2011) reported that the concentrations of polysaccharides and proteins increased at lower temperatures in membrane bioreactors fed with real wastewater. Further, polysaccharide concentrations were higher than proteins and contributed a greater fraction of the SMPs at lower temperatures. Viewed collectively, polysaccharide concentrations tended to be impacted more by low temperature than proteins. The information on polysaccharide and protein concentrations was subsequently employed to estimate the contributions of UAP and BAP to the SMP in the effluents.

Table 3-2. Estimated concentrations of major SMP components.

Samples	SMP concentration (average ± standard deviation ug/L)	
	Polysaccharides	Proteins
20℃	231±58	180±47
14℃	713±89	437±68
8℃	1245±100	581±42

3.3.3 Development of SMP production models

A conceptual model describing SMP production (Aquino & Stuckey, 2008) was modified by incorporating the UAP production from floc-associated EPS hydrolysis into biomass decay to provide a framework for quantitative analysis of the experimental results (Figure 3-3). In the model the raw wastewater contains biodegradable soluble organic matter (OM), biodegradable particulate OM, non-biodegradable soluble OM and non-biodegradable particulate OM. This fractionation is consistent

with conventional biological process modelling where COD is employed to quantify OM (Melcer et al., 2003). Biodegradable OM can be utilized by biomass whereas non-biodegradable soluble OM passes through treatment while non-biodegradable particulate OM contribute to sludge production. In the model UAP is generated as a product of biodegradable OM utilization while BAP originates from active biomass decay. Since the generation of UAP and BAP is associated with bioprocesses it was hypothesized that their generation would be sensitive to the operating temperature.

UAP and BAP have been reported to consist of mixtures of polysaccharides and proteins where the ratio of polysaccharide to protein in BAP ranged from 2.5 to 4.1 while it ranged from 0.7 to 1.3 in UAP (Jiang et al., 2010; Tian et al., 2011). The concentrations of UAP and BAP (C_{UAP} and C_{BAP}) and the contributions of proteins and polysaccharides to these concentrations were estimated by solving mass balances on polysaccharides and proteins and assuming average values from the literature for the polysaccharide/protein ratios of UAP and BAP. A sensitivity analysis on the impact of the values of the polysaccharide/protein ratios on the estimated UAP and BAP concentrations was conducted and it was found that the conclusions were not substantially impacted for ratio's spanning the range of values reported in the literature.

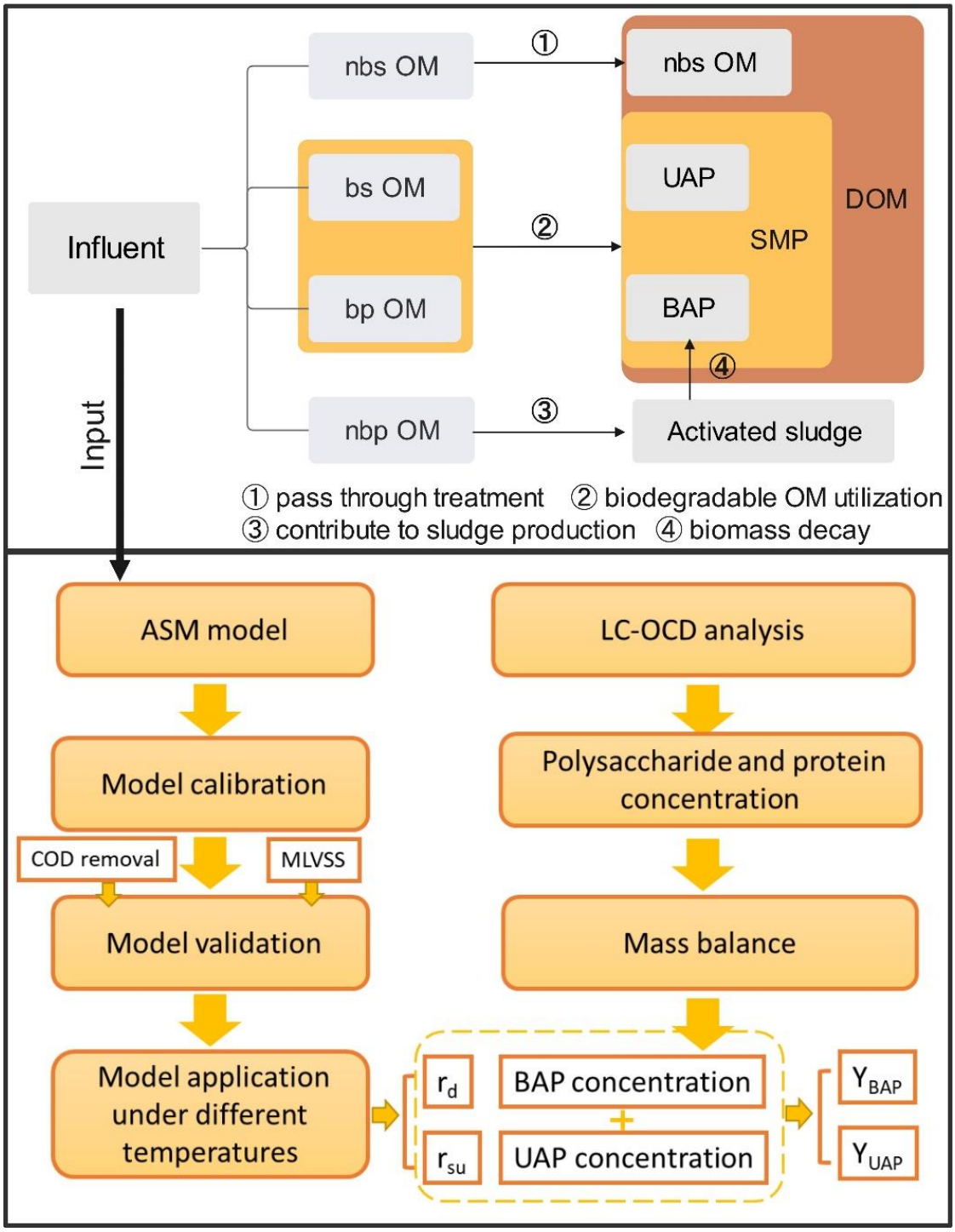

Figure 3-3. Conceptual model describing the generation of SMP and the estimation of UAP/BAP yields.

As will be subsequently described, an activated sludge process model was developed to quantify the rates of substrate utilization and endogenous decay processes that were active in the SBRs (Figure 3-3). As present, the application of the process model required a detailed fractionation of the organic matter in the raw wastewater into biodegradable, non-biodegradable soluble, and non-biodegradable particulate components. Chemical oxygen demand (COD) was employed as the basis for this fractionation (Melcer et al., 2003) and the protocols described in Melcer et al. (2003) were employed to conduct the fractionation. The detailed fractionation methodology and the outcomes of this analysis are presented in the Supplementary Materials (Table A1-A4).

In the conceptual SMP model, UAP and BAP generation are assumed to be proportional to the substrate utilization and endogenous decay respectively. Hence, a steady state analytical process model of the activated sludge process was developed as per Metcalf and Eddy (2013) and a summary of the process model equations is provided in the Supplementary Materials. The activated sludge process model was implemented using typical values for biokinetic parameters (Metcalf and Eddy, 2013) with rate constants corrected for temperature using the Arrhenius relationship. The calculated COD fractions developed from the detailed wastewater fractionation were employed as inputs to the activated sludge process model.

Upon completion of the activated sludge process model simulations, the model predicted values for active biomass and effluent biodegradable COD (S) concentrations were employed to estimate the rates of substrate utilization and endogenous decay as per equations 3-1 and 3-2, respectively.

$$r_{su} = kX_{VSS,bio}S/(K_s + S) \qquad \textbf{Equation 3-1}$$

Where: r_{su} is the rate of substrate utilization ($mgL^{-1}d^{-1}$),

k is the maximum specific substrate utilization rate (d^{-1}),

K_s is half-velocity constant (mg bCOD/L),

$X_{VSS,bio}$ is viable biomass concentration in SBR (mg COD/L),

S is effluent biodegradable soluble COD (mg bCOD/L).

$$r_d = k_d X_{VSS,bio} \qquad \textbf{Equation 3-2}$$

Where: r_d is the rate of biomass decay ($mgL^{-1}d^{-1}$),

k_d is specific endogenous decay coefficient (d^{-1}).

The results of the activated sludge process modelling and the UAP/BAP fractionation were integrated by calculating yield coefficients for BAP and UAP as per equations 3-3 and 3-4 respectively. The ratios were based upon the rates of generation observed in the SBR effluents and the rates of generation by the associated bioprocess.

$$Y_{BAP} = \frac{QC_{BAP}}{Vr_d}$$ **Equation 3-3**

Where: Y_{BAP} is the yield coefficient for BAP (mg BAP/mg COD),

Q is the flow rate (L/d),

C_{BAP} is the concentration of BAP (mg/L),

V is the volume of SBR (L).

$$Y_{UAP} = \frac{QC_{UAP}}{Vr_{su}}$$ **Equation 3-4**

Where: Y_{UAP} is the yield coefficient for UAP (mg UAP/mg COD),

C_{UAP} is the concentration of UAP (mg/L).

3.3.4 Application of SMP production models

The validity of the wastewater fractionation and the analytical modelling exercises was initially assessed by comparing the observed and modelled MLVSS concentrations in the SBRs as an overall indication of the growth and solids accumulation processes (Figure 3-4). As illustrated a close correspondence between the observed and modelled values were observed over the range of operating temperatures. Hence, it was concluded that the modelling exercise was able to adequately simulate the growth and decay processes that were occurring in the SBRs.

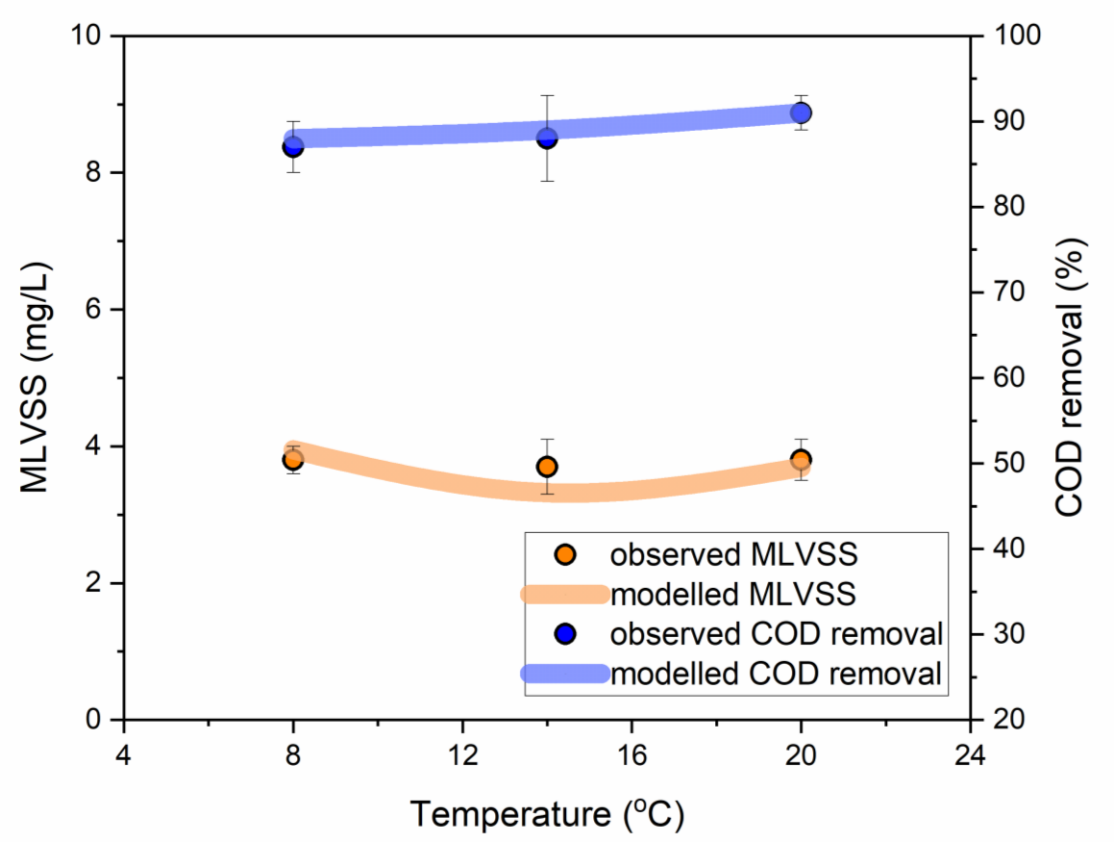

Figure 3-4. Observed and modeled MLVSS concentration and COD removal (mean ± standard deviation, N = 8).

The proposed approach was further validated by comparing the observed and modelled COD removal as a second indicator of the fit of the model to the data. The modelled effluent COD was determined as the sum of non-biodegradable soluble COD in the effluent and modelled residual biodegradable COD in the effluent with non-biodegradable particulate COD contributing to sludge production. It can be observed from Figure 3-4 that the difference between observed and modelled COD removals was less than 2% over the range of operating temperatures. Hence, model and experimental data agree well suggesting the validity of this approach for effluent quality determination under different temperatures.

The viable biomass concentrations and the rates of biomass growth and endogenous decay were extracted from the activated sludge process model to obtain insight into how temperature impacted growth and decay processes (Figure 3-5). From Figure 3-5 it can be observed that a decrease in

temperature from 20 ℃ to 14 ℃ led to a 39% increase in the viable biomass concentration and an additional 21% increase was observed when the temperature decreased from 14 ℃ to 8 ℃. The increase in viable biomass at lower temperatures was attributed to the differential impacts of temperature on growth versus endogenous decay. At the extended SRT employed in the SBR, growth was primarily limited by substrate availability and hence the reduced temperatures caused only a modest reduction in the rate of growth. In contrast the rate of endogenous decay was more sensitive to temperature and the substantial reduction in this rate at lower temperatures led to a net increase in the biomass production. The bioprocess conditions that were established by the modelling established the rates of substrate use and endogenous decay that were subsequently employed to estimate the UAP and BAP yields.

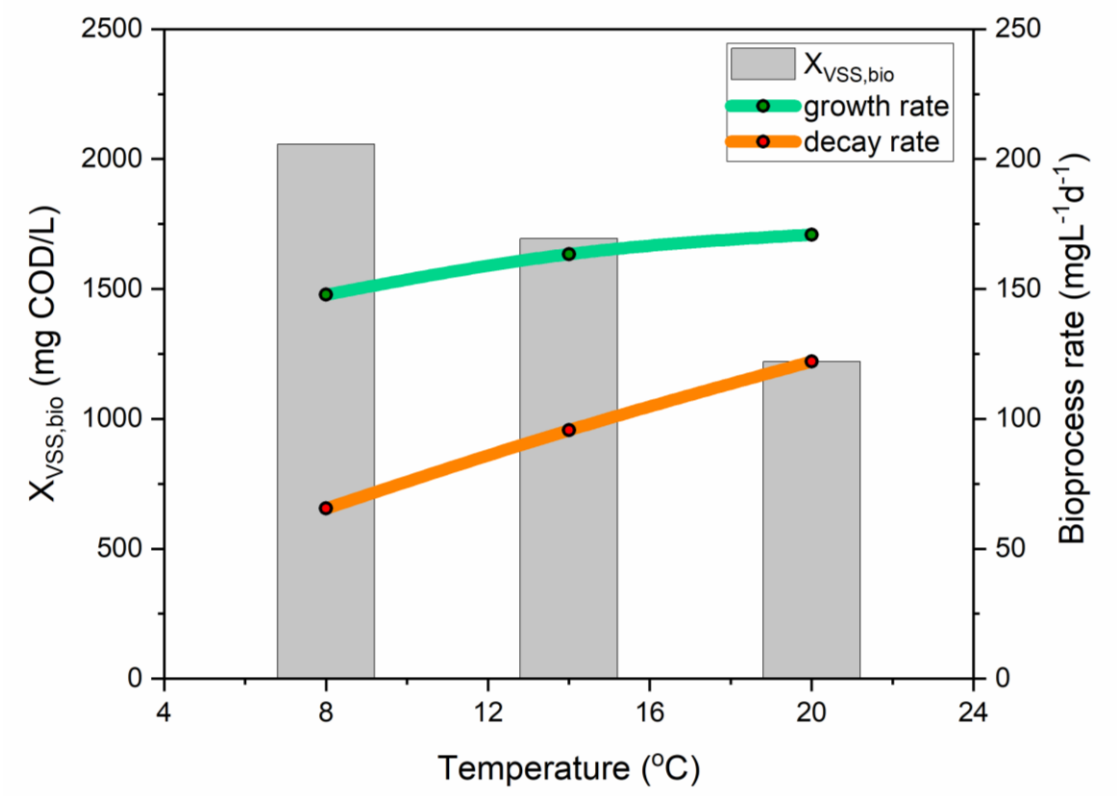

Figure 3-5. Estimated biomass concentration and bioprocess rates.

The concentrations of UAP and BAP and their protein and polysaccharide components that were estimated from the LC-OCD data are presented as a function of operating temperature in Figure 3-6A. The relative contributions of protein and polysaccharide in the two SMP fractions reflected the ratios that were assumed from the literature and it can be observed that the UAP had relatively similar contributions of the two fractions while the BAP composition was dominated by polysaccharides. From Figure 3-6A it can be observed that the concentrations of UAP were consistently higher than the BAP concentrations and both species increased substantially in concentration as temperature decreased. Further, the concentrations of BAP were considerably more temperature dependent when compared to the UAP concentrations.

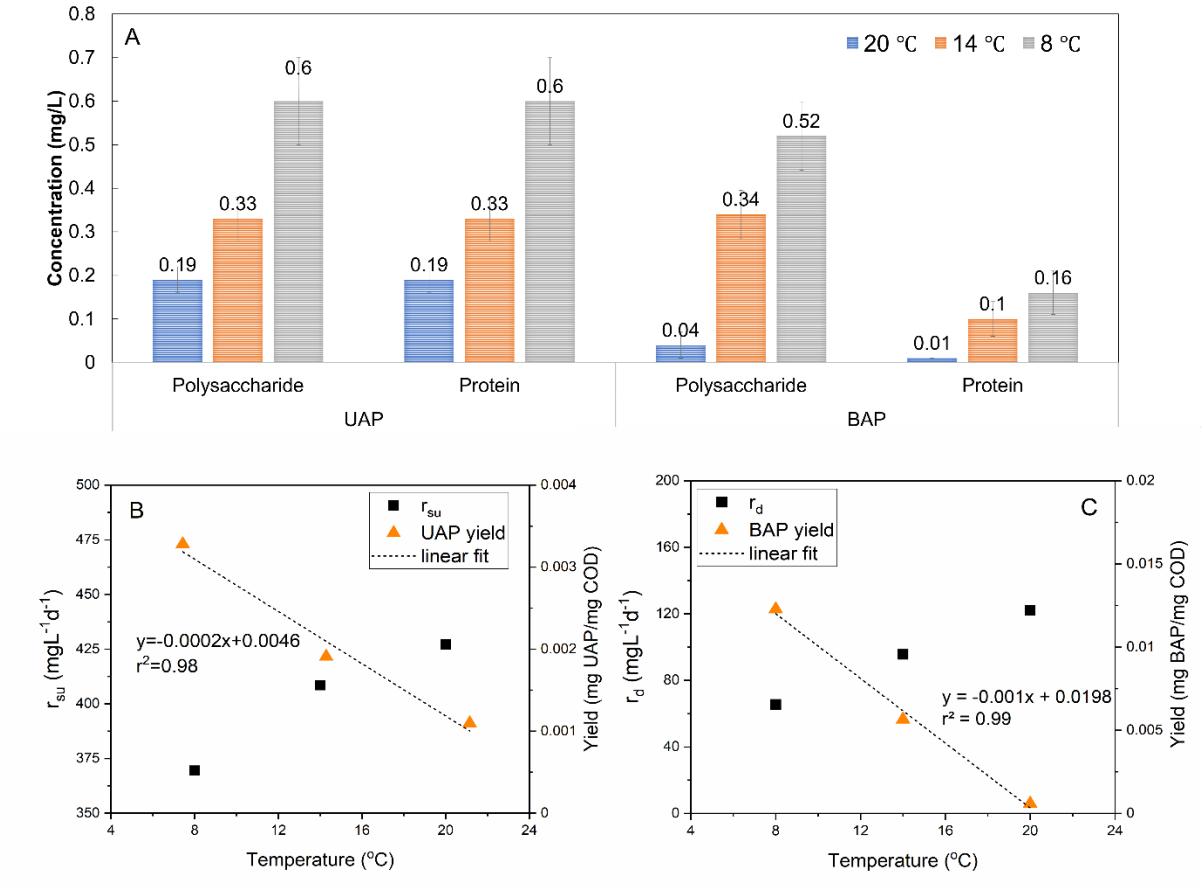

Figure 3-6. (A) Estimated UAP and BAP concentrations (mean ± standard deviation), (B) UAP yield coefficients and substrate utilization rate versus operating temperature, and (C) BAP yield coefficients and biomass decay rate versus operating temperature.

Aquino & Stuckey (2008) demonstrated that UAP and BAP production are proportional to substrate utilization and endogenous decay respectively. Hence, yield coefficients were calculated as the ratio of the observed production of these species to their associated bioprocesses as described in Equations (3-3) and (3-4). Figure 3-6 B and C present the calculated yield coefficients and the bioprocess rates versus operating temperature. It can be observed that both the rate of substrate utilization and the rate of endogenous decay increased with temperature. By contrast both Y_{UAP} and Y_{BAP} values declined substantially as temperature increased. The results clearly indicate that the biomass generated more of the SMP products per unit of biomass activity as temperature declined suggesting a shift of the underlying metabolic processes as temperature decreased.

Linear regression was employed to quantify the dependence of the Yield coefficients on temperature (Figure 3-6 B and C). It can be observed that the r^2 values were quite high and there was only a modest deviation of the data points from the regression line indicating that the linear relationship could adequately fit the data. The slopes of the regressions were 0.0002 and 0.001 mg/(mg·°C) for the UAP and BAP yields, respectively. Hence, the results suggest that the generation of BAP was more temperature sensitive than UAP.

The UAP yields in present study estimated ranged from 0.001-0.003 mg UAP/mg COD. Jiang et al. (2008) reported UAP yields of 0.09 mg COD/mg COD using activated sludge model No. 2d-SMP when acetate was employed as a carbon source at 15 °C. To facilitate a comparison of the values obtained in the present study with that of Jiang et al. (2008), conversion factors of 1.5 and 1.07 g COD/g substrate were used to convert polysaccharide and protein concentration to their COD equivalents (Jiang et al., 2008). On this basis the UAP yields ranged between 0.001-0.006 mg COD/mg COD in the present study and hence were considerably lower than that of Jiang et al. (2008). UAP production is known to be substrate specific and hence, the difference in values was likely due to the different substrate properties employed in the two studies. In addition, UAP production has been reported to depend upon the Food/Microorganism (F/M) ratio with higher F/M leading to increased UAP production (Ferrer-Polonio et al., 2018). The F/M ratio of 0.07 g bCOD/VSS·d employed in this study was somewhat lower than the value of 0.097 g bCOD/VSS·d reported by Jiang et al. (2008) and may also have contributed to the different yields.

The BAP yields in the present study were compared with that reported by Jiang et al. (2008) (0.0215 mg COD/mg COD) which was obtained at 15 °C. After conversion to a COD basis using a similar approach to that employed for UAP, the BAP yields in the current study range between 0.001-

0.02 mg COD/mg COD. Hence, the values estimated in the current study were similar to that of Jiang et al. (2008). The similarity in BAP yields between the two studies suggests that the products of biomass decay were similar and hence the approach employed in the current study could be generalized to estimate BAP production in other applications.

The observed temperature impacts in the current study were consistent with those of Wang & Zhang (2010) that demonstrated both low and high extremes in temperature impacted the production of UAP and BAP. It was suggested that the observed generation of UAP in bioreactor reflects the net of UAP production and consumption within the reactor (Jiang et al., 2008). The greater UAP yields observed at lower temperatures suggest that the rates of consumption in the reactor are slowed to a greater extent than the production process as temperature is reduced.

The generation of BAP has been attributed to both decay of bacterial cells and hydrolysis of bound EPS (Menniti & Morgenroth, 2010). In the present study the contributions of the two pathways to BAP production could not be distinguished. However, Watanabe et al. (2017) observed increased EPS hydrolysis products at 10 ℃ than 25 ℃ suggesting that this pathway may be more significant at low temperature. This trend was consistent with the higher yields observed in the current study.

The results of the present study provide valuable insights into the impact of temperature on the generation of soluble microbial products in activated sludge processes that are known to be important membrane foulants. A significant contribution of the study is the development of SMP yields in real municipal wastewater treatment as a function of temperature. It is apparent that changes in microbial metabolic processes at low temperatures result in increases in SMP generation. Further, the methodology employed to link conventional wastewater process treatment modelling to SMP generation can be employed to assess the impact of activated sludge design and operating conditions on foulant generation. Such process modelling can be employed to assist with the optimization of the design and operation of membrane processes when treating wastewaters under challenging conditions like low temperature.

3.4 Conclusions

The present study characterized SMP generation during the treatment of real municipal wastewater and fills a knowledge gap since previous studies of SMP generation were conducted with synthetic wastewater. This was achieved by linking process engineering analysis to direct measurements of SMP production. Further, the impact of low operating temperatures on SMP production which has

received relatively little attention was studied in detail. The use of LC-OCD analysis revealed that temperature significantly affected the SMP composition with much higher concentrations of polysaccharides and proteins as temperature decreased. Low temperatures led to greater UAP and BAP concentrations and yields with a greater impact on BAP values. The estimated yield coefficients can be employed to estimate the impact of wastewater quality and process operating conditions on the generation of membrane foulants.

Chapter 4

Assessing the role of cold temperatures on irreversible membrane permeability of tertiary ultrafiltration treating municipal wastewater

GRAPHICAL ABSTRACT

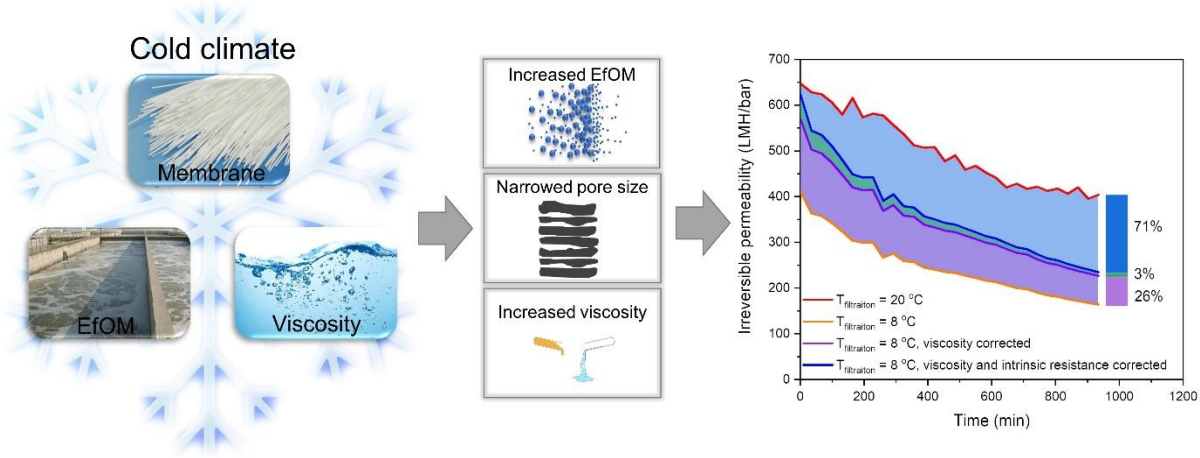

4.1 Introduction

Ultrafiltration (UF) is gaining increasing acceptance for tertiary treatment of wastewaters as it is able to effectively and efficiently produce high quality treated water (Qu et al., 2021). However, membrane fouling, especially hydraulically irreversible fouling, has impeded widespread adoption of this technology for tertiary filtration with effluent organic matter being major foulants (Alresheedi & Basu, 2019). The loss in permeability resulting from hydraulically irreversible fouling increases energy consumption even when reversible fouling is managed (Zhan et al., 2020). The control of hydraulically irreversible fouling remains a key concern for tertiary membrane operations.

Cold water temperatures (≤20 °C), typical of Northern regions (Canada, Russia, Northern Europe and Northern China), can result in greater costs for membrane maintenance and replacement (Ozgun et al., 2015). Previous studies of membrane bioreactors (MBRs) for secondary treatment of

wastewaters have examined hydraulically irreversible fouling behavior in response to operating temperature (Krzeminski et al., 2012). Low temperature operation has been reported to impact the nature of dissolved organic matter leading to severe hydraulically irreversible fouling in MBRs (Ma et al., 2013; Zhao et al., 2015). In addition, the particle size distribution in MBRs was observed to shift from larger particles (average particle size 190 nm) towards smaller particles (average particle size 130 nm) at low temperatures and this led to rapid pore narrowing or blocking (van den Brink et al., 2011).

Less information on low temperature hydraulically irreversible fouling of tertiary membranes is available. (Abu-Obaid et al., 2020) reported increased irreversible fouling of tertiary membranes at full-scale during periods of low temperatures and elevated flows, but the underlying mechanisms of the elevated irreversible fouling were not investigated. Further, the impact of elevated wastewater flows during cold temperature periods could not be separated from that of low temperature itself. Therefore, while MBR-focused research has suggested adverse effects of low temperature on hydraulically irreversible fouling, the factors influencing this response, and the magnitude of the fouling in tertiary applications, have not been directly assessed.

Reductions in tertiary membrane permeability at low temperatures may be attributed to increased concentrations of foulants in secondary treatment effluents. However, low temperature will also reduce membrane permeability by directly impacting viscosity (Chu et al., 2016) and intrinsic membrane resistance by causing a shrinkage in pore sizes (Cui et al., 2017). Further, it is hypothesized that an interaction between changes in membrane properties and foulant properties may exist. In this regard changes in pore size with temperature may modify the nature of the interactions with foulants that lead to hydraulically irreversible fouling. There is limited knowledge on the extent to which temperature influences the relative contribution of these factors to hydraulically irreversible fouling in tertiary applications.

The development of a detailed understanding of the factors leading to reduced permeabilities at low temperatures will be of interest to designers and operators of these systems. In this regard it will facilitate an assessment of the extent to which fouling mitigation measures can enhance permeabilities. Changes in viscosity and intrinsic membrane resistance with temperature are not controllable and need to be factored into membrane sizing. The development of increased hydraulically irreversible fouling at low temperatures might be reduced by pretreatments (Chen et al., 2020; He et al., 2021) or through membrane cleaning practices (Rabuni et al., 2015; Yu et al., 2017).

The objective of the present study was to identify and quantify the contributors to hydraulically irreversible fouling of tertiary membranes at cold temperatures. A comprehensive test plan that allowed for separate assessment of the impacts of temperature on the secondary and tertiary systems was developed. Bench scale SBRs provided secondary treatment of real municipal wastewater over a range of temperatures to generate feed water for filtration tests. Filtration tests were then conducted at bench scale over a range of temperatures to investigate how temperature-dependent secondary effluent characteristics, water rheological properties, and membrane properties affect the development of hydraulically irreversible fouling. Combined fouling models, fitted to the data, were used to facilitate comparisons between operating conditions and to gain insights into mechanisms leading to hydraulically irreversible fouling. The methodology and outcomes of the present study provide insights that can be employed to assist in the design and operation of tertiary membrane systems.

4.2 Experimental Methods

4.2.1 Apparatus

(a) SBR: Bench scale SBRs were operated for extended periods (ranging from October 2018 to March 2020) of time at one of the three temperatures (8, 14 and 20 °C). The temperatures were selected to be representative of summer and winter operating conditions in Ontario, Canada. Briefly, the SBRs were fed with real municipal wastewater collected from the City of Waterloo sewer system and sieved with a 2 mm mesh to remove large particles. The hydraulic retention time (HRT) of the SBRs was 20 h, and the solids retention time (SRT) was maintained at 25 days. A detailed description of the design and operation of the SBRs has been provided by Tao et al. (2021).

(b) Filtration system: The SBR effluents were employed as feed water for the filtration tests. The filtration tests were conducted using bench scale membrane modules immersed in a filtration tank with a volume of 2 L. In the present study, three ZeeWeed-1000 hollow-fibres were used in the bench scale membrane tests. The nominal pore size of the membrane was 0.02 μm. The length of each hollow-fibre was 500 mm and the total membrane surface area of each module was 4,475 mm2. A programmable peristaltic pump (OF-07582-00, Cole-Parmer, USA) was used to control the timing of permeation and back pulsing as described in Section 2.2. The permeate was continuously returned to the filtration tank to maintain a consistent water level and feed composition. An air diffuser (coupled with an air flow meter), located at the bottom of tank, provided aeration for mixing and membrane scouring. The aeration flow was set to 0.75 L/min as optimized by Akhondi et al. (2014). A water

jacket was used to control the water temperature in the filtration tank. During filtration tests the transmembrane pressure (TMP) was measured every 30 s using a pressure transducer (PX209, Omega, Canada) that was coupled to a data acquisition module (37 NI USB-6001, National Instruments Corporation, USA).

4.2.2 Filtration tests

Filtration tests were conducted with either clean water or the effluents from the SBRs (Figure 4-1). Tests with clean water were conducted with virgin membranes to establish the intrinsic membrane resistance as a function of temperature. Filtration tests of the SBR effluents were conducted at room temperature (~20 ℃) and at the corresponding temperature of the source SBR. For example, filtration tests with the effluent from the SBR operated at 8 ℃ were conducted at 20 ℃ and 8 ℃, respectively. This enabled the impact of temperature on the characteristics of the SBR effluent, the rheological properties of the water, and membrane properties to be considered independently.

Each filtration test was operated in dead-end mode and consisted of 30 permeation cycles that included filtration for 30 min and a combination of back pulsing and air scouring for 120 s. Back pulsing and air scouring were employed to remove hydraulically reversible fouling from the membrane surface and/or in the pores of the membrane. The filtration and back pulsing fluxes were 24 and 48 LMH, respectively. All filtration tests were conducted in triplicate. After each test, the fouled membranes were chemically cleaned using a 250 mg/L NaOCl solution for 2 h and then rinsed by soaking in DI water for 2 h.

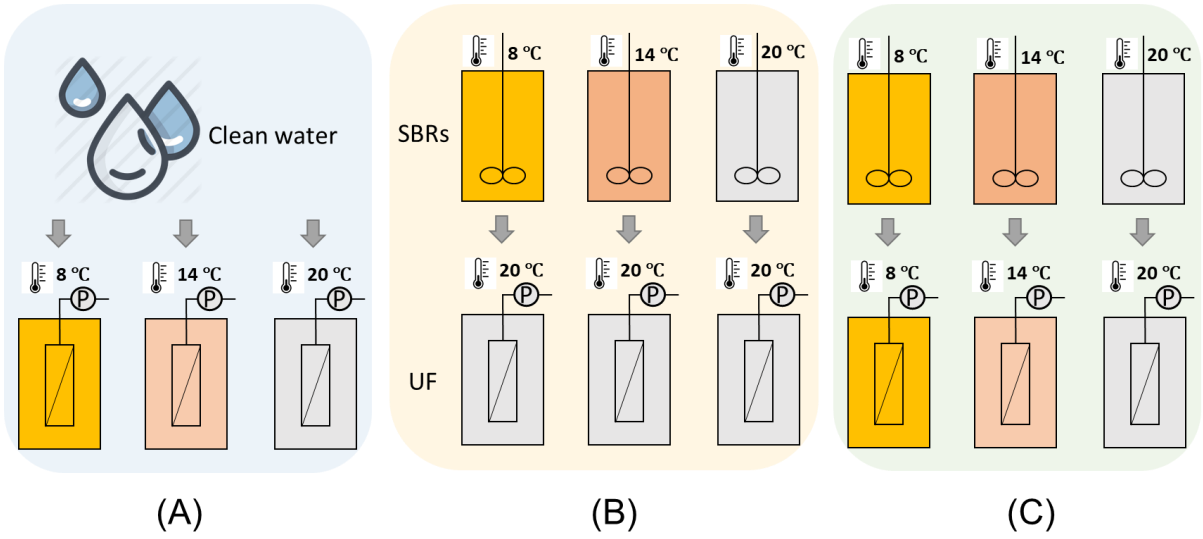

Figure 4-1. Schematic diagram of experimental plan for (A) filtration tests with clean water, (B) filtration tests at 20 ℃ and (C) filtration tests at source SBR operating temperature.

4.2.3 Membrane performance indices

The present study focused on the hydraulically irreversible permeability that was observed at the beginning of each permeation cycle after back pulsing and air scouring had been completed.

The observed permeability (K) was calculated using Equation 4-1 (Sharma et al., 2003), and the values incorporated the influence of temperature on viscosity and intrinsic membrane resistance.

$$\boldsymbol{K = \frac{J}{TMP}} \qquad \textbf{Equation 4-1}$$

where J is measured flux (LMH) and TMP is measured transmembrane pressure (bar).

To assess the effects of viscosity, the K values that were observed in filtration tests conducted at temperatures other than 20 ℃ were corrected for viscosity to 20 ℃ (K_{20}) as presented in Equation 4-2 (Robles et al., 2013).

$$\boldsymbol{K_{20} = \frac{\mu_T}{\mu_{20}} \times K} \qquad \textbf{Equation 4-2}$$

where μ_T is viscosity of water at temperature T (Pa·s), μ_{20} is viscosity of water at 20 ℃ (Pa·s) and viscosity values were calculated using Equation 4-3 (van den Brink et al., 2011).

$$\mu_T = 0.497\,(T + 42.5)^{-1.5}$$ **Equation 4-3**

To assess the effect of temperature on intrinsic membrane resistance, K_{20} values were corrected for the intrinsic membrane resistance at the filtration temperature ($K_{m\text{-}20}$). This was achieved by replacing the intrinsic resistance at the filtration temperature with that observed at 20 ℃ (Equation 4-4).

$$\frac{1}{K_{m-20}} = \mu_{20} \times (R_t - R_m^T + R_m^{20}) = \frac{1}{K_{20}} - \mu_{20} \times \Delta R_m$$ **Equation 4-4**

where R_t is total resistance at the filtration temperature and $\triangle R_m$ is calculated with data gathered from clean water tests as outlined in Equation 4-5.

$$\Delta R_m = R_m^T - R_m^{20}$$ **Equation 4-5**

where R_m^T and R_m^{20} are the intrinsic membrane resistances at temperature T and 20 ℃ (m^{-1}), respectively.

The hydraulically irreversible fouling rate (F_{irr}) was calculated from the initial permeability of each filtration cycle as presented in Equation 4-6. The linear relationship between the initial permeability values and filtration time was verified by linear fit models with $P < 0.05$.

$$F_{irr} = \frac{K_{n+1} - K_n}{\Delta T}$$ **Equation 4-6**

where K_{n+1} and K_n are initial permeabilities in the $(n+1)^{th}$ and nth cycle, $\triangle T$ is the cycle duration.

4.2.4 Modelling analysis

Combined fouling models established by Bolton et al. (2006) were fitted to observed irreversible TMP data to gain insight into the mechanism governing hydraulically irreversible permeability. The combined fouling models include cake-complete, cake-intermediate, complete-standard, intermediate-standard and cake-standard models with K_c, K_b, K_i and K_s as fitted parameters to quantify cake fouling, complete blocking, intermediate blocking and standard blocking, respectively (Table 4-1). The observed irreversible TMP data consisted of initial TMP in each cycle during the whole filtration test. The best fit was determined by minimizing the sum of squared residuals (SSR) where the residual was equal to the difference between measured data and model prediction.

Table 4-1. Summary of the five constant flow combined fouling models (Bolton et al. 2006).

Model	Equation	Fitted parameters
Cake-complete	$\frac{P}{P_0} = \frac{1}{(1-K_b t)}(1 - \frac{K_c J_0^2}{K_b}\ln(1-K_b t)$	K_c (s/m^2), K_b (s^{-1})
Cake-intermediate	$\frac{P}{P_0} = \exp(K_i J_0 t)(1 + \frac{K_c J_0}{K_i}(\exp(K_i J_0 t) - 1))$	K_c (s/m^2), K_i (m^{-1})
Complete-standard	$\frac{P}{P_0} = \frac{1}{(1-K_b t)(1 + \frac{K_s J_0}{2K_b}\ln(1-K_b t)^2}$	K_b (s^{-1}), K_s (m^{-1})
Intermediate-standard	$\frac{P}{P_0} = \frac{\exp(K_i J_0 t)}{(1 - \frac{K_s}{2K_i}(\exp(K_i J_0 t) - 1)^2}$	K_i (m^{-1}), K_s (m^{-1})
Cake-standard	$\frac{P}{P_0} = \left(1 - \frac{K_s J_0 t}{2}\right)^{-2} + K_c J_0^2 t$	K_c (s/m^2), K_s (m^{-1})

4.2.5 Liquid chromatography–organic carbon detection (LC-OCD) analysis

LC-OCD analysis was used to provide insights into potential foulants in the SBR effluents. The samples were filtered with 0.45 μm nylon filters before analysis. The LC-OCD system was equipped with an HPLC pump (S-100, Knauer, Germany) that was operated at a flow rate of 1.1 mL/min to an autosampler and a chromatographic cation exchange column . The LC-OCD employed three detectors including fixed wavelength UV (UVD), organic carbon (OCD) and organic nitrogen (OND) detection in series. The UVD measured the spectral absorption coefficient at 254 nm. The OCD oxidized organic matter in a UV reactor and the organic carbon was quantified from the produced CO_2. The OND oxidized organic nitrogen and measured the produced nitrate using a UVD operated at 220 nm. Based upon the multiple signals, the LC-OCD analysis reports dissolved organic matter as biopolymers, humic-like substances, building blocks, low molecular weight (LMW) acids and LMW neutrals (Huber et al., 2011).

4.2.6 Data Analysis

When fitting models to data, OriginPro 2020 software was used. One-way ANOVA tests were used to determine if there was a significant difference between parameters. Values were considered statistically different at a 95% confidence interval ($P < 0.05$). Linear regression analysis was used to assess the relationship between hydraulically irreversible fouling rate and water quality characteristics.

4.3 Results

The present study sought to comprehensively investigate the impact of temperature on the hydraulically irreversible permeability in tertiary membrane systems. The analysis involved characterization of SBR effluents and permeability reductions calculated from observed filtration data and considered the influence of temperature-dependent changes in viscosity and intrinsic membrane resistance. Combined fouling models were then used to facilitate comparisons between operating conditions and to gain insights into mechanisms leading to hydraulically irreversible fouling.

4.3.1 Hydraulically irreversible permeability evolution

The effects of SBR operating temperature on hydraulically irreversible permeability was initially assessed by conducting all filtration tests at 20 ℃. With this experimental design, differences in hydraulically irreversible permeability associated with the different SBR operating temperatures could be quantified. Examples of the observed permeability profiles that developed during filtration tests, which were typical of the triplicate tests that were conducted, are illustrated in Figure 4-2 (A1-A3). In the subsequent analysis of this data it was assumed that the back pulsing and air scouring between cycles removed all the fractions responsible for the hydraulically reversible fouling (Peiris et al., 2013). Thus, the development of hydraulically irreversible fouling was estimated from the permeability measurements obtained immediately after back pulsing and air scouring. The hydraulically irreversible permeability is highlighted in the permeability decline responses.

The permeabilities observed at the beginning of the filtration tests conducted at 20 ℃ were compared to verify that the filtration of effluents from the SBRs operated at different temperatures had similar initial conditions. As illustrated in Figure 4-2 (A1-A3), the initial permeability in the first cycle was approximately 650 ± 10 LMH/bar for all SBR effluents indicating that the initial membrane permeabilities were similar. Hence, subsequent declines in permeability were attributed to SBR effluent properties and not initial membrane conditions.

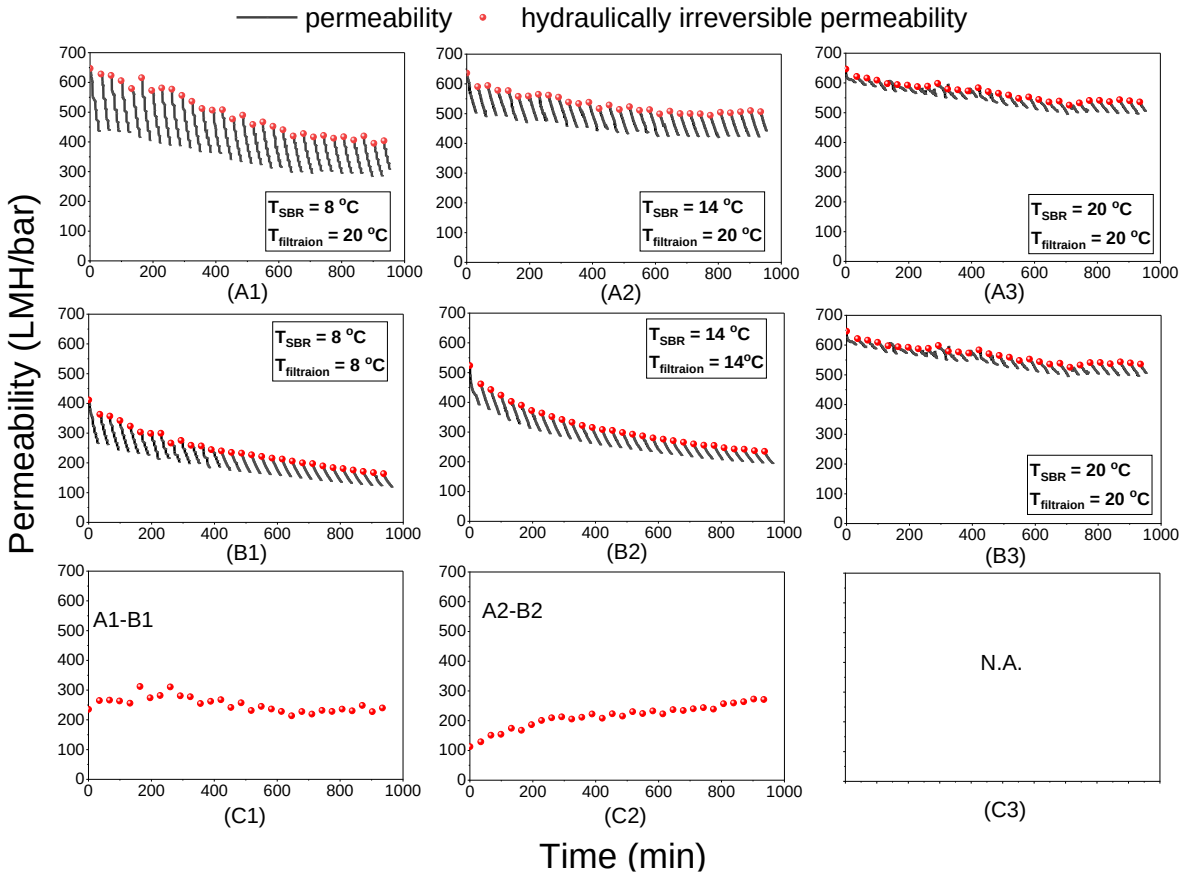

Figure 4-2. Typical permeability profiles during ultrafiltration when (A) filtered at 20 ℃; (B) filtered at SBR operating temperature; and (C) the difference in hydraulically irreversible permeability for each SBR effluents filtered at 20 ℃ and corresponding SBR operating temperature; N.A, no difference for the effluent from SBR operated at 20 ℃.

The decreases in hydraulically irreversible permeability with time during filtration tests conducted at 20 ℃ were compared to assess the impact of the effluents from SBRs operated at different temperatures. From Figure 4-2 (A1-A3) it can be observed that the development of irreversible permeability was similar for the three SBR operating temperatures for the first 10 cycles. However, after 10 cycles, the trends in irreversible permeability were distinct for the SBRs operated at different temperatures. After 30 cycles, the irreversible permeability values decreased to 536, 506 and 403 LMH/bar for the effluents from the SBRs operated at 20, 14 and 8 ℃, respectively. Overall, the irreversible permeability decreased by 17, 22 and 38% during the filtration tests as SBR operating temperature decreased from 20 to 14, and 8 ℃, respectively. The reduction of irreversible

permeability increased as SBR operating temperature decreased, suggesting a change in EfOM concentration and/or fraction in SBR effluents.

The filtration tests at 20 ℃ revealed that SBR effluent properties led to a decreased propensity for irreversible permeability at low SBR operating temperatures; however, they did not provide insight into the extent of permeability that could be expected when filtration tests are conducted at the SBR temperature. Therefore, additional filtration tests were conducted where the effluents from SBRs operated at 8 ℃ and 14 ℃ were filtered at the corresponding SBR temperatures (Figure 4-2 (B1-B2)). Unlike the similar initial permeability that were observed in the filtration tests conducted at 20 ℃ (Figure 4-2 (A1-A3)), the initial permeability values were distinct at the different filtration temperatures (650 ± 10, 523 ± 17 and 411 ± 11 LMH/bar at filtration temperature of 20, 14 and 8 ℃, respectively). The different initial permeability values at different filtration temperatures were expected and attributed to changes in the membrane intrinsic resistance and water viscosity with temperature.

Intrinsic membrane resistance values were estimated from the filtration tests conducted with clean water at 8, 14 and 20 ℃. The average intrinsic membrane resistance was observed to increase by 5% and 14% as filtration temperature decreased from 20 to 14 and 8 ℃, respectively. The measured intrinsic resistances were subsequently employed to correct the irreversible permeabilities from filtration tests using the effluent from the SBRs operated at different temperatures.

The impact of filtration temperature on observed irreversible permeability decline was initially assessed by calculating the difference in permeabilities between the filtration tests conducted at 20 ℃ and filtration tests conducted at the corresponding SBR operating temperatures (Figure 4-2 (C1-C2)). From Figure 4-2 (C1-C2) it can be observed that the differences in irreversible permeability for the filtration tests at 8 ℃ were approximately 250 LMH/bar, and greater than those of the filtration tests at 14 ℃. Moreover, the differences in irreversible permeability for the filtration tests at 8 ℃ were more constant over the cycles implying a consistent decline with time at both filtration temperatures. However, the differences in irreversible permeability for the filtration tests at 14 ℃ increased with time suggesting a diverging trend in declines.

The observed differences in irreversible permeabilities when filtration tests were conducted at 20 ℃ and filtration tests conducted at the corresponding SBR operating temperatures (Figure 4-2 (C1-C2)) indicated a clear impact of filtration temperature on irreversible permeability development. The results from clean water filtration tests demonstrated that this was partially due to changes in viscosity

and intrinsic membrane resistance. To quantify the contribution of viscosity and intrinsic membrane resistance, the observed irreversible permeabilities from the filtration tests conducted at 8 ℃ and 14 ℃ were adjusted to 20 ℃. The adjusted irreversible permeabilities are presented in Figure 4-3. Also presented in Figure 4-3 are the observed irreversible permeabilities at 20 ℃. The difference between the temperature adjusted irreversible permeabilities and the observed irreversible permeabilities at 20 ℃ corresponded to the irreversible fouling that could not be explained simply by changes in viscosity and intrinsic membrane resistance with filtration temperature.

The contributions of viscosity and intrinsic membrane resistance to the differences between the temperature corrected irreversible permeabilities and those observed at 20 ℃ are of practical interest as they cannot be controlled through fouling mitigation practices. From Figure 4-3 it can be observed that at the end of the filtration test, the viscosity and increased intrinsic membrane resistance contributed to 20% of the difference in permeabilities between filtration tests conducted at 20 ℃ and 14 ℃ while at 8 ℃ the contribution increased to 29%. The results demonstrate that the effects of filtration temperature on viscosity and intrinsic membrane resistance on permeability decline cannot be neglected. The influence of viscosity and intrinsic membrane resistance were observed to be substantial and characterize the upper boundary to which fouling mitigation strategies can reduce irreversible permeability declines at low filtration temperatures.

The results also demonstrate that low filtration temperatures changed the interaction between the membrane and foulants leading to increased development of irreversible fouling. From Figure 4-3 it can be observed that there was a substantial difference between viscosity and intrinsic membrane resistance adjusted irreversible permeabilities and the irreversible permeabilities observed at 20 ℃ for both effluents from the SBRs operated at 8 ℃ and 14 ℃. As illustrated, the difference between the irreversible permeability at 20 ℃ and that at 14 ℃, adjusted to 20℃, progressively increased. At the end of the filtration test, the difference between the irreversible permeability at 20 ℃ and that at 14 ℃, adjusted to 20℃, accounted for 80% of the total difference. The difference between the irreversible permeability at 20 ℃ and that at 8 ℃, adjusted to 20℃, rapidly increased over the first few hundred minutes of operation, but then remained relatively constant. At the end of the filtration test, the difference between the irreversible permeability at 20 ℃ and that at 8 ℃, adjusted to 20 ℃, accounted for 71% of the total difference. At lower filtration temperatures, the pores of membranes are expected to be smaller and therefore more foulants are likely to be retained (Cui et al., 2017). The

foulants retained by the membranes under different filtration temperatures and fouling mechanisms are further discussed.

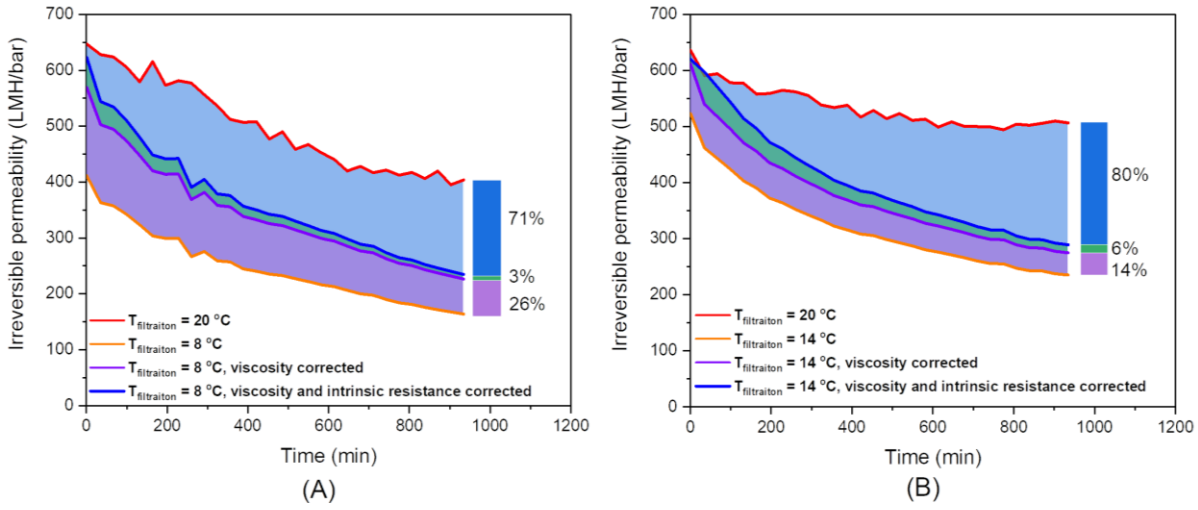

Figure 4-3. Observed and corrected hydraulically irreversible permeability for the effluents from SBRs operated at (A) 8 ℃ and (B) 14 ℃.

4.3.2 Foulant identification and quantification

The operating temperature of the SBRs was observed to result in distinct trends in the hydraulically irreversible permeability indicating that the foulants present in the effluents were affected by temperature. The concentrations of the DOC fractions reported by LC-OCD analysis in the SBR effluents and UF permeates were examined to obtain insights into the foulants.

Concentrations of different DOC fractions in the SBR effluents are presented in Figure 4-4A. The concentrations of high MW organics (polysaccharides and proteins) in the SBR effluents increased as SBR operating temperature decreased. The average concentrations of polysaccharides in the effluents from the SBR operated at 8 ℃ were 62% and 402% higher than those in the effluents from the SBRs operated at 14 ℃ and 20 ℃, respectively. Similarly, proteins in the effluents from the SBR operated at 8 ℃ were 13% and 170% higher than those operated at 14 ℃ and 20 ℃, respectively. The increase in polysaccharides was more impacted by temperature than that of proteins, which is consistent with previous research on MBRs for secondary treatment of wastewater (Ma et al., 2013; van den Brink et

al., 2011). The great influence on polysaccharide and protein concentrations may have been because they were highly associated with UAP/BAP generation which was substantially affected by low SBR operating temperatures (Tao et al., 2021). The concentrations of low MW organics (building blocks, LMW neutrals and LMW acids) also increased as SBR temperature decreased with total concentrations of 2673, 2910 and 4392 μg/L for the effluents from SBRs operated at 20, 14 and 8 ℃, respectively. In contrast, no obvious trend between SBR operating temperature and the concentration of intermediate MW humic-like substances was detectable. The relatively constant concentration of humic-like substances is consistent with prior reports of their biological recalcitrance (Tao et al., 2021). It is likely that the greater decline in hydraulically irreversible permeability observed when the SBRs were operated at low temperatures was due to the higher concentrations of high and low MW organic matter.

As previously discussed, the intrinsic membrane resistance increased at lower filtration temperatures suggesting that the pore size decreased with temperature, and therefore greater removal of organic materials could potentially be achieved at lower filtration temperatures. To test this hypothesis, the DOC removal efficiencies for the effluent from the SBR operated at 8 ℃ and filtered at both 8 ℃ and 20 ℃ were compared (Figure 4-4A). The total DOC removal efficiency of the filtration test conducted at 8 ℃ increased by 14% as compared to that conducted at 20 ℃, confirming that at low filtration temperatures more organic material can be retained. The removal efficiencies of high MW and low MW organics also significantly increased by 10% and 78%, respectively, at 8 ℃ compared to removal at 20 ℃ (Figure 4-4B). The removal of intermediate MW organics was not impacted by filtration temperature. These results suggest that the removal of organic material during tertiary filtration is not only related to membrane pore size but also the hydrophobicity of the foulants with hydrophobic humic-like substances less trapped on/in the membranes (Bessiere et al., 2009).

To investigate the correlation between the specific organic fractions and hydraulically irreversible fouling, linear regression analyses of the DOC fractions in effluents from SBRs operated at different temperatures and hydraulically irreversible fouling rates from filtration tests conducted at 20 ℃ were analysed (Figure 4-5) (see Supplementary materials). The regression analysis revealed that the relationships between irreversible fouling rates and polysaccharides, proteins and LMW matter were statistically significant ($P<0.05$). The good correlation between hydraulically irreversible fouling rates and polysaccharides ($r^2 = 0.89$) is consistent with prior studies which reported that hydraulically irreversible fouling is mainly due to polysaccharide in MBRs treating municipal wastewater (Paul,

2011). A strong correlation was also observed between hydraulically irreversible fouling rate and LMW matter ($r^2 = 0.89$) suggesting a significant role of LMW matter in hydraulically irreversible fouling. However, a poor correlation ($r^2 = 0.52$) was observed between protein concentrations and hydraulically irreversible fouling rates. This indicates that protein as a single fraction was not sufficient to explain hydraulically irreversible fouling and may impact fouling combined with other fractions. However, prior studies have demonstrated that microbially-derived effluent organics, especially proteins, were the key EfOM foulants that were responsible for irreversible fouling in UF membranes (Henderson et al., 2011; Jutaporn et al., 2021; Poojamnong et al., 2020). The difference in the role of protein between the present study and prior studies might be due to the different membranes (ZeeWeed-500, pore size 0.04 μm) used by Jutaporn et al. (2021) and Poojamnong et al. (2020). Furthermore, the different characteristics of the protein generated in various secondary systems with specific influent properties could be another factor for the different correlation.

Prior studies have reported that each organic fraction plays a different role in the development of fouling (Henderson et al., 2011). Polysaccharides have been demonstrated to affect membrane fouling through forming cake/gel layers while protein and LMW organic matter contribute more to pore blocking (Sun et al., 2014). On the basis of linear regression results it was anticipated that cake fouling and pore blocking were potentially responsible for the observed hydraulically irreversible fouling.

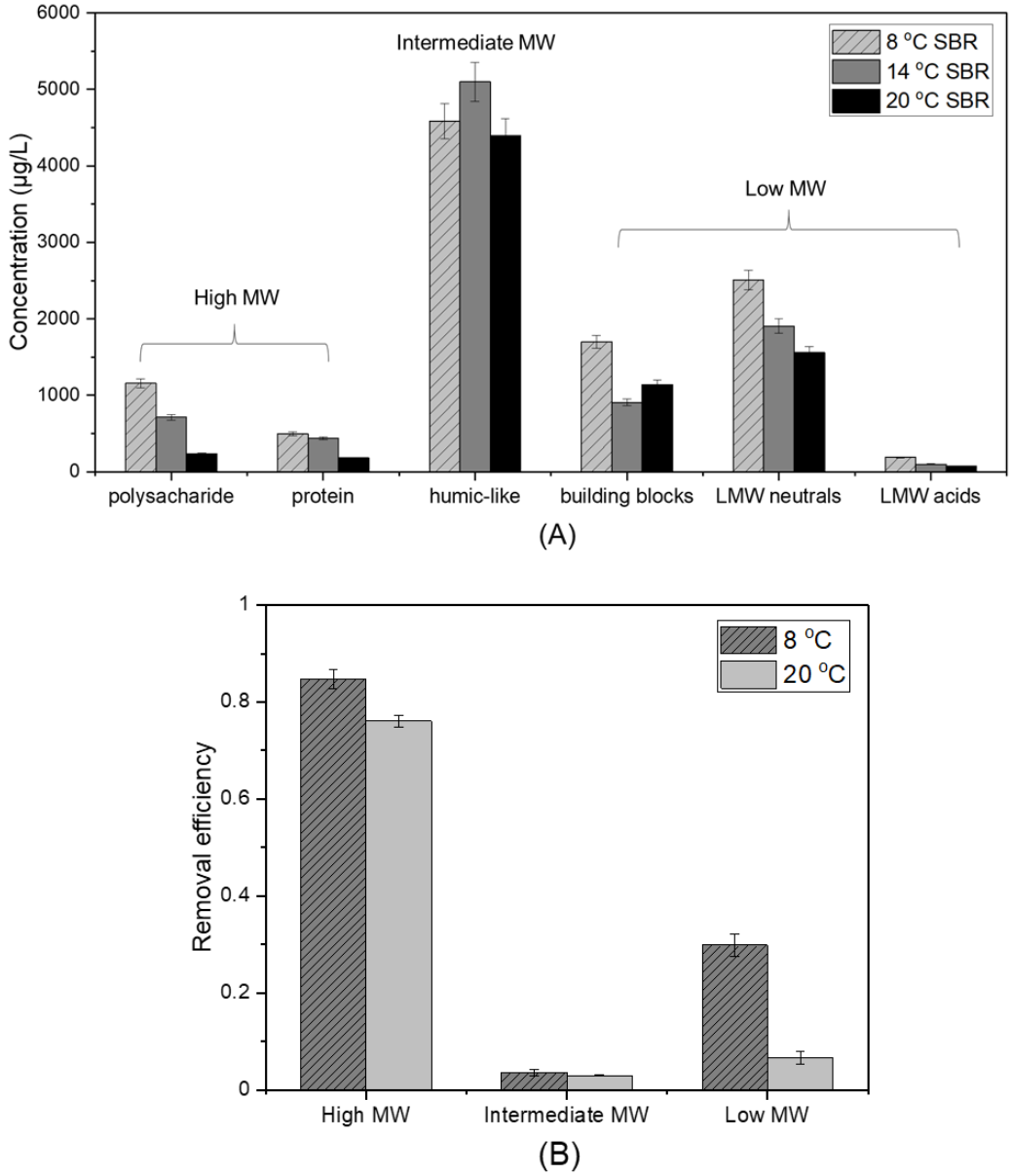

Figure 4-4. (A) DOC concentrations (µg/L) (mean ± standard deviation) of the effluents from SBRs operated at different temperatures and (B) DOC removal efficiencies (mean ± standard deviation) with the effluent from SBR operated at 8 ℃ and filtered at 8 ℃ and 20 ℃.

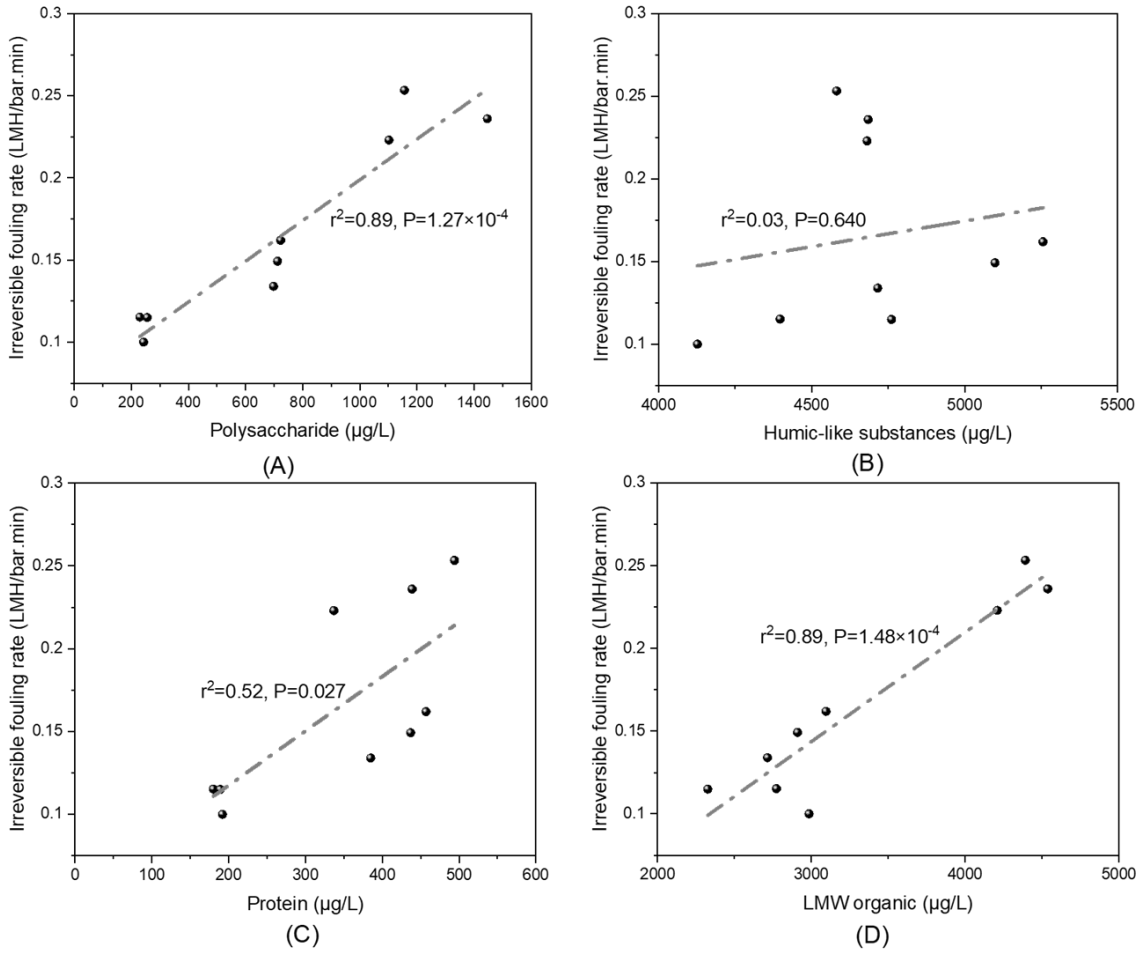

Figure 4-5. Hydraulically irreversible fouling rate versus (A) polysaccharide; (B) humic-like substance; (C) protein; and (D) LMW organic concentrations.

4.3.3 Mechanism in hydraulically irreversible permeability development

The observed irreversible permeabilities were derived from irreversible TMP data. In order to gain insight into the mechanism governing hydraulically irreversible permeability, established fouling models (Bolton et al., 2006) were fitted to observed irreversible TMP data for the filtration tests with the effluents from SBRs operated at different temperatures and filtered at different temperatures. It was observed that a combined cake-intermediate pore blocking model could best fit all data sets, suggesting the significant roles of cake fouling and pore blocking on hydraulically irreversible permeability decline observed in section 4.3.1.

Kimura et al. (2015) suggested a two-step mechanism in the evolution of hydraulically irreversible fouling in MBRs when treating municipal wastewater. In this evolution, initial adsorption of low MW organics is followed by a gradual accumulation of large polysaccharides and proteins which leads to pore blocking and subsequent cake fouling. The two-step mechanism proposed by Kimura et al. (2015) for MBRs is consistent with the results observed in the current study that indicated low MW organics, polysaccharides and proteins contributed to hydraulically irreversible permeability reduction and that combined cake-intermediate pore blocking was the dominant permeability reduction mechanism.

The model coefficients for the combined cake-intermediate pore blocking model were examined to quantify the impact of cake fouling (K_c) (Figure 4-6A), intermediate pore blocking (K_i) (Figure 4-6B), and their relative contribution (K_c*J_0/K_i) (Figure 4-6C), on hydraulically irreversible fouling. The effect of SBR operating temperature on hydraulically irreversible permeability through changes in the effluent quality was assessed by examining the coefficients derived from the filtration tests conducted at 20 ℃. From Figure 4-6A it can be observed that Kc values increased by 85% as SBR operating temperature decreased from 20 ℃ to 8 ℃ indicating an increased role of cake fouling. The increased cake fouling might have been due to increased high MW polysaccharide concentrations in the effluents from SBRs operated at lower temperatures. Similarly, the values of K_i also increased by 66% as SBR operating temperature decreased from 20 ℃ to 8 ℃ whereas the increased extent was lower than that of polysaccharide (Figure 4-6B). The increased Ki could be attributed to greater low MW organics generated at low SBR operating temperatures.

The relative contributions of cake fouling and pore blocking indicated by K_c*J_0/K_i were then evaluated with the effects of SBR operating temperature (Figure 4-6C). From Figure 4-6C it can be observed that the values of K_c*J_0 were always greater than K_i for all SBR operating temperatures, indicating a greater contribution of cake fouling than intermediate pore blocking. However, the magnitude of the ratio was substantially greater when SBR was operated at 8 ℃ suggesting the dominant impact of the elevated polysaccharide concentrations at 8 ℃.

The fouling model was also fit to the observed irreversible TMP data from filtration tests carried out at the source SBR operating temperature to investigate how filtration temperature affected hydraulically irreversible permeability development. It can be observed that K_c (Figure 4-6A) and K_i (Figure 4-6B) values both increased when filtered at the source SBR operating temperature as compared to filtered at 20 ℃ for both effluents from SBRs operated at 14 ℃ and 8 ℃. In addition,

the increase was greater for the effluents from SBR operated at 8 ℃ than 14 ℃. The results were consistent with those of Shang et al. (2015). They reported that the extent of pore blocking increased as membrane pore size decreased. Hence, the increased Ki values could be attributed to decreased pore sizes as a result of low filtration temperature. This would then further lead to increased cake fouling (K_c) as a result of the initial pore blocking (Guo et al., 2012). The trends of the model coefficients (K_c and K_i) were consistent with the previously discussed results that showed fewer polysaccharides and low MW organics passed through the membrane pores when filtered at the source SBR operating temperature.

From Figure 4-6C it can be observed that for the effluent from SBR operated at 8 ℃, the value of K_c*J_0/K_i filtered at 8 ℃ was significantly greater than that of corresponding filtration at 20 ℃. By contrast there was no significant difference in the ratio between the filtration temperature of 14 ℃ and 20 ℃ for the effluent from SBR operated at 14 ℃. The increased relative contribution of cake fouling can be associated with the changes of DOC fraction retained by membrane due to smaller pore size at lower filtration temperature. In the present study, for the filtration test with the effluent from the SBR operated at 8 ℃ the concentrations of polysaccharide and low MW organics in the permeates decreased by 55% and 25% respectively when filtration temperature decreased from 20 ℃ to 8 ℃. The greater concentration of polysaccharides retained at 8 ℃ than low MW organics may result in a subsequent larger contribution of cake filtration then pore blocking.

Upon the above fouling model fitting, the degree of cake fouling and intermediate pore blocking was significantly affected under cold temperature operations of SBRs and filtration due to changed effluent organics and membrane pore size. For a practical point of view, the heating of wastewater would be cost prohibitive to mitigate fouling in cold climates due to high specific heat capacity of water. Therefore, improved cleaning strategies to remove mainly high and low MW foulants should be considered for cold weather conditions, and pretreatment of effluents prior to filtration such as pre-coagulation would be another strategy to mitigate hydraulically irreversible fouling by converting charge and changing size of the foulants.

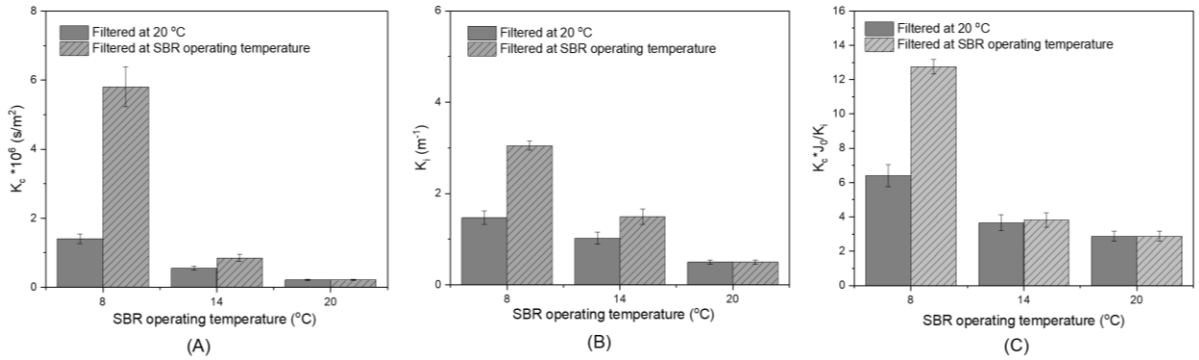

Figure 4-6. Modelling coefficients of (A) cake fouling constant, K_c; (B) intermediate pore blocking constant, K_i; and (C) the contributions of cake fouling and intermediate pore blocking to the combined model, K_c*J_0/K_i.

4.4 Conclusions

The effect of upstream biological treatment temperature and filtration temperature on hydraulically irreversible permeability of tertiary ultrafiltration membranes was quantified in the present study. Reduced SBR operating and filtration temperatures impacted hydraulically irreversible permeability by changing EfOM characteristics, water viscosity, membrane intrinsic resistance, and membrane-foulants interactions. Increased generation of EfOM induced more rapid decline of hydraulically irreversible permeability at low SBR operating temperatures with high and low MW matter playing significant roles. Higher viscosity and intrinsic membrane resistance at low filtration temperatures further deteriorated hydraulically irreversible permeability, which cannot be neglected. Moreover, narrowed membrane pore size retained more organic matter and further decreased hydraulically irreversible permeability. The results suggest that cake formation and pore blocking were the major fouling mechanisms for hydraulically irreversible fouling. These results provide insights that can be employed as a basis to optimize filtration operation by mitigating hydraulically irreversible fouling.

Chapter 5

Evaluation of the impact of SBR temperature and filtration temperature on fouling of tertiary membranes

GRAPHICAL ABSTRACT

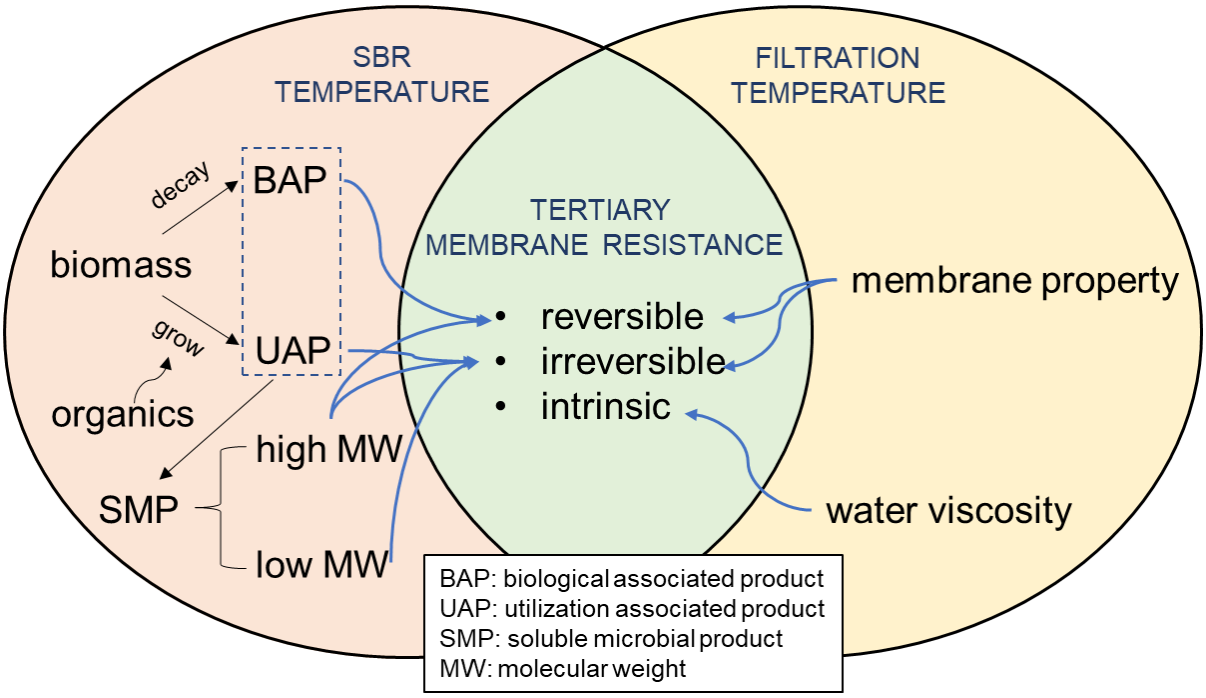

5.1 Introduction

As water resources become increasingly strained, the need for production of high quality treated municipal wastewaters continues to grow. Membrane technologies, which can effectively remove particulate/colloidal matter, macromolecules, and pathogens, have gained increasing acceptance in tertiary treatment of wastewater (Krzeminski et al., 2017). However, although there has been rapid development of tertiary filtration, the application of this technology is significantly hindered by membrane fouling caused by effluent organic matter (EfOM) (Qu et al., 2021). Moreover, fouling of tertiary membranes can be intensified due to the impacts of temperature on EfOM generation and membrane properties in cold climates resulting in greater need for fouling control and membrane

replacement (Ozgun et al., 2015; Cui et al., 2017). Abu-Obaid et al. (2020) reported increased fouling of tertiary membranes at full-scale during periods of low temperatures and elevated flows but the underlying causes of the elevated fouling were not conclusively identified. An improved understanding of the fouling mechanisms of tertiary membranes in cold climates will support the development of fouling control strategies.

Previous studies of fouling behavior in membrane bioreactors (MBRs) have demonstrated that cold temperatures (7 to 12.7 ℃) caused rapid membrane fouling by inducing changes to biomass concentration and biodegradation of wastewater in the mixed liquor (Kakuda et al., 2020; Krzeminski *et al.*, 2012; Miyoshi et al., 2009; Drews, 2010). In a pilot-scale MBR treating real municipal wastewater in Mikkeli Finland (7 to 20 ℃) it was reported that membrane fouling accelerated during low temperature periods with a 75% decrease in membrane permeability (Gurung et al., 2017). Reduced particle back transport velocity and elevated hydrophobicity of the mixed liquor were demonstrated to be responsible for the severe fouling. In other studies of MBRs, fouling has been observed to correspond to elevated mixed liquor concentrations of organics (humic-like substances, polysaccharides and proteins) when operated under cold temperatures (Ma et al., 2013). In addition, the particle size distribution in MBRs was reported to shift towards smaller particles when temperature was lower than 15 ℃ leading to rapid pore narrowing or blocking (van den Brink et al., 2011). Furthermore, the alteration of membrane structure and properties under cold temperatures has been demonstrated to intensify membrane fouling (Cui et al., 2017). Viewed collectively, the MBR-focused research has suggested several potential mechanisms for increased fouling under low temperatures, however, the extrapolation of these results to tertiary treatment is challenging due to differences in the exposure of the membranes to the various foulants.

Tertiary membranes are less exposed to settleable components (Sánchez et al., 2011). It is anticipated that there will be less cake formation on tertiary membranes than that which would be expected with MBR membranes. Therefore, the fouling mechanisms in MBRs and tertiary membrane treatments could be fundamentally different. In tertiary configurations, the extent of membrane fouling has been attributed to the chemical composition and concentration of EfOM in the secondary effluents (Ly et al., 2018). Soluble microbial products (SMPs) have been reported to constitute a dominant part of EfOM in secondary effluents and are biologically derived from substrate metabolism (utilization-associated products, UAP) and biomass decay (biomass-associated products, BAP) (Barker & Stuckey, 1999). The generation of SMPs has been demonstrated to be temperature

dependent since substrate utilization and biomass decay, that lead to UAP and BAP generation, depend on operating temperatures (Hu et al., 2019). Tao et al. (2021) observed a strong correlation between temperature and BAP/UAP yields from treating real wastewater with the generation of BAP more temperature sensitive than UAP. However, a comprehensive evaluation of the effect of temperature on UAP and BAP generation with a linkage to fouling of tertiary membranes has not been reported.

In this context, the objectives of the present study were to investigate the effects of temperature, including secondary treatment operating temperature and filtration temperature, on fouling of tertiary membranes. Bench scale sequencing batch reactors (SBRs) were employed to treat real municipal wastewater over a range of temperatures (8, 14 and 20 ℃) to generate feed water for filtration tests. Bench scale filtration tests were conducted at 20 ℃ to investigate the impact of SBR temperature on fouling of tertiary membranes and at the source SBR temperatures (i.e. 8 and 14 ℃) to characterize the effect of filtration temperature on fouling of tertiary membranes. The relationships between membrane fouling indices and DOC fractions were investigated by correlation analysis. The outcomes of the present study provide insights into the combined effects of temperature on biological and filtration processes that influence fouling behavior of tertiary membranes and can be employed to assist with the design of fouling mitigation measures in cold climates.

5.2 Materials and methods

5.2.1 Apparatus

Bench scale SBRs were operated on real municipal wastewater for extended periods (October 2018 to March 2020) at temperatures of 8, 14 and 20 ℃ to provide feed water for filtration tests. The temperatures were selected to span summer and winter operating conditions in a northern climate (e.g. Ontario, Canada). The hydraulic retention time (HRT) of the SBRs was 20 h, and the solids retention time (SRT) was maintained at 25 days. A detailed description of the design and operation of the SBRs has been provided by Tao et al. (2021).

Bench scale membrane modules were employed to assess membrane performance in a batch configuration. Each membrane module consisted of three ZeeWeed-1000 hollow-fibres (Suez, Canada). The nominal pore size of the ZeeWeed-1000 membrane is 0.02 μm. The length of each hollow-fibre was 500 mm. A programmable peristaltic pump (OF-07582-00, Cole-Parmer, USA) was used to control the timing of permeation and back pulsing as described in Section 5.2.2. An air

diffuser (coupled with an air flow meter), located at the bottom of tank, provided aeration for mixing and membrane scouring. A detailed description of the design and operation of the filtration systems has been provided by Tao et al. (2022).

5.2.2 Filtration tests

Filtration tests were conducted with either clean water or the effluents from the SBRs as illustrated in Figure 5-1. Tests with clean water were initially conducted with virgin membranes to establish the intrinsic membrane resistance as a function of filtration temperature. Subsequent filtration tests were conducted with SBR effluent at both room temperature (approx. 20 ℃) and at the source SBR temperature (Figure 5-1). This enabled independent evaluations of the impact of SBR temperature and filtration temperature on fouling of tertiary membranes.

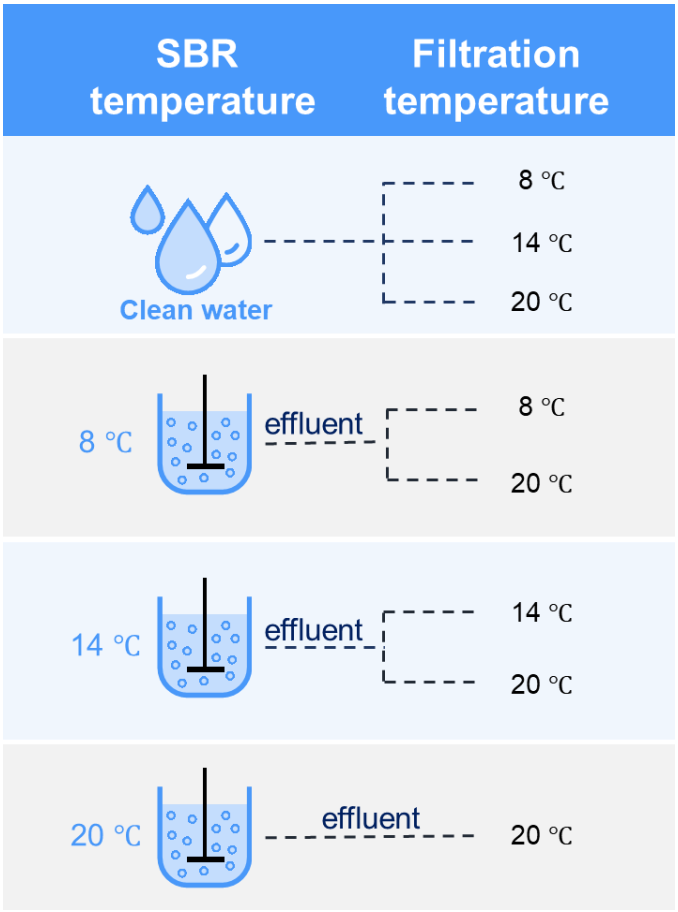

Figure 5-1. Schematic diagram of filtration test plan.

The filtration tests were operated in dead-end mode and consisted of 30 cycles that each included permeation for 30 min and fouling mitigation for 2 min. The permeate was continuously returned to the filtration tank to maintain a consistent feed composition. A combination of back pulsing and air scouring was employed for fouling mitigation. Parallel filtration tests with only flux interruption (FI) were conducted to provide a reference condition which allowed for an assessment of the effectiveness of the back pulsing and air scouring. The permeation flux was 24 LMH and was established on the basis of flux step tests that were conducted as described by Vera et al. (2015) (see Supplementary materials). The back-pulsing flux was twice the permeation flux. All filtration tests were conducted in triplicate. Prior to conducting the filtration tests, the virgin membranes were cleaned by soaking in a 250 mg/L NaOCl solution overnight and then DI water for 2 h. After each test, the fouled membranes were chemically cleaned using a 250 mg/L NaOCl solution for 2 h and then rinsed by soaking in DI water for 2 h.

5.2.3 Membrane performance indices

Four resistance-based fouling indices were employed to quantify the evolution of fouling of the membranes and enable a quantitative comparison of the various filtration conditions.

Total resistance ($R_{t,i}$) quantified the sum of intrinsic membrane (R_m), hydraulically reversible ($R_{rev,i}$) and irreversible ($R_{irr,i}$) resistances at the end of cycle i, and was calculated from the test data using Equation 5-1:

$$\boldsymbol{R_{t,i} = \frac{TMP}{\eta J}} \qquad \textbf{Equation 5-1}$$

where TMP was the measured transmembrane pressure (Pa), η was the permeate viscosity (Pa·s), and J was the measured flux ($m^3m^{-2}s^{-1}$). Permeate viscosity was calculated according to Equation 5-2 (van den Brink et al., 2011):

$$\boldsymbol{\eta = 0.497\,(T + 42.5)^{-1.5}} \qquad \textbf{Equation 5-2}$$

with temperature (T) in degrees Celsius.

The fouling rate (F_i) in cycle i was examined as it can provide insight into the possible mechanisms responsible for fouling (Meng et al., 2017), and was calculated as per Equation 5-3.

$$\mathbf{F_i} = \boldsymbol{\frac{Rt_i^f - Rt_i^i}{\Delta t}} \qquad \textbf{Equation 5-3}$$

where Rt_i^f and Rt_i^i were the final and initial membrane resistances (m^{-1}) of cycle i, and Δt was the duration of the cycles (min).

The values of R_m, $R_{rev,i}$ and $R_{irr,i}$ were assessed to determine how SBR temperature influenced the contribution of each resistance to R_t. R_m values were determined from the filtration tests conducted with clean water. $R_{rev,i}$ quantified the resistance that accumulated in one cycle and was recovered during physical cleaning between cycles and was calculated for each cycle as per Equation 5-4.

$$\boldsymbol{R_{rev,i} = Rt_i^f - Rt_{i+1}^i} \qquad \textbf{Equation 5-4}$$

where Rt_i^f was the final membrane resistance of cycle i, and Rt_{i+1}^i was the initial membrane resistance of filtration cycle i+1.

$R_{irr,i}$ was defined as the resistance that accumulated during a cycle and that was not removed by physical cleaning and was calculated for each cycle as per Equation 5-5.

$$\boldsymbol{R_{irr,i} = R_{t,i} - R_{rev,i} - R_m} \qquad \textbf{Equation 5-5}$$

5.2.4 SBR effluent characterization

5.2.4.1 Conventional parameters

Soluble COD (sCOD) was analyzed according to Standard Methods 5220 (APHA, 2005) using a spectrophotometer (DR2600, HACH, USA). DOC was measured using a Shimadzu DOC analyzer (Japan). UV absorbance at 254 nm (UV_{254}) was determined by a SHARP spectrophotometer (Japan).

5.2.4.2 DOC fractionation

Liquid chromatography with organic carbon detection (LC-OCD) (Model 8, DOC-LABOR, Germany) was used to provide insight into the composition of dissolved organic matter in the SBR effluents. The LC-OCD analysis classifies dissolved organic matter as biopolymers, humic substances, building blocks, low molecular weight (LMW) acids and LMW neutrals (Huber et al., 2011). The concentration of biopolymers reported by the LC-OCD analysis were then divided into polysaccharide and protein assuming all of the DON in the biopolymers was bound in proteinaceous matter and employing a typical C:N mass ratio of 3 for proteins (Huber et al., 2011).

5.2.4.3 BAP and UAP

BAP and UAP have been reported to consist of mixtures of polysaccharides and proteins (Tian et al., 2011). The concentrations of UAP and BAP and the contributions of proteins and polysaccharides to these concentrations were estimated by solving mass balances on polysaccharides and proteins. The detailed approach was described in our previous study (Tao et al., 2021).

5.2.5 Statistical analysis for tertiary membrane fouling

Correlation analysis was used to assess the relationships between the fouling indices (F_i, $R_{t,i}$, $R_{rev,i}$ and $R_{irr,i}$) and SBR effluent characteristics (sCOD, DOC, UV_{254}, polysaccharide, protein, humic substances, building blocks, LMW organics, UAP and BAP). The fouling indices at the end of each filtration test were used in the correlation analysis. The correlation coefficients range between -1 and +1 and quantifies the direction and strength of the linear association between the two variables. The correlation analysis was conducted using OriginLab 2020 (USA).

Five combined fouling models as proposed by Bolton et al. (2006) were fit to the experimental data. The combined fouling models included cake-complete, cake-intermediate, complete-standard, intermediate-standard and cake-standard models with K_c, K_b, K_i and K_s as fitted parameters to quantify cake fouling, complete blocking, intermediate blocking and standard blocking, respectively. The normalized TMP values (P/P_0) over time from the triplicate runs were simultaneously used in the model fitting. The best fit was determined by minimizing the sum of squared residuals (SSR) where the residuals were equal to the difference between measured data and model prediction. One-way ANOVA was used to determine if there was a statistically significant different between the fitted parameters.

Linear regression was subsequently conducted (OriginLab 2020, USA) to determine the relationship between the concentrations of selected DOC fractions and the fitted parameters of the fouling models. The relationships were considered statistically significant at a 95% confidence interval ($P<0.05$).

5.3 Results and discussion

The present study sought to comprehensively investigate the impact of SBR temperature and filtration temperature on fouling of tertiary membranes. The experimental design for the filtration tests allowed for separate assessment of the impact of SBR and filtration temperature on the fouling indices.

Correlation analyses were employed to provide insight into the foulants responsible for the development of total, hydraulically reversible and irreversible membrane resistances from the perspective of molecular weight and biological origin. Combined fouling models were then used to facilitate comparisons between operating conditions.

5.3.1 Effect of SBR temperature on fouling indices

Tao et al. (2021) demonstrated that the concentrations of soluble microbial products, which are potential membrane foulants in secondary treated effluents, were impacted by SBR temperature. The current study sought to assess if the generated soluble microbial products would also impact fouling of tertiary membranes. Hence, the effluents from the SBRs operated at different temperatures were all filtered at a reference temperature of 20 ℃ to assess whether there was a corresponding impact on the fouling of tertiary membranes. The mean and standard deviations of the four fouling indices over the triplicate filtration tests were computed for the different conditions. In all cases, the standard deviations were consistently less than 20% of the corresponding means indicating good reproducibility of the filtration tests.

Values of $R_{t,i}$ were initially examined to assess the impact of SBR temperature on the trends in the combined resistances over the multiple filtration cycles (**Figure 5-2**). It can be observed that the increase in values of $R_{t,i}$ in the initial cycles of the filtration tests was strongly influenced by SBR temperature. For the effluent from the SBR operated at 20 ℃, the $R_{t,i}$ value estimated for the first cycle was 5.8×10^{11} m^{-1} and the corresponding values for the effluents from the SBRs operated at 8 and 14 ℃ increased by 50% and 23% . Subsequent values of $R_{t,i}$ were consistently higher for the effluents from the SBRs operated at lower temperatures over the multiple filtration cycles. At the end of the filtration tests, the value of $R_{t,i}$ for the effluent from the SBR operated at 20 ℃ increased by 27% relative to the first cycle while the corresponding increases for the effluents from the SBRs operated at 8 and 14 ℃ were 82% and 45%, respectively. The results demonstrate that low SBR temperature resulted in a substantial increase in the total membrane resistance ($R_{t,i}$).

The values of R_m were compared to obtain insight into its contribution to $R_{t,i}$ over the multiple filtration cycles. R_m had an average value of $4.2 \times 10^{11} \pm 0.9 \times 10^{10}$ m^{-1} and was similar for all the filtration tests conducted at 20 ℃. Hence, differences in R_t values as a function of SBR temperature were attributed to differences in $R_{rev,i}$ and $R_{irr,i}$ values that are subsequently discussed in detail.

The trends in values of $R_{rev,i}$ and $R_{irr,i}$ over the multiple filtration cycles for the effluent from the SBR operated at 20 ℃ were assessed as a reference condition for fouling development. It can be observed from **Figure 5-2** that for this condition the values of $R_{rev,i}$ were relatively constant while values of $R_{irr,i}$ increased by 43% over the multiple filtration cycles. Although the values of $R_{irr,i}$ increased, the total contribution of $R_{rev,i}$ and $R_{irr,i}$ accounted for a relatively small portion (8-28%) of the $R_{t,i}$ values. Hence, for the effluent from the SBR operated at 20 ℃, $R_{rev,i}$ and $R_{irr,i}$ were relatively well controlled by the back pulsing and air scouring employed in the filtration tests. The results indicate that the effluent from the SBR operated at 20 ℃ had a relatively low fouling propensity although there was a modest increase in hydraulically irreversible fouling over the multiple filtration cycles.

The values of $R_{rev,i}$ and $R_{irr,i}$ for the effluents from the SBRs operated at 8 and 14 ℃ were compared to that of 20 ℃ to obtain insight into the effect of SBR temperature on fouling reversibility. Similar to those observed at 20 ℃, the values of $R_{rev,i}$ were relatively constant over the multiple filtration cycles for the lower SBR temperatures. However, the values of $R_{rev,i}$ for the effluents from the SBR operated at 8 ℃ and 14 ℃ were approximately 7 and 2 times higher respectively than those of the effluent from the SBR operated at 20 ℃. In contrast, the values of $R_{irr,i}$ for the lower SBR temperatures increased over the multiple filtration cycles, with the extent of the increase greater as the SBR temperature decreased. At the end of the filtration tests, the values of $R_{irr,i}$ for the effluents from the SBRs operated at 8 and 14 ℃ were 255% and 84% higher than those of effluents from 20 ℃ SBR. Hence, the lower SBR temperatures induced greater hydraulically reversible and irreversible membrane fouling which collectively contributed to the previously described increases in $R_{t,i}$.

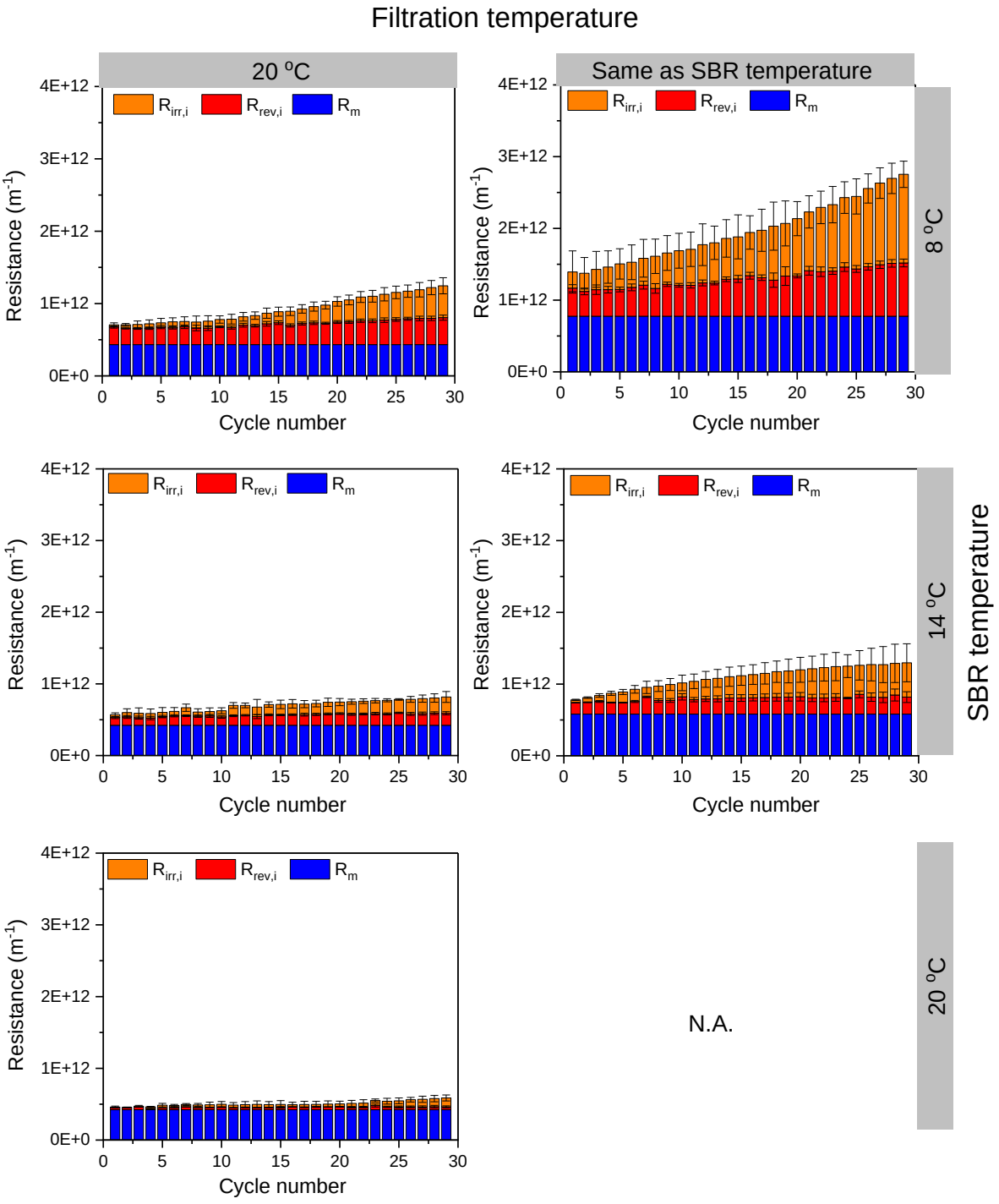

Figure 5-2. Membrane resistances (mean ± standard deviation) observed at different SBR and filtration temperatures. (Rt,i values are indicated by the total height of the column in each cycle.)

The trends in fouling rate (F_i) were examined to obtain insight into possible fouling mechanisms (Figure 5-3). The slopes from linear regression of the F_i values versus cycle number were used to assess the different stages of fouling development. The regression equations where the slopes were significantly different from 0 are presented in Figure 5-3. It was observed the values of F_i with the effluent from the SBR operated at 20 ℃ increased only slightly with a slope of 3.5×10^7 m^{-1}/cycle. The relatively constant and small values of F_i reflected slight membrane fouling and a singular fouling mechanism when the SBR was operated at 20 ℃.

The values of F_i for the effluents from the SBRs operated at low temperatures were similarly analyzed to assess how the temperature of the biological treatment impacted the rate of fouling. In general, the values of F_i were higher for the SBRs operated at low temperatures than that of the 20 ℃ effluent. As illustrated in Figure 5-3, a two-stage pattern of F_i development was observed over the multiple filtration cycles for the lower temperatures. Hence, the F_i values were regressed separately for the different stages. For the effluent from the SBR operated at 8 ℃, the slope of the regression was 8.9×10^7 m^{-1}/cycle for the first ten cycles and then it increased to 2.4×10^8 m^{-1}/cycle over the rest of the cycles, indicating accelerated fouling development. In contrast the slopes of the two stages observed with the effluent from the SBR operated at 14 ℃ (not significant; 8.0×10^7 m^{-1}/cycle) were lower than that of the SBR operated at 8 ℃ and the duration of the first stage was longer (14 cycles), The two-stage development in F_i values at the lower temperatures suggests an alteration of fouling mechanism as the filtration tests proceeded. This was consistent with a two-step fouling mechanism that has been reported for MBRs treating municipal wastewater (Kimura et al., 2015). Kimura et al. (2015) indicated that initial membrane fouling was due to pore blocking by low molecular weight (MW) organics and this was followed by cake fouling with relatively high MW organics. Hence, it was concluded that the SBR temperature impacted the effluent properties in a manner that influenced the rate and type of fouling mechanisms of tertiary membranes.

The trends in fouling indices indicated that as SBR temperature decreased, the fouling of tertiary membranes increased significantly. Further, the trend in the increase in $R_{rev,i}$ and $R_{irr,i}$ values differed between SBR temperatures. As the SBR temperature was the only experimental variable that differed between the filtration tests, the observed difference in fouling of tertiary membranes was attributed to differences in the effluent composition. The characteristics of the DOC and DOC fractions generated in the SBRs operated at the different temperatures and their correlation with fouling indices are subsequently discussed in Section 5.3.3.

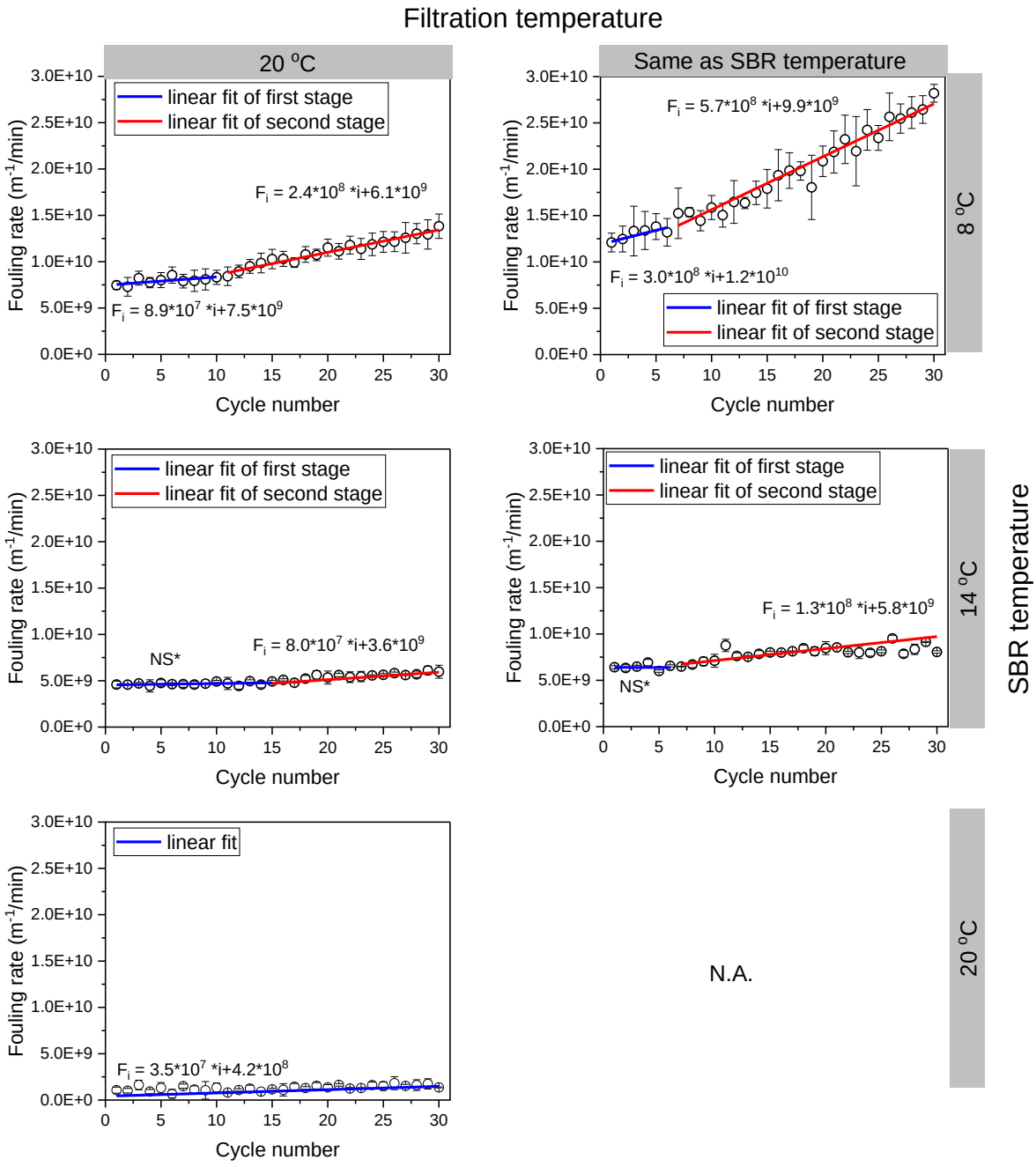

Figure 5-3. F_i values (mean ± standard deviation) versus cycle number (i) observed at different SBR and filtration temperatures. (NS*: slope is not significantly different from 0).

5.3.2 Effect of filtration temperature on fouling indices

As previously demonstrated, low SBR temperatures resulted in increased membrane fouling when the filtration tests were all conducted at 20 ℃. However, low filtration temperatures have also been reported to cause changes in water viscosity and membrane pore size, both of which can affect membrane fouling (Cui et al., 2017). To quantify the contribution of the effect of viscosity and the membrane pore size with filtration temperature to membrane fouling, additional filtration tests were conducted at the source SBR temperature.

Values of $R_{t,i}$ were compared at the different filtration temperatures as an indicator of the overall effect on total membrane fouling (Figure 5-2). It was observed that the values of $R_{t,i}$ for the effluent from the SBR operated at 8 ℃ were significantly higher (97-122%) when the filtration temperature was 8 ℃ as compared to filtration at 20 ℃. The corresponding increase in values of $R_{t,i}$ for the effluent from the SBR operated at 14 ℃ ranged from 34-55%. The increase in values of $R_{t,i}$ for the tests conducted under low filtration temperatures indicates the cumulative impacts of filtration temperature are substantial and should not be ignored in cold climates .

It was expected that intrinsic membrane resistance would be impacted by filtration temperature (Cui et al., 2017) and therefore values of R_m and their contribution to $R_{t,i}$ were estimated from the filtration tests conducted with clean water. It can be observed from Figure 5-2, when the filtration temperature reduced from 20 to 8 ℃, the value of R_m increased by 80% and the percentage of R_m to $R_{t,i}$ increased from 35% to 72%. Similarly, the value of R_m increased by 35% as filtration temperature decreased from 20 to 14 ℃ and accounted for 52% of $R_{t,i}$. Hence, reducing filtration temperature resulted in a significant increase in R_m that cannot be controlled through fouling mitigation measures.

The values of $R_{rev,i}$ were investigated to examine how filtration temperature affected the accumulation of hydraulically reversible fouling over the multiple filtration cycles. Since the values of $R_{rev,i}$ remained relatively constant in all cases, the average values over the multiple filtration cycles were compared between the two filtration temperatures. For the effluent from the SBR operated at 8 ℃, the average value of $R_{rev,i}$ increased 128% as the filtration temperature decreased from 20 to 8 ℃. Similarly, an increase of 107% in average $R_{rev,i}$ was observed for the effluent from the SBR operated at 14 ℃. The increase in $R_{rev,i}$ values as filtration temperature decreased indicates increased accumulation of hydraulically reversible foulants at the reduced filtration temperatures.

The response of $R_{irr,i}$ to filtration temperature was assessed in terms of the increase in these values over the multiple filtration cycles as this was considered to be indicative of the foulant-membrane

interaction (Liu et al., 2020). For the effluent from the SBR operated at 8 ℃, the values of $R_{irr,i}$ increased by 170–650% times when filtration temperature reduced from 20 to 8 ℃. The corresponding values for the effluent from the SBR operated at 14 ℃ were 110–260% times as filtration temperature decreased from 20 to 14 ℃. The increases in accumulation of $R_{irr,i}$ as filtration temperature decreased suggests a change in foulant-membrane interaction with more foulants attaching and blocking membrane pores that could not be recovered by back pulsing and air scouring.

The trends in F_i values with cycle number were evaluated for the tests with low filtration temperatures and compared with those that were conducted at 20 ℃. As illustrated in Figure 5-3 for both effluents from the SBRs operated at 8 and 14 ℃, the values of F_i were substantially higher at the lower filtration temperature when compared to 20 ℃. A two-stage development of F_i values was also observed at the lower filtration temperatures, with the duration of the stages the same (6 and 24 cycles) for both temperatures but the slopes were different. For the effluent from the SBR operated at 8 ℃, the first and second stage slopes were 3.8×10^8 and 5.7×10^8 m^{-1}/cycle, respectively. The corresponding values for the effluent from the SBR operated at 14 ℃ were 0 and 1.3×10^8 m^{-1}/cycle. The results indicate accelerated initial pore blocking and subsequent cake formation at the lower filtration temperatures which might be attributed to changes in membrane properties at the reduced filtration temperatures.

Tao et al. (2022) demonstrated that an increase in hydraulically irreversible membrane permeability at lower filtration temperatures was attributed to reduced membrane pore size. Increased retention of high and low molecular weight effluent organics was also observed at low filtration temperatures. Therefore, the increased $R_{rev,i}$ and $R_{irr,i}$ at low filtration temperatures were attributed to smaller membrane pore sizes and that led to more effluent organic matter being retained as hydraulically reversible and irreversible foulants in the cake layer/pores.

5.3.3 Investigation of foulants

Low temperature operation of SBRs has been reported to generate elevated effluent concentrations of high and low MW organics that were attributed to the generation of BAP and UAP (Tao et al., 2021). Hence, a correlation analysis was conducted between the fouling indices (F_i, $R_{t,i}$, $R_{rev,i}$, $R_{irr,i}$) and the concentration of the DOC fractions (polysaccharides, proteins, humic substances, LMW organics) and UAP and BAP to identify those most associated with membrane fouling. In this analysis the concentration of LMW organics represented the sum of the concentrations of building blocks, LMW neutrals and acids. The values of the fouling indices used in the correlations were from the last cycle

of each filtration test and hence represent the cumulative fouling over all of the cycles. For comparison, the conventional bulk parameters of effluent quality, including DOC, sCOD and UV_{254}, were also included in the correlation analysis. Only the fouling indices obtained from the filtration tests conducted at 20 °C were included in the correlation analysis to exclude the additional impacts of filtration temperature on fouling.

The results of the correlation analysis (Figure 5-4) summarized the extent to which the variability in the fouling indices could be explained by the various water quality parameters. The correlation between the fouling indices and the conventional water quality parameters was assessed firstly to provide a point of comparison for the analysis of the DOC fractions. The fouling indices were not correlated with either sCOD or UV_{254} as their concentrations were not significantly different at the three tested SBR temperatures (Tao et al., 2021). As illustrated in Figure 5-4, it was found that the only conventional parameter to which the fouling indices were correlated with was DOC. The correlation coefficients between the three membrane resistances and DOC concentrations were all over 0.85 indicating strong correlations. However, fouling rates were not correlated with DOC concentrations which might be because fouling rates presented patterns with multiple stages and could not be simply explained by single DOC concentrations. The significant correlations between membrane resistances and DOC concentrations were consistent with that reported by Abu-Obaid et al. (2020) for full-scale tertiary membranes.

The correlations between the fouling indices and DOC fractions (Figure 5-4) were then assessed to obtain insights whether DOC fractions could be better indicators of membrane fouling. The correlation between $R_{t,i}$ and F_i and DOC fractions can reflect the responsible fractions for the total membrane fouling. Generally, $R_{t,i}$ and F_i values were not correlated with humic-like substances concentrations, which was due to their relative constant concentration at different SBR temperatures (Tao et al., 2021). It was observed that $R_{t,i}$ values were positively correlated with the total DOC ($r = 0.98$), polysaccharide ($r = 0.97$), protein ($r = 0.83$), and LMW organic concentrations ($r = 0.88$). The strong correlations between $R_{t,i}$ values and both high and low MW organics were consistent with cake fouling and intermediate pore blocking as the dominant fouling mechanisms (Liu et al., 2018). This is further addressed through modelling in a subsequent section. In contrast, F_i values were only correlated with LMW organic concentrations with a relatively low correlation coefficient ($r = 0.73$), which was attributed to the use of only the end-of-test values.

The correlations were then assessed to obtain insights into responsible foulants for $R_{rev,i}$ and $R_{irr,i}$. $R_{rev,i}$ and $R_{irr,i}$ values were also not correlated with humic-like substances concentration. $R_{rev,i}$ presented the highest correlation with polysccharidie (r = 0.98), which was consistent with the generally larger molecular weight and higher tendency of polysaccharides to contribute to hydraulically reversible fouling (Zhao et al., 2017). Moreover, $R_{irr,i}$ was observed to correlate with polysaccharides (r = 0.95) and LMW organics (r = 0.87). It is generally accepted that LMW organics contribute to hydraulically irreversible fouling due to their ready absorbance on membranes through hydrophobic and electrostatic interactions (Liu et al., 2020). However, a portion of biopolymers, with sizes close to the pore size of membranes, have also been reported to be responsible for hydraulically irreversible fouling (Kimura & Kume, 2020), and the observations in the present study are consistent with this phenomena. Hence, the results indicate that hydraulically reversible resistance was mainly contributed by polysaccharides while hydraulically irreversible resistance was associated with both polysaccharides and LMW organics.

The previous correlation analysis examined the relationship between fouling indices and DOC fractions with the focus on the molecular weight. However, the foulants are of biological origin and in order to better link membrane fouling with the biological processes responsible for foulant generation, additional correlational analyses were conducted. In this regard correlations between the fouling indices and BAP/UAP which describe the mixtures of effluent organics generated during biomass decay and substrate utilization were evaluated (Kunacheva & Stuckey, 2014). The methodology for estimating the BAP and UAP concentrations and the data employed in the analyses were previously reported (Tao et al., 2021).

The impacts of BAP and UAP on total membrane fouling was assessed by their correlation with $R_{t,i}$ and F_i. It was observed that $R_{t,i}$ values were highly correlated with BAP (r = 0.99) and UAP (r = 0.92) concentrations. BAP and UAP are mixtures of polysaccharides and proteins which represent the high MW organics. Hence, the strong correlation between $R_{t,i}$ and BAP/UAP was consistent with the previous correlation between $R_{t,i}$ and polysaccharides(r = 0.97) and proteins (r = 0.83). By comparing the correlation coefficients, it was found that the BAP/UAP responses were similar to polysaccharides and proteins as predictors of $R_{t,i}$. In contrast, F_i values were only correlated with BAP concentrations (r = 0.71), which was also because only the end values included in the analysis. Hence, the high MW organics can explain the total membrane fouling from both classifications of molecular weight and

biological origin, while they are less effective to predict fouling rates when multiple stages of fouling occur.

The correlations between $R_{rev,i}$ and $R_{irr,i}$ with BAP and UAP were examined to assess the impact of the biological origin of effluent organics on fouling reversibility. It was observed that $R_{rev,i}$ and $R_{irr,i}$ values were correlated with both BAP (r = 0.99 and 0.97) and UAP (r = 0.94 and 0.89) concentrations which was consistent with the previous observation that polysaccharides (r = 0.98 and 0.95) and proteins (r = 0.86 and 0.79) contributed to both reversible and irreversible fouling. BAP and UAP have been previously reported to contribute with cake fouling and complete pore blocking in MBRs (Tian et al., 2011). The correlations developed between BAP/UAP and fouling indices can contribute a better understanding of the linkage between factors that impact secondary biological processes rates (i.e. wastewater properties, temperature and operating conditions) and fouling potentials of the SMPs in tertiary membranes.

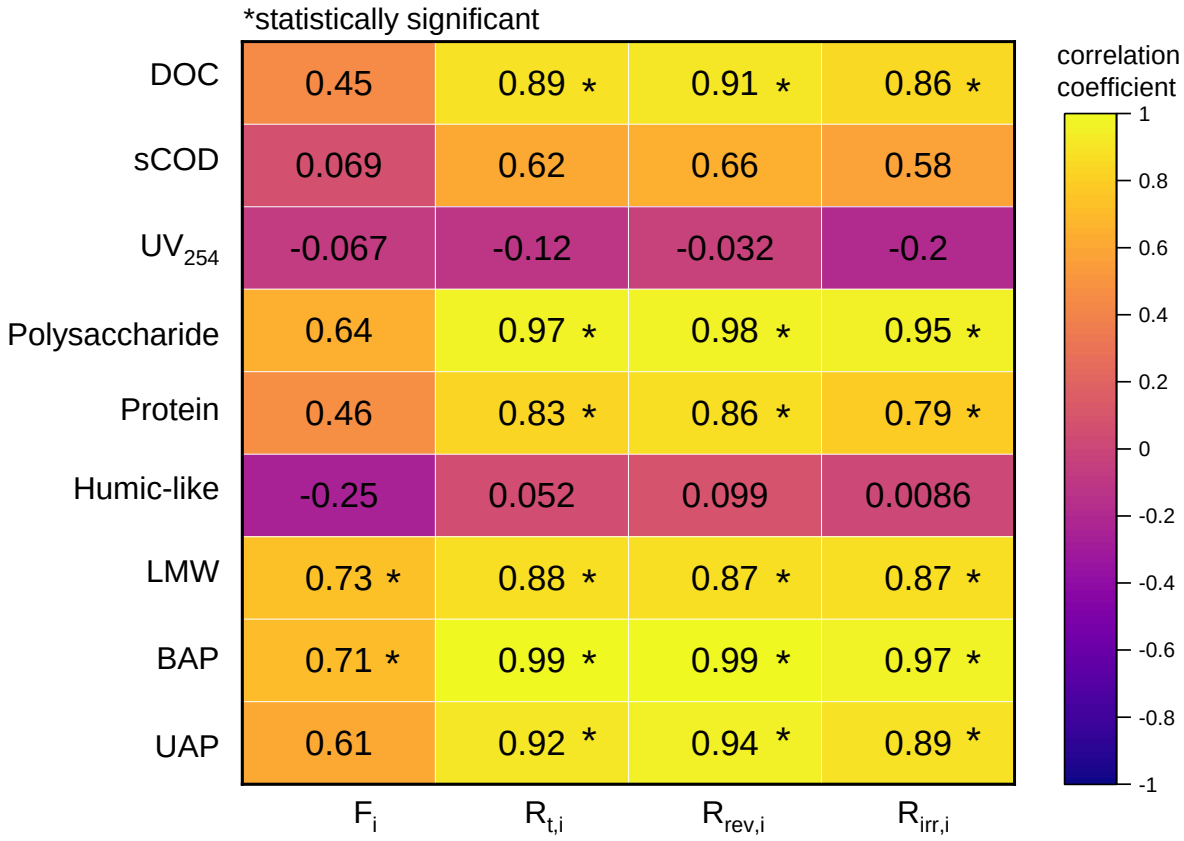

Figure 5-4. Correlation between fouling indices and water quality parameters.

5.3.4 Impact of SBR and filtration temperature on fouling development

The filtration tests generated transient data on TMP development over multiple filtration cycles. The combined fouling models described by Bolton et al. (2006) were therefore employed to translate the transient data into the values of a fixed number of fitted model parameters that could be compared between tests. The fitted model parameters were compared to better understand the impact of SBR and filtration temperatures on fouling development. In the model fitting exercise, the combined cake-intermediate pore blocking model was found to provide the best fit of the data with the lowest value of SSE, indicating the component models (cake and intermediate blocking) were the major contributors to membrane fouling. Hence, only the parameters estimated for the combined cake-intermediate pore blocking model are presented and discussed.

The impact of SBR temperature on the extent of cake fouling and intermediate pore blocking was evaluated by comparing the fitted K_c and K_i values respectively for the filtration tests conducted at 20 ℃ (Table 5-1). The changes in K_c and K_i were statistically tested. It was observed that the values of K_c consistently increased by 140% as SBR temperature decreased from 20 to 8 ℃ ($P<0.05$). In contrast the values of K_i for the effluents from the SBRs operated at 20 and 14 ℃ were similar ($P>0.05$) whereas they increased by over 150% when the SBR temperature decreased to 8 ℃. The increased K_c and K_i values indicate that low SBR temperatures led to both greater cake fouling and intermediate pore blocking while their response to filtration temperature was different.

The effect of filtration temperature on the fouling mechanisms was evaluated by comparing K_c and K_i values obtained at a filtration temperature of 20 ℃ with those obtained when filtration was conducted at SBR temperatures. For the effluent from the SBRs operated at 8 and 14 ℃, the values of K_c significantly increased by over 10 % when the filtration tests were conducted at their corresponding SBR temperatures as compared to 20 ℃. In comparison, the increase of K_i for the effluent from the SBRs operated at 14 and 8 ℃ were both over 11%. The results revealed that reducing the filtration temperature resulted in increases in both cake fouling and intermediate pore blocking.

Table 5-1. Fitted model parameters under different SBR and filtration temperatures.

SBR temperature (℃)	Filtration temperature (℃) (mean ± standard error)	
	20 ℃	Same as SBR temperature
8	$K_c = 5.7 \times 10^6 \pm 1.4 \times 10^5$ $K_i = 9.6 \pm 0.8$	$K_c = 6.3 \times 10^6 \pm 2.0 \times 10^5$ $K_i = 3.8 \pm 0.1$
14	$K_c = 4.0 \times 10^6 \pm 1.1 \times 10^5$ $K_i = 3.4 \pm 0.4$	$K_c = 4.8 \times 10^6 \pm 1.2 \times 10^5$ $K_i = 10.8 \pm 0.7$
20	$K_c = 2.4 \times 10^6 \pm 1.2 \times 10^5$ $K_i = 3.1 \pm 0.4$	N.A.

Linear regression analysis was conducted between the fitted model parameters and the major foulants identified in Section 5.3.3 to further identify the fractions most impacting the fouling model parameters (Figure 5-5). From Figure 5-5 it was observed that the values of K_c were significantly associated with the concentrations of polysaccharides and LMW organics ($P<0.05$), and the regression coefficient was much higher for polysaccharide ($r^2 = 0.89$) than LMW organics ($r^2 = 0.52$). The results indicate that polysaccharides were the dominant contributor to cake fouling and LMW organics has less contribution in this regard.

Similarly, the relationship between K_i and major foulants was studied to identify foulants associated with intermediate pore blocking. The regression analysis revealed that the values of K_i were significantly associated with LMW organics, indicating their dominant role in intermediate pore blocking. This was consistent with a prior study that reported the significant role of LMW fractions in pore blocking when treating secondary municipal wastewater effluent (Gupta & Chellam, 2020).

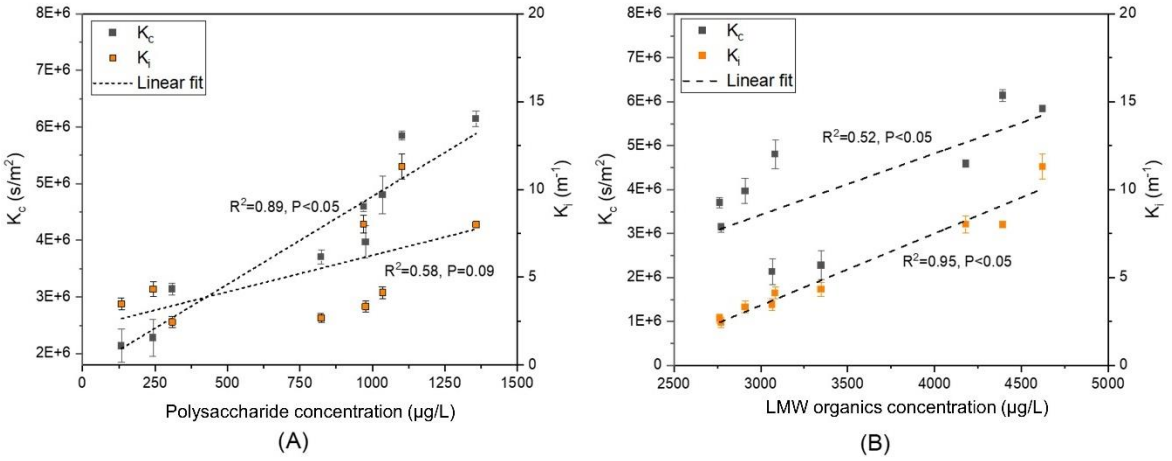

Figure 5-5. Regression between fitted model parameters (K_c and K_i) and concentrations of (A) polysaccharides, and (B) LMW organics.

5.3.5 Effectiveness of back pulsing and air scouring on mitigation of tertiary fouling

In order to provide a point of comparison for assessing the effectiveness of BP/AS for fouling mitigation, additional tests were conducted with flux interruption (FI) alone as a reference condition. The results obtained with FI also provided a qualitative indication of the strength of the attachment of foulants to the membrane for the various effluents. The membrane resistances including $R_{t,i}$, $R_{rev,i}$ and $R_{irr,i}$ that developed in the filtration tests were compared in this regard.

Values of $R_{t,i}$ were compared to evaluate the overall effectiveness of the BP/AS strategy. As illustrated in Figure 5-6, for the effluent from the SBR operated at 8 ℃, the values of $R_{t,i}$ obtained with BP/AS increased less rapidly than those of FI. The vales of $R_{t,i}$ with FI reached a value of 4.7×10^{12} m^{-1} at the 10^{th} cycle at which point the TMP exceeded the range of the pressure transducer. Similarly, the $R_{t,i}$ values for the effluent from the SBR operated at 14 ℃ also developed at a slower rate with BP/AS than FI. In contrast, the values of $R_{t,i}$ for the effluent from the SBR operated at 20 ℃ were similar with BP/AS and FI. The different responses for the three effluents demonstrates that BP/AS presented substantially higher efficiency than FI to control $R_{t,i}$ for low temperature SBR effluents and hence was able to substantially able to remove potential foulants. Since BP/AS provided few additional benefits to reduce R_t due to low level of foulants in the effluent from SBR operated at 20 ℃, the following discussion focused on low SBR temperatures.

The $R_{rev,i}$ and $R_{irr,i}$ were then compared to provide additional insight into the strength of attachment of foulants. It was observed that for the effluent from the SBR operated at 8 ℃ the values of $R_{rev,i}$

were similar for BP/AS and FI. For the effluent from the SBR operated at 14 °C the values of $R_{rev,i}$ with FI were lower than those of BP/AS in the first 15 cycles and then reached similar levels as BP/AS after that. Hence the results indicate a weak attachment between hydraulically reversible foulants and membranes, especially for the SBR operated at 8 °C. In contrast, the values of $R_{irr,i}$ significantly increased when employing FI as compared to BP/AS for both effluents, which suggests a high removal efficiency of irreversible foulants by BP/AS. Hence the test conditions in the present study provided a reasonable delineation of hydraulically reversible and irreversible fouling.

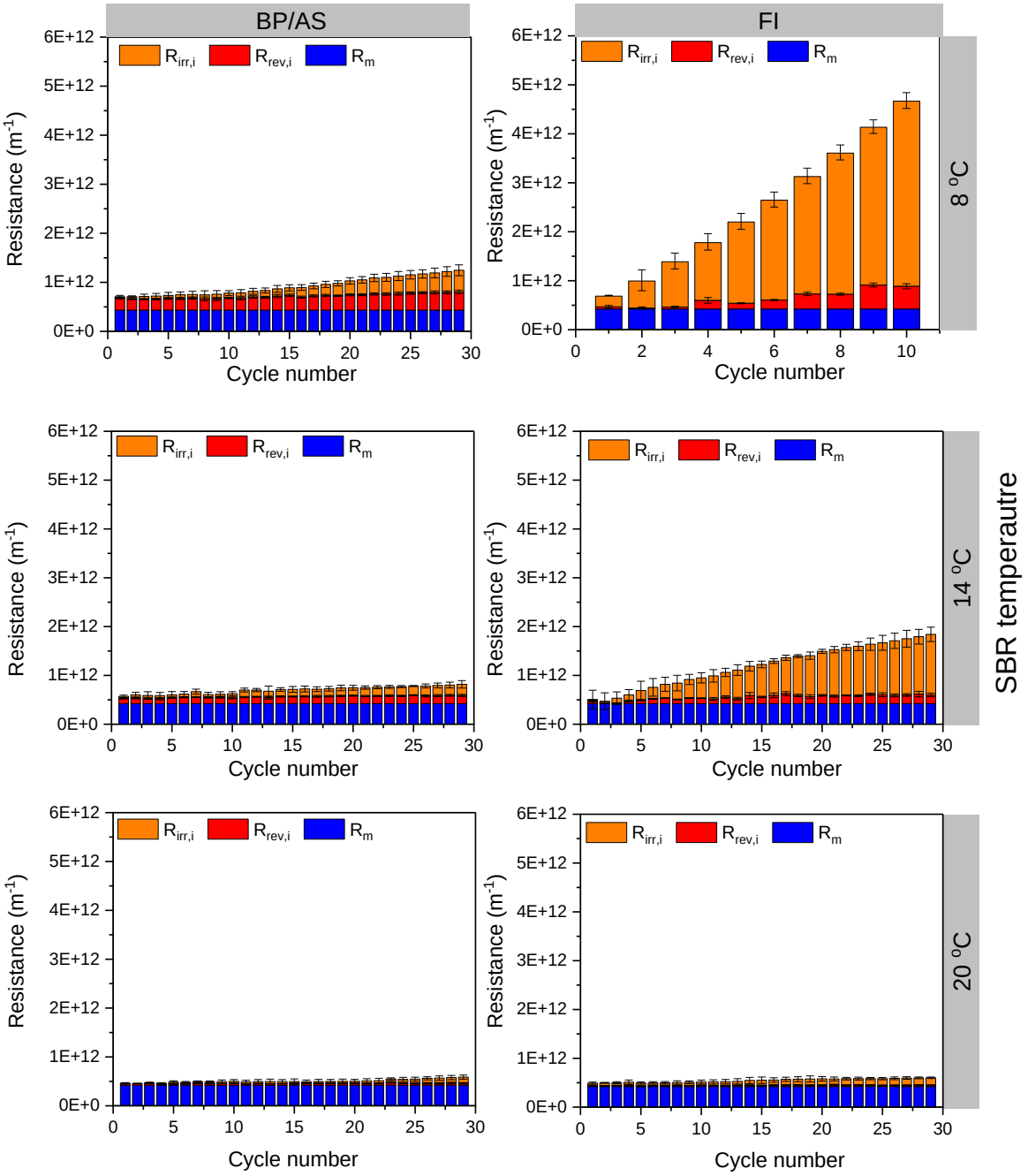

Figure 5-6. Membrane resistances (mean ± standard deviation) with BP/AS and FI.

5.4 Conclusions

The present study for the first time evaluated the impact of secondary operating temperature and filtration temperature on fouling of tertiary membranes. At SBR temperature of 20, 14 and 8 ℃, the increase in total membrane resistances was 27%, 45% and 82% over the multiple filtration cycles, respectively. The increased total membrane resistances accumulated at low SBR temperatures were contributed by both hydraulically reversible and irreversible resistances. Reduction in filtration temperature further induced 122% and 55% increases in total membrane resistances when compared to the filtration temperature of 20 ℃ with the effluents from the SBRs operated at 8 and 14 ℃, respectively. The additional increase in total membrane resistance was attributed to increased intrinsic resistance (35-80%) and viscosity which further induced changed interaction between foulants and membranes. Correlation analyses suggest that total membrane resistance correlated well with DOC ($r = 0.98$) and DOC fractions including polysaccharides, proteins and low MW organics ($r = 0.97$, 0.88 and 0.83). Hydraulically reversible resistance was mainly contributed by polysaccharides ($r = 0.98$) while hydraulically irreversible resistance was explained by both polysaccharides ($r = 0.95$) and LMW organics ($r = 0.87$). Membrane resistances were also strongly correlated to BAP and UAP concentrations that represented mixtures of polysaccharides and proteins. Cake fouling and intermediate pore blocking were dominant fouling mechanisms and they were intensified as SBR temperature decreased from 20 to 8 ℃. The outcomes of the present study provide insights into the combined effects of temperature on biological and filtration processes that influence the fouling behavior of tertiary membranes and can be employed to assist with the design of fouling mitigation measures in cold climates.

Chapter 6

The effect of secondary treatment HRT on SMP production and fouling of tertiary membranes at different temperatures

GRAPHICAL ABSTRACT

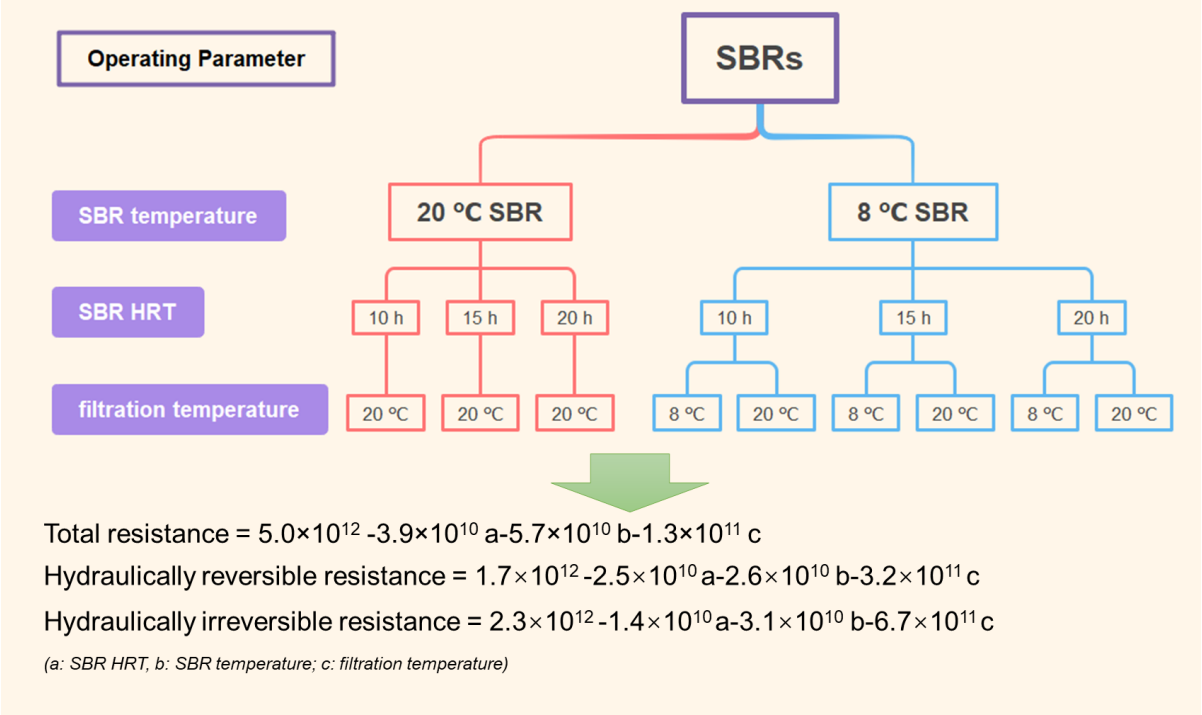

6.1 Introduction

Ultrafiltration (UF) has been considered a promising process for wastewater reuse (Sánchez et al., 2011) due to its efficient removal of particulate/colloidal matter, macromolecules, and pathogens. The application of UF membranes for wastewater treatment and water reclamation is increasing in North America (Yang et al., 2006), Europe (Krzeminski et al., 2017) and China (Yu et al., 2020). Despite the large-scale applications, a major limitation that constrains implementation of UF membrane filtration is membrane fouling. When employed downstream of biological processes (tertiary UF), the

presence of soluble microbial products (SMP) can result in significant fouling leading to increases in transmembrane pressure (TMP) and operating costs (Liu et al., 2019).

The operating conditions of full scale water resource recovery facilities (WRRF) often vary with time of year. In temperate regions WRRFs often need to operate during periods of elevated flow and low temperature that results from processes like snow melt. It is anticipated that climate change will increase the frequency of extreme weather events and cause earlier snowmelts that may accentuate the periods of low temperature and high flow. These challenging operating conditions can be expected to impact on both secondary biological and tertiary UF processes in WRRFs (Holloway et al., 2021).

The impacts of temperature and flow on the production of SMPs in biological processes have been attributed to their influences on substrate utilization, biomass growth and cell decay (Ferrer-Polonio et al., 2018; Soh et al., 2020). Increases in SMP production have been observed in a secondary system when operated at low temperature (Tao et al., 2021). Further, a reduction in HRT was found to enhance growth of biomass and accumulation of SMPs (Tian, et al., 2011; Khan et al., 2013). Low HRTs have also been found to result in increased growth of filamentous bacteria with associated SMP production (Meng et al., 2007). However, the impacts of the interaction between these factors, that may be exacerbated by climate change, on membrane fouling has received little attention.

The performance of tertiary UF membranes can also be directly affected by temperature due to changes in water viscosity and membrane properties. Even without changes in SMP production in the upstream biological process, low temperatures can enhance membrane fouling due to increased viscosity, decreased membrane pore size and reduced shear stress from aeration (van den Brink et al., 2011; Ma et al., 2013). Tao et al. (2022) demonstrated that changes in water viscosity and intrinsic membrane resistance, when the temperature was reduced from 20 to 8 ℃, were responsible for 20–29% of the total decrease in hydraulically irreversible permeability. Despite some studies that have showed the effect of low temperature on physical membrane process, little attention has been paid to the superimposed influence of high flows that often occur simultaneously. In a full-scale tertiary membrane treatment plant in Canada, it was found the fouling rate substantially increased during the period from March to May when seasonally low temperatures and elevated flows were present (Abu-Obaid et al., 2020). It was however not possible to isolate the factors responsible for the elevated fouling in this study.

The primary objective of the present study was to evaluate the impact of secondary system HRT on fouling of tertiary UF membranes over a range of temperatures. This was achieved by using bench scale sequencing batch reactors (SBRs) and filtration tests. The SBRs treated real municipal wastewater over a range of temperatures and HRTs to generate feed water for the tertiary filtration tests. Filtration tests were conducted at 20 ℃ to investigate the effect of secondary system HRT and temperature on tertiary membrane fouling. Subsequent filtration tests were conducted at the source SBR operating temperatures to characterize the effect of filtration temperature on tertiary fouling. The results from LC-OCD and conventional wastewater quality characterization were coupled with activated sludge modelling to interpret the generation of SMP fractions that are relevant to membrane fouling. Fouling models were employed to facilitate data analysis such that the results from the filtration tests could be compared between tests. Correlation analyses were conducted to assist with foulant identification. The outcomes of the present study provide insights into the interaction between HRT and temperature on tertiary membrane fouling which can be employed when designing mitigation strategies.

6.2 Materials and methods

6.2.1 Experimental set-up and operation

Bench-scale SBRs: Two parallel bench-scale SBRs were operated on real municipal wastewater for extended periods (October 2020 to April 2021) at temperatures of 20 ℃ and 8 ℃, respectively. The temperatures are representative of summer and winter operating conditions in a northern climate (e.g. Ontario, Canada). Over the course of the study the HRTs of the SBRs were reduced from 20 h to 15 h and then to 10 h. In each HRT condition, both SBRs reached pseudo steady state before sampling for effluent characterization. The effluents from the two SBRs were collected and analyzed once per week. A detailed description of the design and operation of the SBRs has been provided by Tao et al. (2021).

Membrane modules: Bench scale membrane modules were employed to assess membrane performance in a batch configuration. Each membrane module consisted of three ZeeWeed-1000 hollow-fibres (Suez, Canada). The nominal pore size of the ZeeWeed-1000 membrane is 0.02 μm. The length of each hollow-fibre was 500 mm. The permeate was continuously returned to the filtration tank to maintain a consistent water level and feed composition. A programmable peristaltic pump (OF-07582-00, Cole-Parmer, USA) was used to control the timing of permeation and back

pulsing. An air diffuser was employed to provide aeration for mixing and membrane scouring. A detailed description of the design and operation of the membrane modules has been provided by Tao et al. (2022).

Experimental design: The experimental design employed in this study is illustrated in Figure 6-1. The effluents from the 8 ℃ SBR and 20 ℃ SBR at the three different HRT were employed as feed to the membrane filtration tests. Filtration tests were then conducted at room temperature (~20 ℃) and at the corresponding temperature of the source SBR. This enabled the impacts of temperature on the characteristics of the SBR effluents, the rheological properties of the water, and the membrane properties to be considered independently. Each filtration test was operated in dead-end mode and consisted of 30 permeation cycles that included filtration for 30 min and a combination of back pulsing and air scouring for 120 s. Back pulsing and air scouring were employed to remove hydraulically reversible fouling from the membrane surface and/or in the pores of the membrane. The filtration and back pulsing fluxes were 24 and 48 LMH, respectively. All filtration tests were conducted in triplicate. After each test, the fouled membranes were chemically cleaned using a 250 mg/L NaOCl solution for 2 h and then rinsed by soaking in DI water for 2 h.

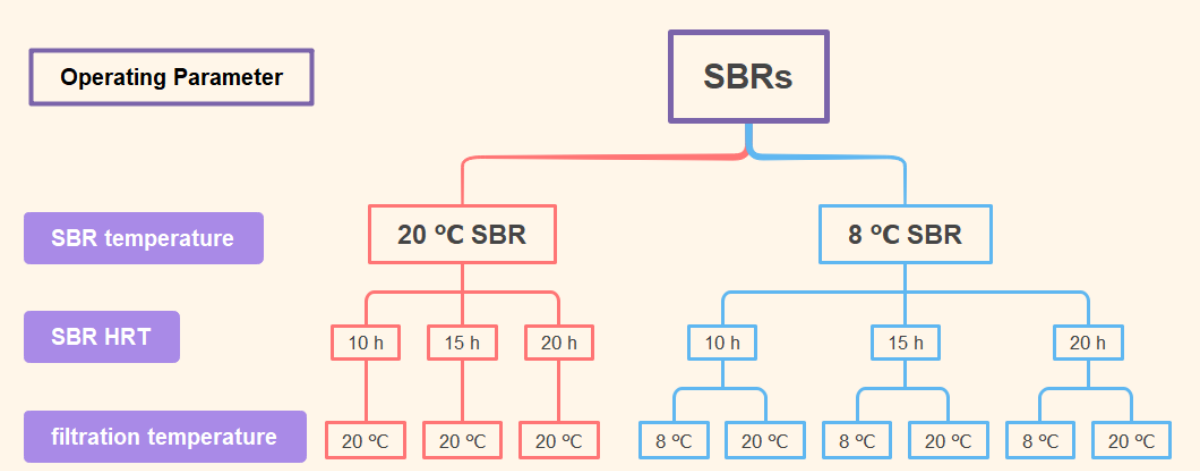

Figure 6-1. Schematic diagram of experiment design.

6.2.2 Membrane fouling analysis

Fouling indices: Four resistance-based fouling indices, based on the resistance-in-series model (Nguyen et al., 2011) were employed to quantify the evolution of fouling in the filtration tests and thereby support a comparison of the various filtration conditions. The total resistance values ($R_{t,i}$) reflected the sum of intrinsic membrane, hydraulically reversible and irreversible resistances in cycle i. Fouling rate values (F_i) quantified the change in total resistance over the multiple filtration cycles. Hydraulically reversible resistance values ($R_{rev,i}$) quantified the resistance that accumulated during a cycle and which was recovered during physical cleaning between cycles. Hydraulically irreversible resistance values ($R_{irr,i}$) were determined as the resistance that accumulated during a cycle which was not removed by physical cleaning. A detailed description of the calculations employed was provided in Chapter 6.

Fouling modelling: Five combined fouling models as proposed by Bolton et al. (2006) were fit to the experimental data. The combined fouling models included cake-complete, cake-intermediate, complete-standard, intermediate-standard and cake-standard models with K_c, K_b, K_i and K_s as fitted parameters to quantify cake fouling, complete blocking, intermediate blocking and standard blocking, respectively. The normalized TMP values (P/P_0) over time from the triplicate runs were simultaneously used in the model fitting. The best fit was determined by minimizing the sum of squared residuals (SSR) where the residual was equal to the difference between measured data and model prediction.

6.2.3 Water quality analysis

Conventional characteristics: Mixed liquor volatile suspended solids (MLVSS) and mixed liquor suspended solids (MLSS) of the SBRs were analyzed in accordance with Standard Methods (APHA, 2005). Total COD (tCOD), soluble COD (sCOD), dissolved organic carbon (DOC), UV_{254} and turbidity of raw wastewater and SBR effluents were measured as indicators of organic matter. Soluble components were obtained by filtering through 0.45 μm nylon filters. tCOD and sCOD were analyzed according to Standard Methods 5220 (APHA, 2005). Filtered samples were analyzed for DOC using a Shimadzu analyzer (TOC-L, Shimadzu, Japan) and for UV absorbance at 254 nm by a spectrophotometer (8453, Agilent, USA). The turbidity of samples was analyzed with a HACH 2100N Turbidimeter. Nitrogen species concentrations were analyzed to indicate the state of nitrification in the SBRs. The filtered samples were analyzed color metrically for Total Kjeldahl nitrogen (TKN), ammonia (NH_4^+-N), nitrate (NO_3^--N) and nitrite (NO_2^--N) (APHA, 2005).

LC-OCD: LC-OCD analysis was used to provide insight into DOC fractions in the raw wastewater and SBR effluents. The samples were filtered with 0.45 μm nylon filters before analysis. The LC-OCD employed three detectors including fixed wavelength UV (UVD), organic carbon (OCD) and organic nitrogen (OND) detection in series. The UVD measured the spectral absorption coefficient at 254 nm. The OCD oxidized organic matter in a UV reactor and the organic carbon was quantified from the produced CO_2. The OND oxidized organic nitrogen and measured the produced nitrate using a UVD operated at 220 nm. Based upon the multiple signals, the LC-OCD analysis reports dissolved organic matter as biopolymers, humic substances, building blocks, low molecular weight (LMW) acids and LMW neutrals (Huber et al., 2011). The biopolymer concentrations reported were then divided into polysaccharide and protein components assuming all of the DON in the biopolymers was bound in proteinaceous matter and employing a typical C:N mass ratio of 3 for proteins (Huber et al., 2011).

6.2.4 SMP modelling

A modified conceptual model describing SMP production (Tao et al., 2021) was employed to explore the effects of SBR HRT and temperature on SMP related biological processes. In the model, BAP originates from active biomass decay while UAP is generated as a product of biodegradable organic matter utilization. The concentrations of BAP and UAP were calculated based on mass balances on polysaccharides and proteins and assuming average values from the literature for the polysaccharide/protein ratios of BAP and UAP (Jiang et al., 2010; Tian et al., 2011). An activated sludge (AS) process model was used to quantify the rates of substrate utilization and endogenous decay processes under the different operating conditions. The modelling was verified by comparing modelled and observed biomass concentrations and total COD treatment performance. Based upon the observed BAP and UAP concentrations and the calculated bioprocess rates, the yields of BAP and UAP were determined for each condition.

6.2.5 Statistical analysis

ANOVA: One-way ANOVA tests were used to determine if there was a statistically significant difference in raw wastewater and SBR effluent characteristics that were generated at the different HRTs. Where appropriate the mean values observed at each operating condition were compared via Tukey tests. Data sets were considered statistically different at a 95% confidence interval ($P<0.05$). The software OriginPro 2020b (OriginLab Inc., USA) was employed to process the ANOVA.

Correlation analysis: Correlation analyses were conducted to assess the relationships between SBR HRT, temperature and conventional effluent quality parameters (turbidity, sCOD, tCOD, DOC, nitrate-N, nitrite-N and ammonia-N). The correlation coefficients ranged between -1 and +1 and quantified the direction and strength of the linear association between the two variables. The software OriginPro 2020b (OriginLab Inc., USA) was employed to process the correlation analysis.

Multiple linear regression: Multiple regression analysis was adopted to describe the relationship between SBR HRT, temperature and filtration temperature and values of total, hydraulically reversible and irreversible membrane resistance determined from the filtration tests. The software SPSS (IBM, USA) was used to process the multiple linear regression.

6.3 Results and discussion

The present study sought to comprehensively investigate the impact of HRT on SMP production and subsequent fouling of tertiary membranes under two secondary and filtration temperature conditions. The analysis involved characterization of SBR performance and conventional effluent qualities, effluent DOC fractions by LC-OCD, and fouling evolution as described by four fouling indices. For the SBR operated at 8 ℃, the additional influence of filtration temperature on water viscosity, membrane property and fouling indices was considered. Combined fouling models were then used to facilitate comparisons between operating conditions. Multiple linear regression analysis was employed to determine the relationships between operating parameters (SBR HRT, temperature and filtration temperature) and membrane resistances ($R_{t,i}$, $R_{rev,i}$ and $R_{irr,i}$), and the relative contribution of each operating parameter was compared.

6.3.1 SBR performance and conventional effluent quality

The steady state secondary effluent quality of the SBRs was assessed at each operating HRT by examining a range of conventional wastewater parameters, including turbidity, sCOD, tCOD, DOC, nitrate-N, nitrite-N and ammonia-N. Since a real wastewater was employed, the characteristics of the raw wastewater observed in this period were initially compared between the three phases of SBR operation using one-way ANOVA to assess the influent stability over long-term operation. The results demonstrated that all of the measured parameters were not significantly different between the phases. Therefore, any difference in SBR effluent quality were attributed to changes in operating parameters rather than raw wastewater properties.

The quantitative correlation between operating parameters of SBRs (HRT and temperature) and conventional effluent quality was elucidated by correlation analysis (Figure 6-2). A P-value below 0.05 was employed to delineate whether the correlations were statistically significant. The overall performance of the biological treatment with respect to carbon removal was assessed by examining effluent tCOD concentrations. Correlation analysis revealed that the tCOD concentrations in the SBR effluents were not significantly correlated with either SBR HRT or temperature ($P>0.05$). This indicates little impact of the two operating parameters on overall biological treatment performance demonstrating the robustness of the SBRs over the range of operating conditions.

The correlation between soluble carbon related metrics (DOC and sCOD) and SBR HRT and temperature was assessed since soluble components have been demonstrated to be major foulants in tertiary fouling (Yang et al., 2021). It was observed that both of the metrics were not significantly correlated with SBR HRT. In contrast, the DOC concentration was negatively correlated with SBR temperature ($P<0.05$) with a correlation coefficient of -0.95. The increased DOC concentrations as SBR temperature decreased were attributed to reduced biological growth and decay at lower temperatures (Lishman et al., 2000). The results indicate that the total soluble carbon concentrations were significantly affected by the operating temperature of the SBRs.

The turbidity, an indicator of the presence of particulate matter, was examined as an indirect measure of the performance of the activated sludge processes. As illustrated in Figure 6-2, effluent turbidity presented no correlation with SBR HRT. However, a strong correlation between effluent turbidity and SBR temperature ($r = -0.93$) was identified. With the decrease in SBR temperature, effluent turbidity significantly increased which suggested a reduction in the capture of particulate matter into the activated sludge floc under low temperature conditions. Hence, it was anticipated that the effluents from the SBR operated at the lower temperature would have a greater fouling potential of the tertiary UF membranes.

The impact of the SBR operating conditions on nitrogen related metrics, and hence associated biological process activities, was examined through correlation analysis. Nitrate-N presented a relatively strong correlation with SBR HRT ($r = 0.81$); however, the removal of ammonia was not correlated with either SBR HRT or temperature (data not shown). Besides nitrification, nitrate-N can also be generated from endogenous decay. It has been demonstrated by Corsino et al. (2020) that the endogenous decay coefficient increased by 85% when HRT was extended from 6 h to 10 h to reach a substrate-limitation condition. In contrast, the nitrogen related metrics were not correlated with SBR

temperature. Hence, the observed increased concentrations of nitrate-N at higher HRTs was attributed to the increased endogenous decay of biomass at the high HRT conditions. The contribution of substrate utilization and endogenous decay to generation of UAP and BAP will be discussed subsequently.

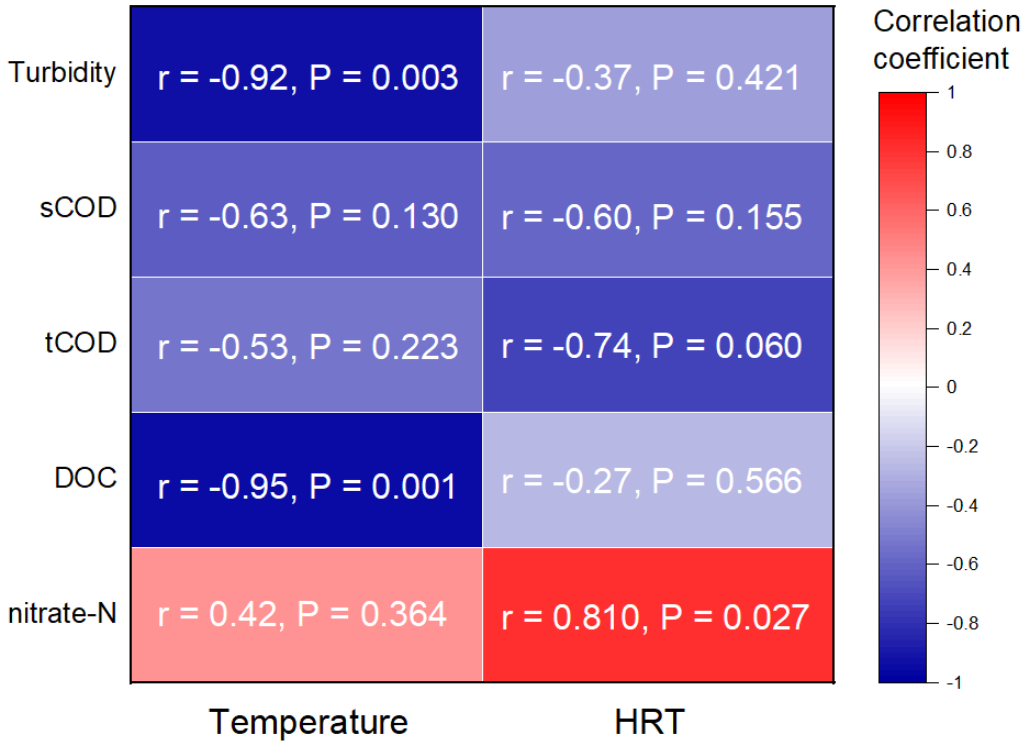

Figure 6-2. Correlations between conventional effluent parameter concentrations and SBR operating conditions.

6.3.2 Dissolved organic matter speciation

Fouling of tertiary membranes has been demonstrated to be associated with specific DOC fractions in secondary effluents (Ferrer-Polonio et al., 2018). Therefore, the effect of SBR HRT on the DOC fractions under the two SBR temperatures was assessed from the perspective of molecular weight and composition as reported by LC-OCD (Figure 6-3).

The polysaccharide and protein fractions are classified as high molecular weight (MW) organics (>10 kDa) and have been reported to cause more severe membrane fouling than the other fractions

(Chen et al., 2021; Huber et al., 2011). The effect of HRT on the concentrations of the high MW organics for the effluent from the SBR operated at 20 ℃ was initially evaluated as a reference condition. It was found the concentrations of high MW organics in the effluent from the SBR operated at 8 ℃ were consistently higher than those of 20 ℃. As illustrated in Figure 6-3A, the concentrations of high MW organics increased 141% for the effluent from the SBR operated at 20 ℃ as HRT decreased from 20 to 10 h. The corresponding increase for the effluent from the SBR operated at 8 ℃ was only 60%. Hence, as HRT decreased the concentrations of high MW organics increased and the increase percentage was greater for the effluent from the SBR operated at 20 ℃.

Polysaccharides and proteins were demonstrated to present different fouling potentials (Tao et al., 2022) and therefore their concentrations were analyzed separately. The concentrations of polysaccharides and proteins were higher in the effluent from the SBR operated at 8 ℃ than that of 20 ℃ regardless of HRT. For the effluent from the SBR operated at 20 ℃, the concentrations of polysaccharides and proteins increased by 201% and 64% respectively as HRT decreased from 20 to 10 h. Similarly, the increases were 77% and 29% respectively for the effluent from the SBR operated at 8 ℃. It was noted that the higher increased percentages for the SBR operated at 20 ℃ were because of their lower initial values; however, the values of polysaccharides and proteins in the effluent from the SBR operated at 8 ℃ were much higher than those of 20 ℃.

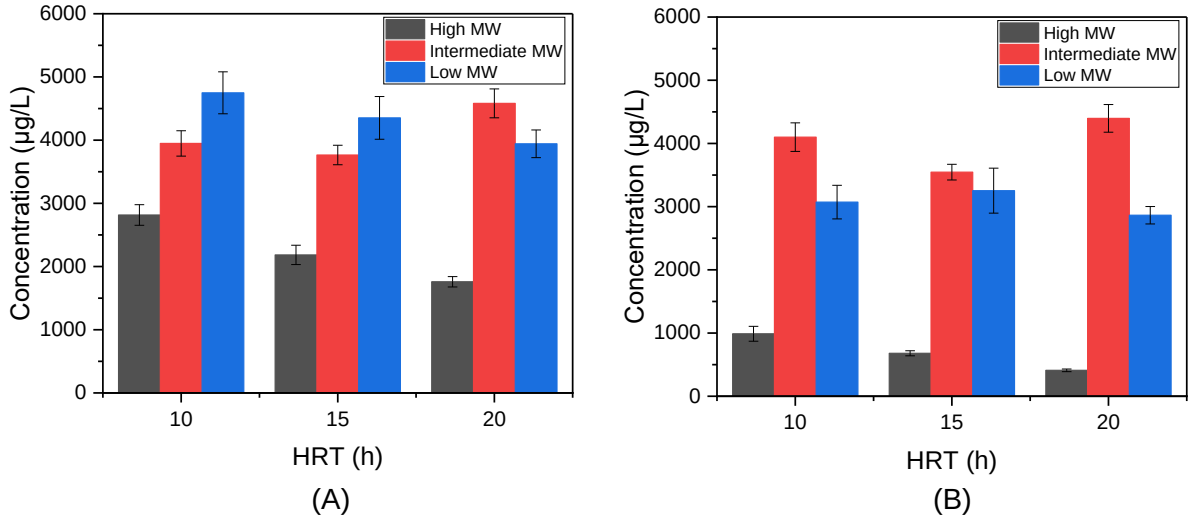

Figure 6-3. Concentrations (mean ± standard deviation) of DOC fractions by LC-OCD for the effluent from the SBR operated at (A) 8 ℃ and (B) 20 ℃.

LMW organics have been reported to adsorb to membranes and result in hydraulically irreversible fouling (Ayache et al., 2013) and therefore they were compared under the different conditions. The concentrations of LMW organics were consistently higher in the effluent from the SBR operated at 8 ℃ than those of 20 ℃. For the LMW organics from the SBR operated at 20 ℃, the concentration increased by 7% as HRT decreased from 20 to 10 h. The corresponding increased percentage for the effluent from the SBR operated at 8 ℃ was 20%. Hence, reduced HRT led to greater generation of LMW organics with the extent of the impact higher for the low temperature SBR.

The remaining DOC fraction reported by the LC-OCD analysis consisted of humic-like substances, that have been reported to make minimal contributions to fouling of membranes in wastewater treatment (Deng et al., 2019; Yu et al., 2016). From Figure 6-3, it was observed there was no particular trend in the concentrations of humic-like substances with either SBR HRT or temperature. The results were consistent with those of Tao et al. (2022) that found their presence in secondary effluents could be attributed to raw wastewater properties with no impact of secondary operating conditions. Hence, humic-like substances were not considered in the subsequent analysis of the impacts of operating conditions on fouling of tertiary membranes.

6.3.3 SMP modelling

The DOC fraction data indicated that the impact of HRT on generation of SMPs was influenced by SBR temperature. Hence, the relationship between SMP generation and the corresponding biomass growth and decay rates were analyzed to obtain insights into the mechanisms of SMP generation. The wastewater was initially fractionated into biodegradable soluble organic matter (OM), biodegradable particulate OM, non-biodegradable soluble OM and non-biodegradable particulate OM as per the protocols described by Melcer et al. (2003). A steady state analytical process model of the SBRs was then implemented using the fractionated wastewater components to allow for estimation of growth and decay rates (Tao et al., 2021).

The wastewater fractionation and activated sludge modelling were verified by comparing the observed and modelled MLVSS concentrations and COD removal as indictors of the fit of the model to the data (Figure 6-4). It was observed that there was a close correspondence between the observed and modelled MLVSS and COD removals over the range of operating HRT for the SBRs operated at 20 and 8 ℃. The differences between observed and modelled MLVSS and COD removal were less than 9% and 3% respectively for both SBRs. Hence, the model predictions and experimental data

agreed well suggesting the validity of this approach for estimating effluent quality and process rates determination under different operating conditions.

In order to obtain insight into how HRT impacted biomass growth and decay processes, the estimated viable biomass concentrations were compared under tested conditions. The viable biomass concentrations were observed to be consistently higher in the SBR operated at 8 ℃ than those of 20 ℃. For the SBR operated at 20 ℃, the decrease in HRT from 20 to 10 h resulted in 146% increase (1,660 mg COD/L) in the viable biomass concentration. In the SBR operated at 8 ℃, the viable biomass concentration presented a similar percentage increase (145%) however, the magnitude of the increase (2,929 mg COD/L) was much higher than that of 20 ℃. Hence the impact of HRT on viable biomass concentrations was greater at low SBR temperature.

The biomass growth and decay rates were then assessed to gain insights into the biological processes that led to the observed impacts of HRT and temperature on the biomass concentrations. For the effluent from the SBR operated at 20 ℃, the biomass growth rates were consistently higher than those of biomass decay rates resulting in a net accumulation of biomass concentration. Furthermore, the difference in biomass growth rates and decay rates increased as HRT decreased for the SBR operated at 20 ℃ and therefore this led to increased viable biomass concentrations. The biomass growth and decay rates for the SBR operated at 8 ℃ presented similar trends to those of 20 ℃, however, the differences between biomass growth and decay rates were higher and also increased to a greater extent as HRT decreased than those of 20 ℃ . Therefore, reducing HRT resulted in increased biomass concentrations, and these concentrations were higher for the SBR operated at 8 ℃ than that of 20 ℃ at each HRT.

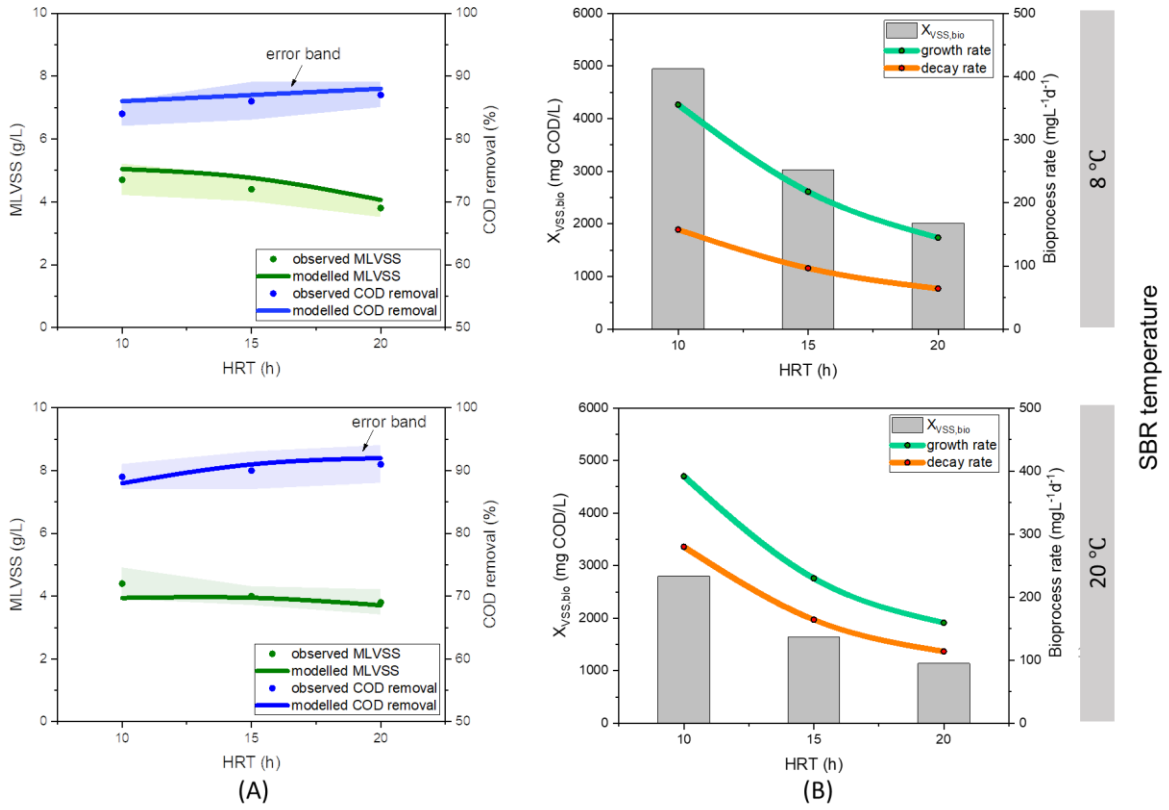

Figure 6-4. (A) Observed and modelled MLSS and COD removal (Error band presents the standard deviation of observed MLVSS and COD removal) and (B) Estimated biomass concentration and bioprocess rates.

The established rates of substrate use and endogenous decay were subsequently employed to estimate the BAP/UAP yields as a function of HRT. UAP yield coefficients were calculated as the ratio of the observed UAP production to substrate utilization (Tao et al., 2021). Figure 6-5 presents the calculated yield coefficients versus HRT at the two SBR temperatures. It can be observed that the UAP yield coefficients substantially decreased as HRT decreased with the data from the SBR operated at 8 ℃ being higher and more sensitive than those of 20 ℃. Despite the UAP yield decrease, total production of UAP which is composed of polysaccharides and proteins increased (data not shown) when HRT decreased, which can be attributed to increased concentration of biomass induced by low HRT.

The BAP yields coefficients were calculated as the ratio of observed BAP production to endogenous decay rates. From Figure 6-5, it was observed that BAP yields were relative stable over the range of HRTs examined. However, the BAP yields coefficients were greater for the SBR operated at 8 ℃ than that of 20 ℃, which indicated SBR temperature presented higher influence on BAP yields than HRT. This might have been due to the more significant role of temperature on biomass decay kinetics (Ni et al., 2011). It has been demonstrated in Chapter 5 that BAP and UAP can provide similar insights with polysaccharides and proteins into total fouling and fouling reversibility of tertiary membranes. The determination of BAP/UAP yields and rates of biomass growth and decay can serve as a guidance for the optimization of secondary operation and fouling mitigation of tertiary membranes (Tian et al., 2011).

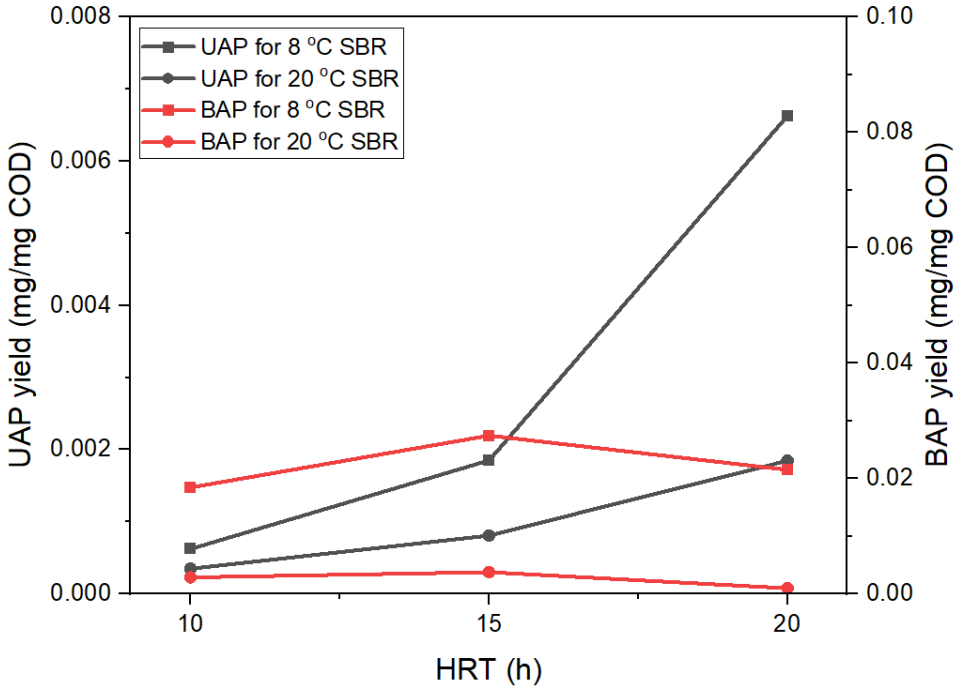

Figure 6-5. BAP/UAP yields coefficients versus HRT.

6.3.4 Tertiary fouling evolution

The effects of SBR HRT and temperature on fouling evolution were evaluated by examining fouling indices that were developed from the filtration tests. The data from the filtration tests that were

conducted at 20 ℃ was initially assessed to obtain insights into the effects of SBR HRT and temperature. Then the results from the filtration tests that were conducted with the effluent from the SBR operated at 8 ℃ and a filtration temperature of 8 ℃ were analyzed to assess the interacted influence of filtration temperature and SBR HRT.

$R_{t,i}$ values (Figure 6-6) were examined to assess the trends in the combined R_m, $R_{rev,i}$ and $R_{irr,i}$ values over the multiple filtration cycles. In general, the $R_{t,i}$ values for the effluent from the SBR operated at 20 ℃ were substantially lower than those of 8 ℃. As the HRT of the SBR that was operated at 20 ℃ was reduced from 20 to 10 h, the final $R_{t,i}$ value increased by 3.6×10^{11} m^{-1} with a percentage increase of 38%. For the effluent from the SBR operated at 8 ℃, the corresponding increase was 4.3×10^{11} m^{-1} (26%). Hence, reducing the HRT induced a moderate increase in the overall R_t values and the increase was similar for SBRs operated at the two tested temperatures.

The values of R_m, $R_{rev,i}$ and $R_{irr,i}$ were then assessed separately to determine how SBR HRT and temperature influenced the contribution of each resistance to $R_{t,i}$. The values of R_m of the used membranes were initially evaluated at 20 ℃ and found to be similar for all the tests ($4.4 \times 10^{11} \pm 5.0 \times 10^{9}$ m^{-1}). Hence, for the filtration tests that were conducted at 20 ℃ the changes of $R_{rev,i}$ and $R_{irr,i}$ values were deemed to be responsible for the changes in $R_{t,i}$ values.

The values of $R_{rev,i}$ were assessed to obtain insights into the reversibility of fouling with effluents generated at the different HRTs (Figure 6-6). The values of $R_{rev,i}$ for the SBR operated at 8 ℃ were consistently higher than those of 20 ℃. Moreover, $R_{rev,i}$ values were observed to be relatively constant over the multiple filtration cycles indicating stable attachment and detachment processes for reversible foulants and hence the average $R_{rev,i}$ over the multiple filtration cycles were compared at different HRT. For the effluent from the SBR operated at 20 ℃, the average $R_{rev,i}$ increased by 1.6×10^{11} m^{-1} (454%) as HRT decreased from 20 to 10 h. The corresponding increase for the effluent from the SBR operated at 8 ℃ was 1.5×10^{11} m^{-1} (52%). The results indicate that reduction in HRT induced more hydraulically reversible fouling and the increase in reversible fouling was greater for the SBR operated at 20 ℃. It has been demonstrated in Chapter 5 that hydraulically reversible resistances were highly contributed by polysaccharides concentrations. Hence the lower increase in $R_{rev,i}$ with HRT for the SBR operated at 8 ℃ was consistent with the reduced increase in high MW organics concentration as reported in section 6.3.2.

The effects of HRT on $R_{irr,i}$ values were assessed as irreversible fouling can significantly impact long-term membrane performance. $R_{irr,i}$ values consistently increased over the multiple filtration

cycle. Hence the increase in $R_{t,i}$ values over the multiple filtration cycles was mostly attributed to the increase in $R_{irr,i}$ values. The values of $R_{irr,i}$ were also consistently higher for the effluent from the SBR operated at 8 ℃ than 20 ℃. As HRT decreased from 20 to 10 h, the final value of R_{irr} increased by 1.3×10^{11} m^{-1} (104%) for the effluent from the SBR operated at 20 ℃. The corresponding increase for the effluent from the SBR operated at 8 ℃ was 2.0×10^{11} m^{-1} (47%). The greater increase in $R_{irr,i}$ values for the SBR operated at 8 ℃ was likely due to the greater production of LWM organics at 8 ℃ (Liu et al., 2020) as presented in section 3.2.

F_i values that reflected the rate of development of $R_{t,i}$ over the multiple filtration cycles were calculated to provide preliminary evidence of fouling mechanisms (Figure 6-7). The slopes from linear regression of the F_i values versus cycle number were used to assess the different stages of fouling development. The regression equations for which the slopes were significantly different from 0 are presented in Figure 6-7. A one stage development of F_i was observed for the effluent from the SBR operated at 20 ℃ with slopes of 3.5×10^7 and 7.6×10^7 m^{-1}/cycle when the HRT was 20 and 15 h, respectively. At an HRT 10 h, the F_i values followed a two stage pattern with slopes of 7.8×10^7 and 1.3×10^8 m^{-1}/cycle for the first and second stages. The different trends in fouling rate development suggest that fouling mechanism changed with the HRT of the SBR.

F_i values with the effluent from the SBR operated at 8 ℃ were then compared with that of 20 ℃ effluent. It was observed that at HRTs of 20 and 15 h, F_i values followed a two-stage pattern with the slopes of the second stage higher than that of the first stage. However, this pattern changed when the HRT further decreased to 10 h. At the lowest HRT of 10 h, the fouling development was faster in the initial cycles and the first phase slope was not observed. Moreover, it was found the slopes of the regression for the SBR operated at 8 ℃ were consistently higher that those observed for 20 ℃. Kimura et al. (2015) indicated that initial membrane fouling was due to pore blocking by low MW organics and this was followed by cake fouling with relatively high MW organics. Hence the increased slope of the first stage might be due to accelerated pore blocking by low MW organics generated at low HRT. The changed pattern of fouling rates also indicate fouling mechanism might change with the HRT for the SBR operated at low temperature.

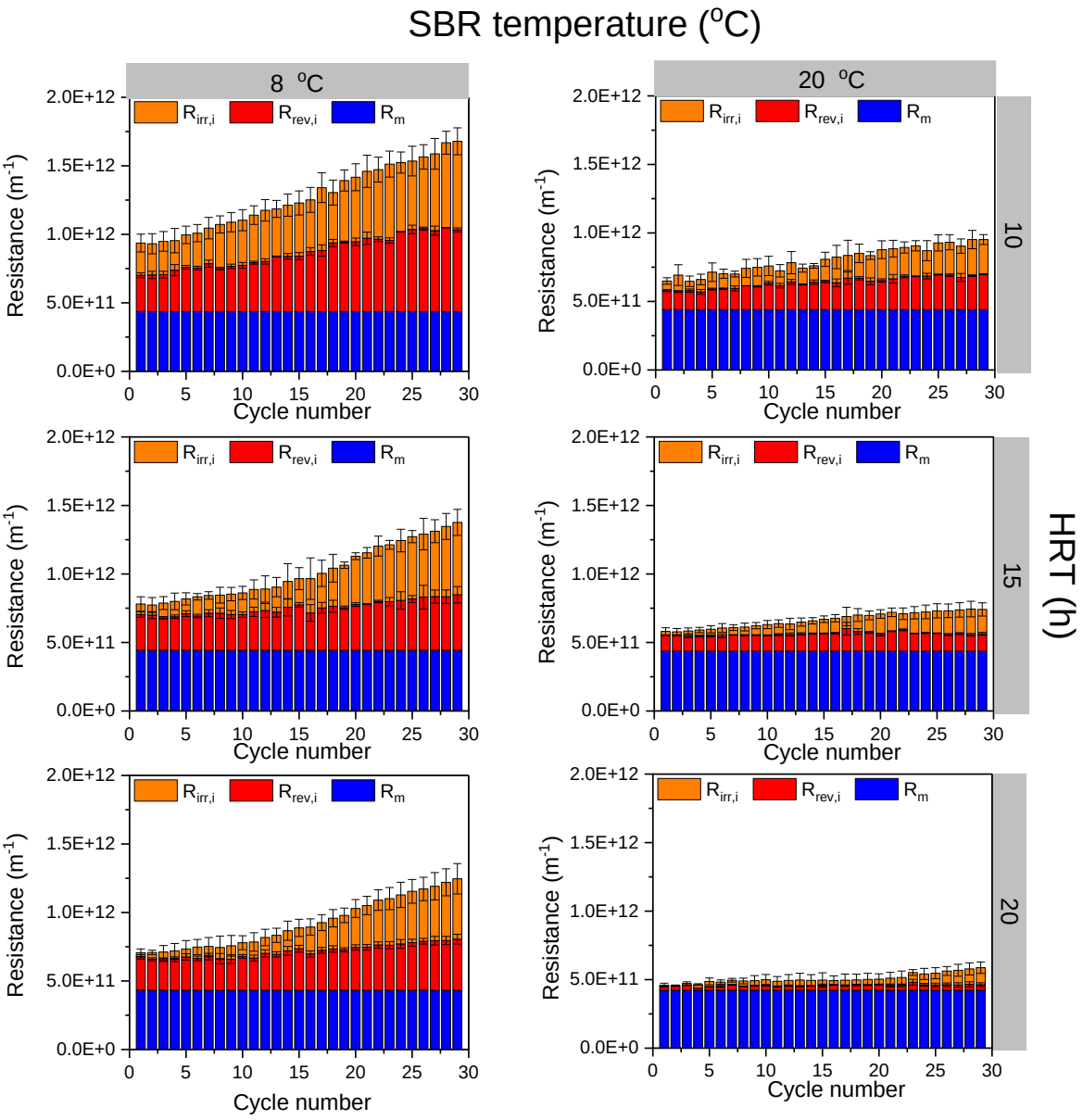

Figure 6-6. Membrane resistances (mean ± standard deviation) observed at different HRT. ($R_{t,i}$ values are indicated by the total height of the column in each cycle.)

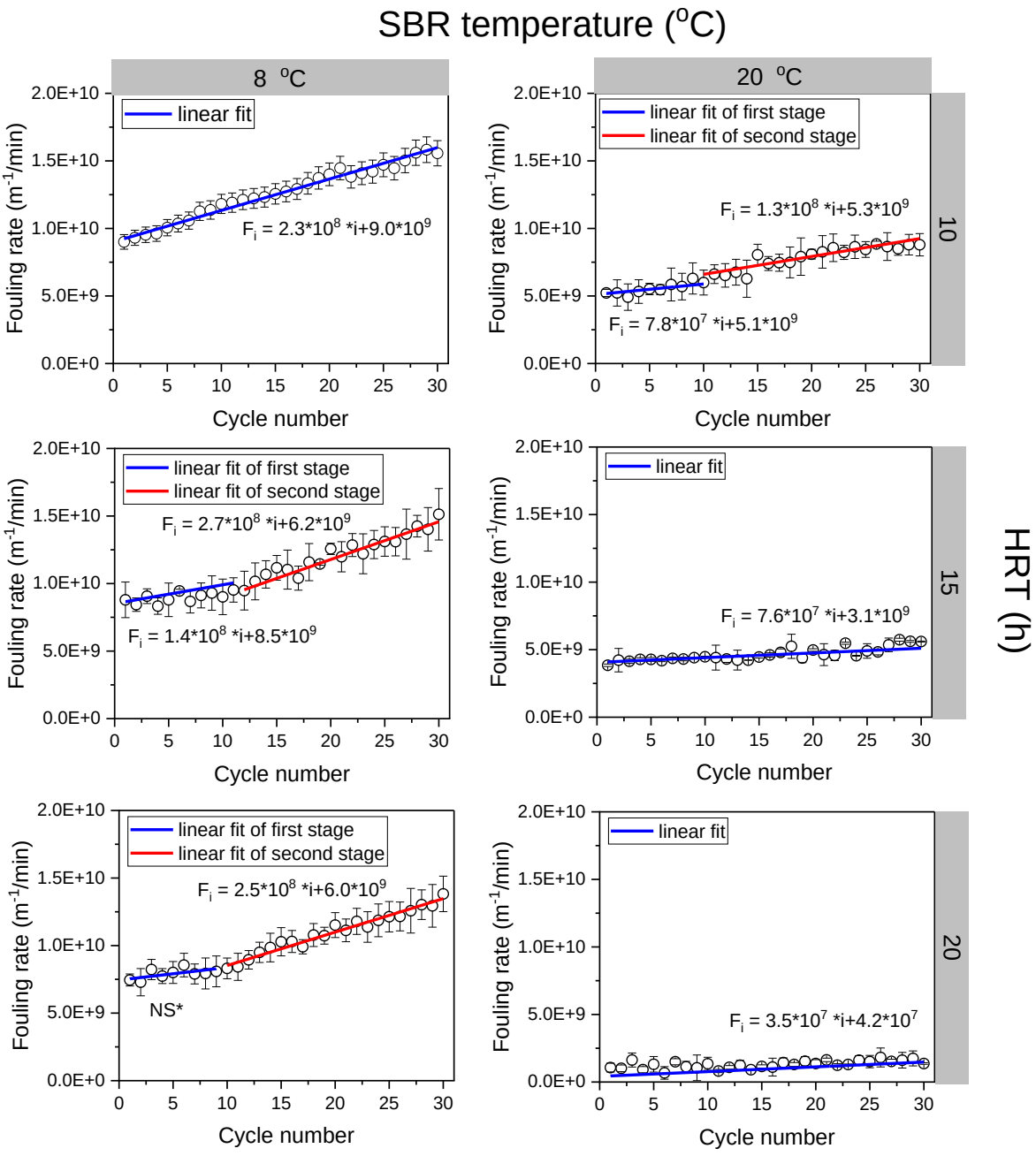

Figure 6-7. Fouling rates (mean ± standard deviation) observed at different HRT. (NS*: slope is not significantly different from 0).

A previous study demonstrated that reducing the filtration temperature can result in increased membrane fouling for tertiary treatment due to increased viscosity and intrinsic membrane resistance and a change in the interaction between the membrane and foulants (Tao et al., 2022). In order to investigate whether this influence would vary under different HRTs, additional filtration tests were conducted at 8 ℃ with the effluents from the SBR operated at 8 ℃.

The values of $R_{t,i}$ for the filtration tests conducted at 20 and 8 ℃ with the effluent from the SBR operated at 8 ℃ were compared to get insights into the influence of filtration temperature on total membrane fouling as a function of HRT (Figure 6-8). It was observed the values of $R_{t,i}$ for the filtration temperature of 8 ℃ were substantially higher than those observed at 20 ℃. At an HRT of 20 h, the difference in $R_{t,i}$ values between filtration temperature of 20 and 8 ℃ at the end of the filtration was 1.2×10^{12} m^{-1}, whereas this value significantly increased to 1.7×10^{12} m^{-1} ($P<0.05$) as HRT reduced to 10 h. Hence the impacts of filtration temperature on total membrane fouling were magnified at low HRT condition.

It has been demonstrated in our previous research that reducing filtration temperature from 20 to 8 ℃ resulted in a 43% increase in R_m (Tao et al., 2022). Therefore, the difference in R_m values ($R_{m,8℃}$ - $R_{m,20℃}$) were deducted from the $R_{t,i}$ values at the filtration temperature of 8 ℃ to exclude the influence on R_m and assess if there were differences in the residual differences as a function of HRT. Figure 6-8 presents the R_m corrected $R_{t,i}$ for the tests at the filtration temperature of 8 ℃. It was observed from Figure 6-8 that after the correction, there was still a substantial difference between the two filtration temperatures, and the difference consistently increased over the multiple filtration cycles. The difference demonstrates that beyond the impact on R_m the low filtration temperatures also changed the interaction between the membrane and foulants leading to increased development of $R_{t,i}$. At lower filtration temperatures, the pores of membranes are expected to be smaller and therefore more foulants are likely to be retained by membranes (Cui et al., 2017). Moreover, it was found the difference at the end of the filtration increased by 64% as HRT decreased from 20 to 10 h. The greater impacts of filtration temperature at low HRT can be attributed to higher concentrations of high and low MW organics generated at low HRT. To sum up, in practice the effect of filtration temperature on membrane fouling cannot be neglected and this effect would result in greater increase in membrane fouling at low HRT conditions.

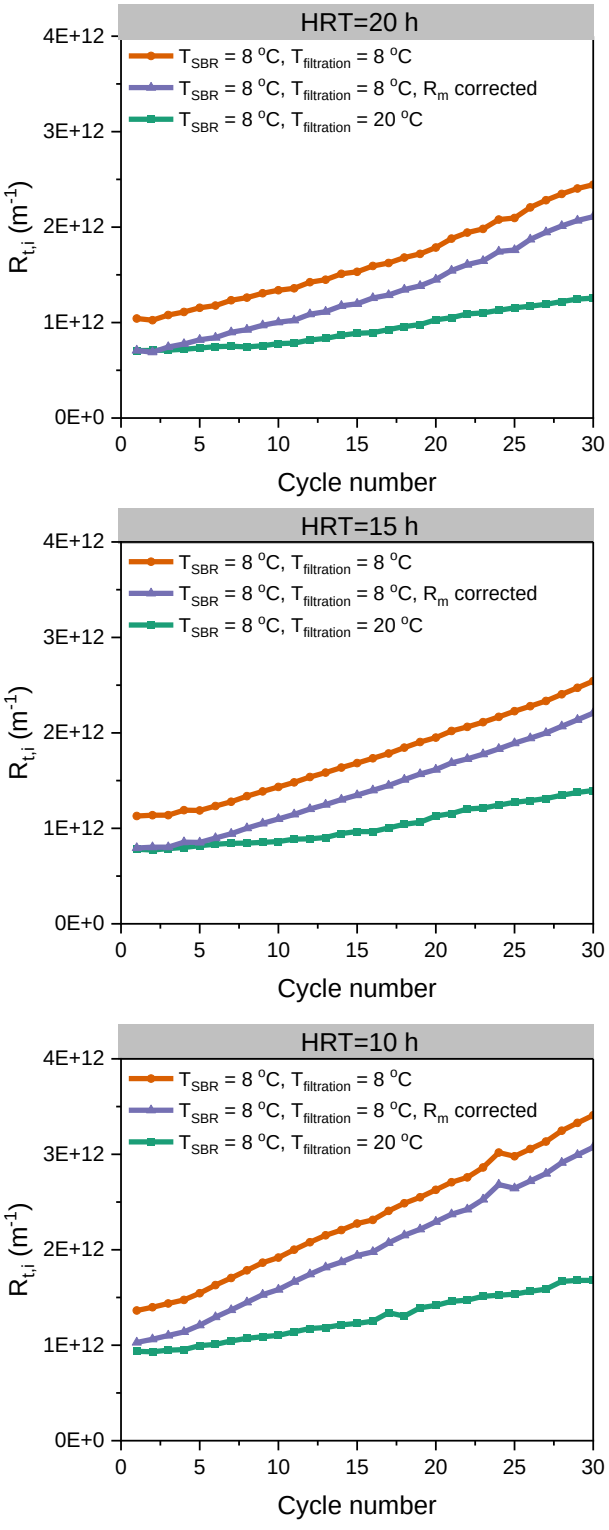

Figure 6-8. Observed and corrected $R_{t,i}$ for the effluents from the SBR operated at 8 °C.

6.3.5 Modelling of membrane filtration process

Combined fouling models were used to facilitate comparisons between operating conditions. It was found that the cake-intermediate blocking model best fit the experimental data. The mean values of SSE for all the filtration tests were less than 2 and r^2 values were greater than 0.87, indicating good fit of the model.

The impact of HRT on the extent of cake fouling was evaluated by comparing the fitted K_c for the filtration tests (Figure 6-9). It was observed that the K_c values presented similar increasing trends with HRT, however, the magnitude of the increases for the SBR operated at 8 ℃ were substantially higher than that of 20 ℃. The higher magnitude of K_c values for the SBR operated at 8 ℃ was likely be due to the higher concentrations of high MW organics in the effluents.

Similarly, the values of K_i were compared to obtain insights into the effect on intermediate pore blocking. At the HRT of 20 h, the value of K_i was higher for the SBR operated at 8 ℃. With the decrease in HRT, the values of K_i significantly increased and the increases for the SBR operated at 20 ℃ were greater than that of 8 ℃. The increased K_i values at reduced HRTs could be attributed to both increased generation of low MW organics and changes in floc formation at short HRTs. Kimura & Kume (2020) has demonstrated that the flocs concentration can reduce pore-blocking in UF by sorption of low MW organics onto the surface of the flocs. It was previously demonstrated in Section 6.3.1 that the flocs concentration was higher in the effluent from the SBR operated at 8 ℃. Hence, despite the concentration of low MW organics increased as HRT decreased for both SBRs, the higher concentration of flocs led to less increase in pore blocking in the effluent from the SBR operated at low temperature.

The relative contribution of the cake layer and pore blocking to overall TMP development was evaluated on the basis of the values of the ratio K_c*J_0/K_i (Figure 6-9) (Bolton et al., 2006). The average values of K_c*J_0/K_i were greater than 2.5 for all SBR temperature and HRT combinations, indicating that cake fouling played a more important role during the filtration. It was also observed that with the decrease in HRT from 20 to 10 h, the contribution of cake fouling increased as indicated by increased values of K_c*J_0/K_i. This change was attributed to different combinations of high and low MW organics at different HRTs. As previously demonstrated, when the HRT was reduced from 20 to 10 h, the ratio of the concentrations of high to low MW organics increased from 14 to 32% for the SBR operated at 20 ℃ and from 44 to 59% for the SBR operated at 8 ℃. Hence the increased ratio of high to low MW organics, as HRT decreased, likely resulted in a greater contribution of cake fouling.

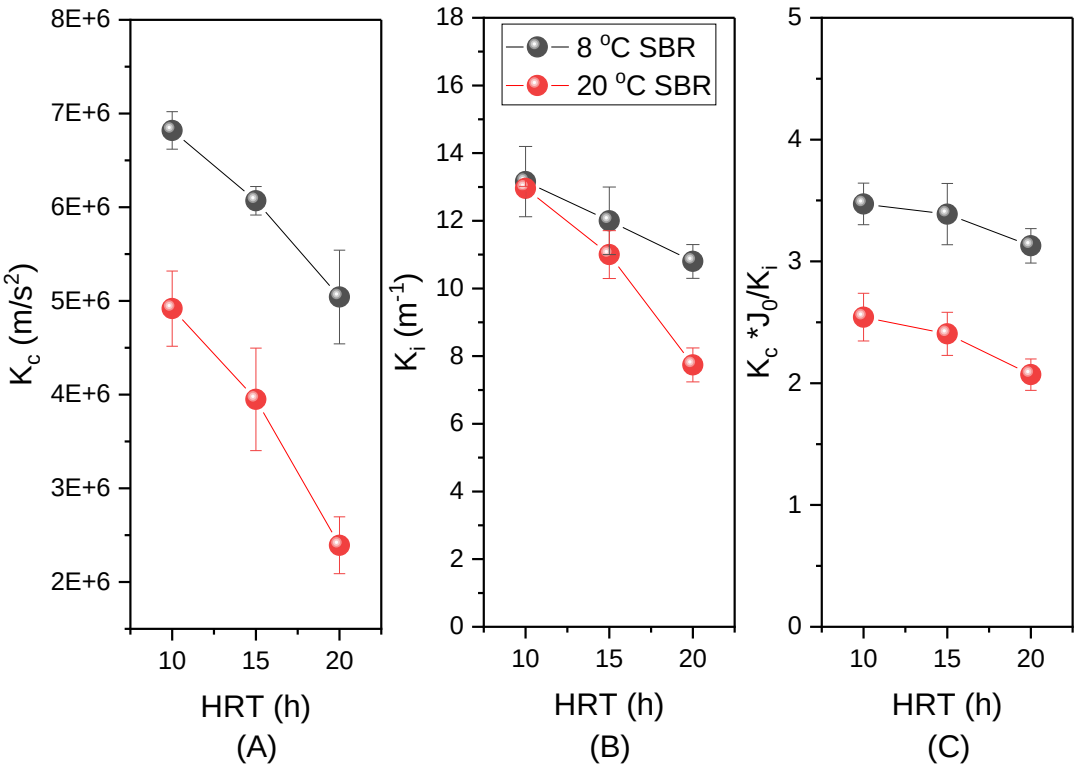

Figure 6-9. Fouling model fitting parameters (A) K_c, (B) K_i and (C)K_c*J_0/K_i as a function of HRT for SBRs operated at 8 and 20 ℃.

6.3.6 Combined factors affecting membrane resistances

The relationship between the operating variables (SBR HRT, temperature, filtration temperature) and fouling indices ($R_{t,i}$, $R_{rev,i}$ and $R_{irr,i}$ in the final cycle of filtration test) were examined using multiple linear regression analysis to obtain insight into the contribution of each operating parameter to fouling. The values of variance inflation factors of independent variables were less than 2 in the present study, indicating no multicollinearity for each of the independent variables (Wang et al., 2018). The regression models were all statistically significant ($P<0.05$), and the values of r^2 were all above 0.95 indicating strong linear relationships. The contribution of SBR HRT, temperature and filtration temperature to membrane resistance was determined by comparing absolute values of standardized coefficients of each operating condition, where the greater the absolute value of standardized coefficients, the greater influence of corresponding variables (Wang et al., 2018).

The contribution to total fouling was initially analyzed and the multiple linear regression results of $R_{t,i}$ are listed in Table 6-1. Generally, $R_{t,i}$ values were negatively related to SBR HRT, temperature and filtration temperature which indicates that increasing the values of these factors would be beneficial to mitigate total membrane resistance. Moreover, it was found filtration temperature was the most important factor influencing $R_{t,i}$ followed by SBR temperature and HRT according to the comparison of standardized coefficients. The substantial influence of filtration temperature on $R_{t,i}$ can be attributed to the significant change in R_m which was previously demonstrated. In addition, reducing filtration temperature resulted in greater retainment of effluent organics due to smaller membrane pore size, which also contributed greatly to $R_{t,i}$. The higher contribution of SBR temperature than HRT indicates that SBR temperature induced higher change in effluent organics concentration and composition, and therefore led to higher impacts on $R_{t,i.}$

The influence and contribution of SBR HRT, temperature and filtration temperature on hydraulically reversible resistances were next assessed by the regression models (see Supplemental materials). From Table 6-1, $R_{rev,i}$ negatively related to SBR HRT, temperature, and filtration temperature. It was observed that the contribution of filtration temperature was the highest (-0.58) which indicates that a great portion of effluent organics contributed to reversible foulants due to reduced pore size. Moreover, the contribution of SBR temperature (-0.48) was higher than HRT (-0.33) which can be due to greater influence of SBR temperature on high MW organics generation.

The effects on hydraulically irreversible resistances were analyzed. Similarly, negative correlation and similar order of contributions were observed for $R_{irr,i}$ and SBR HRT, temperature and filtration temperature. However, it was found the difference in the contributions of SBR HRT (-0.11), temperature (-0.35) and filtration temperature (-0.76) were higher for $R_{irr,i}$ than those of $R_{rev,i}$ indicated by the greater difference among standardized coefficients. The contribution of filtration temperature in $R_{irr,i}$ was more dominant compared to that of SBR operating parameters, which indicates the role of membrane property on irreversible fouling accumulation was greater than the change in DOC concentration and composition caused by SBR HRT and temperature tested in the present study.

In practice, HRT and temperature are conditions that cannot be controlled during periods of low temperature and high flow. The results suggest that designing systems with extended HRTs may result in reduced fouling of the tertiary filters however the costs of the larger tankage would need to be considered. The use of physical-chemical pretreatment of secondary effluents during periods of low temperature or high flow may be a viable alternative to either reduce organic concentrations

(Feng et al., 2015) or modify the composition of high and low MW organics (Liu et al., 2019) to reduce fouling .

Table 6-1. Multiple linear regression analysis between operating parameters and membrane resistances.

Membrane resistances	Regression equation	Standardized coefficient	r^2	Sig.
$R_{t,i}$	$R_{t,i} = 5.0\times10^{12} - 3.9\times10^{10}\,a - 5.7\times10^{10}\,b - 1.3\times10^{11}\,c$	a = -0.17 b = -0.34 c = -0.76	0.99	<0.001
$R_{rev,i}$	$R_{rev,i} = 1.7\times10^{12} - 2.5\times10^{10}\,a - 2.6\times10^{10}\,b - 3.2\times10^{11}\,c$	a = -0.33 b = -0.48 c = -0.58	0.95	<0.001
$R_{irr,i}$	$R_{irr,i} = 2.3\times10^{12} - 1.4\times10^{10}\,a - 3.1\times10^{10}\,b - 6.7\times10^{11}\,c$	a = -0.11 b = -0.35 c = -0.76	0.98	<0.001

a: SBR HRT; b: SBR temperature; and c: filtration temperature

6.4 Conclusions

This study demonstrated for the first time the interacting impacts of secondary HRT and temperature and filtration temperature on fouling of tertiary membranes. Reducing HRT from 20 to 10 h resulted in a substantial increase in high and low MW organics for both SBR effluents. The results of SMP modelling revealed that UAP yields decreased with HRT whereas BAP yields kept constant with all the yields for the SBR operated at 8 ℃ higher than those of 20 ℃. Reducing HRT from 20 to 10 h induced moderate increase in total membrane resistance (26–38%) for SBRs operated at both temperatures. The increase in hydraulically reversible resistance was greater for SBR operated at 20 ℃ (454%) than 8 ℃ (52%) due to the higher increase in high MW organics. In contrast, the greater increase in hydraulically irreversible fouling was observed for the SBR operated at 8 ℃ with the greater increase in low MW organics. Further reducing the filtration temperature resulted in significant increase in total membrane resistance even with the correction on intrinsic membrane

resistances, and the impacts of filtration temperature were magnified as HRT decreased. The relationship between membrane resistances and SBR HRT, temperature and filtration temperature were determined by multiple linear regression with the contribution of filtration temperature > SBR temperature > SBR HRT for all cases. The pretreatment of secondary effluents would be a possible strategy to reduce fouling under the low HRT and temperature operating conditions.

Chapter 7

The impact of pre-coagulation on fouling of tertiary membranes at low temperatures

GRAPHICAL ABSTRACT

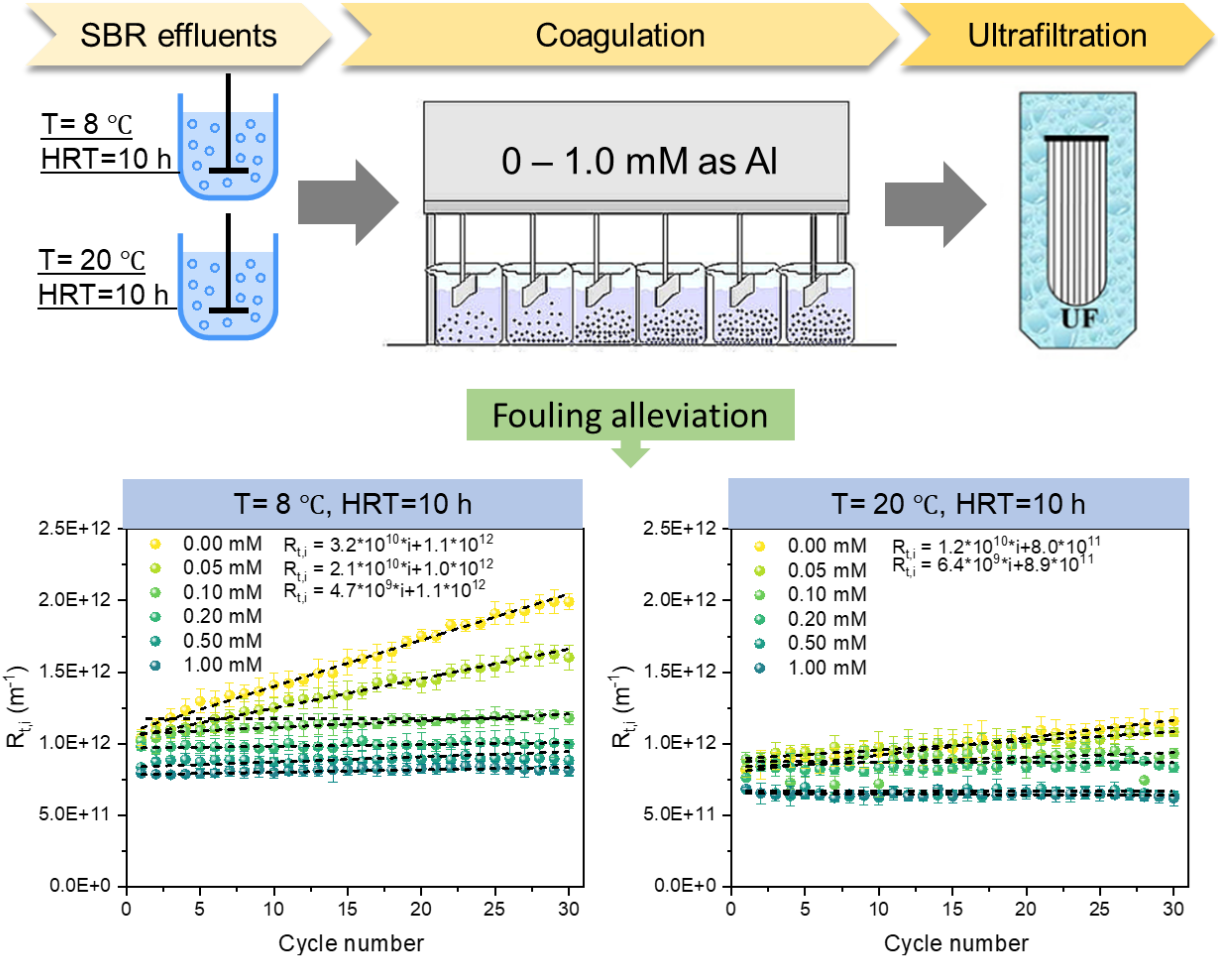

7.1 Introduction

Water reuse and wastewater reclamation are becoming increasingly important due to the growing demands for clean water that are spurred by economic growth, urbanization, and population growth (Wang et al., 2017). Membrane technologies have become key elements of the treatment systems that are being employed for this purpose. However, membrane fouling remains a major challenge that limits the wide application of these technologies (Meng et al., 2017).

The occurrence of extreme weather events and earlier snowmelts can increase the risk for the control of biological treatment process and subsequent tertiary membranes (Holloway et al., 2021). Several studies have indicated that the combination of low temperatures and high flows can negatively impact the performance of ultrafiltration (UF) membranes when employed for tertiary treatment. Abu-Obaid et al. (2020) reported that in a full-scale tertiary membrane treatment process seasonal variations of low temperature and high flow resulted in increased release of soluble microbial products (SMPs) from biomass and this subsequently led to higher membrane fouling and worsened dewaterability of the activated sludge. High influent flows have also been demonstrated to cause adverse effects on membrane fouling with a decrease in foulant size and increase in specific cake resistance when a synthetic municipal wastewater was treated (Salazar-Peláez et al., 2011). In the face of these challenges to fouling of tertiary membranes, it is hypothesized that pretreatment of the UF influent may be an effective strategy to mitigate tertiary fouling during seasons with high fouling potential.

Pore blocking and cake layer formation by SMPs have been reported to be the dominant mechanisms of membrane fouling in tertiary treatment when operated at low temperatures and high flows. Tao et al. (2021) observed that polysaccharides and low molecular weight (MW) organics were the major foulants responsible for cake fouling and pore blocking. Hence the primary foulants during these challenging conditions are associated with biomass metabolism in the upstream secondary treatment. Coagulants have been widely used as a pretreatment prior to membrane filtration to mitigate fouling by removing SMPs or changing their physical-chemical characteristics (Chen et al., 2020; Peleato et al., 2017). In these prior studies the DOC concentration of the UF influent ranged from 4.5–8 mg/L (Chen et al., 2021; Liu et al., 2019). However, it has been reported in Chapter 6 that low temperature operation (8 ℃) and high flows (HRT=10 h) of secondary treatment resulted in DOC concentrations as high as 15 mg/L and the fraction of high and low MW organics substantially increased. It is expected that the preferred dosage of coagulants and the mechanisms of membrane fouling alleviation may change under low temperature and high flow condition however, there is little information in this regard.

In this study, the impact of pre-coagulation on tertiary fouling was assessed when applied to the effluent of secondary systems that were operated at different temperatures. Alum was selected as coagulant as it has been demonstrated to provide effective pretreatment prior to membranes in other studies (Yu et al., 2013; Jutaporn et al., 2021). Bench-scale sequencing batch reactors (SBRs) treating real municipal wastewater were operated at 20 and 8 ℃ to provide feed water to bench-scale membrane tests that assessed fouling. The SBR effluents were coagulated with different dosages of alum prior to the filtration tests to assess the impact of coagulant dose on fouling responses. LC-OCD analysis was employed to quantify SMP concentrations of the SBR effluents and coagulated effluents to provide insight into the types of potential foulants that were impacted by coagulation. Fouling models were employed to facilitate data analysis such that the results from the filtration tests could be compared between tests with different coagulant dosages. The outcomes of the present study provide insights into how coagulant dosing should be modified to mitigate fouling of tertiary membranes during periods of low temperature operation.

7.2 Materials and methods

7.2.1 Secondary treatment operation

The secondary effluents used in the present study were obtained from SBRs that were treating real municipal wastewater at an HRT of 10 hours and an SRT of 25 days and different temperatures. A control SBR was operated at 20 ℃ that was considered to represent regular temperature and high flow operating condition of secondary treatment. A test SBR was operated at 8 ℃ to reflect stressed operating conditions that have been reported in Ontario, Canada (Abu-Obaid et al., 2020). A detailed description of SBR operation has been previously described (Tao et al., 2021).

7.2.2 Coagulation and filtration tests

The coagulation tests were conducted in 1 L beakers using a programmable jar test apparatus (PB-700, PHIPPS&BIRD, USA). The effluents from the SBRs were heated to 20 ℃ prior to coagulation tests to exclude the influence of water temperature variation. Alum powder (Sigma-Aldrich, USA) was added into the beakers to achieve a range of dosages (0, 0.05, 0.1, 0.2,0.5, 1.0 mM). The dosed water samples were mixed rapidly at 200 rpm for 1 min and then at 35 rpm for 20 min. After coagulation, the water samples were transferred to the membrane setup for filtration tests. The experiments were designed to be representative of an in-line coagulation immediately prior to UF filtration without sedimentation. Dosages were selected based on previous research on in-line coagulation with alum (Peleato et al., 2017). All coagulation tests were conducted in duplicate.

The membrane filtration set-up employed in this study has been described by Tao et al. (2022). The filtration tests were conducted in dead-end mode where each test consisted of 30 permeation cycles that included 30 min of filtration and 2 min of back pulsing and air scouring. Back pulsing and air scouring were employed to remove hydraulically reversible fouling from the membrane. The filtration and back pulsing fluxes were 24 and 48 LMH, respectively. All filtration tests were conducted in duplicate.

7.2.3 Water quality analysis

Samples of the SBR effluents and coagulated effluents were filtered through 0.45 μm nylon filters prior to analysis of soluble components. Soluble chemical oxygen demand (sCOD) dissolved organic carbon (DOC) and UV_{254} were measured as indicators of dissolved organic matter using Standard Methods 5220 (APHA, 2005), a total organic carbon analyzer (TOC-L, Shimadzu, Japan) and a spectrophotometer (8453, Agilent, USA), respectively. pH was measured using a portable pH meter (SP80PD, VWR, USA). Suspended solids (SS) and turbidity were analyzed as indicators of particulate matter using Standard Method 2540D (APHA, 2005) and a turbidity meter (2100N, Hach, USA) respectively. Total phosphorus (TP) was measured according to Standard Methods (APHA, 2005) to indicate the P removal performance achieved with the coagulation.

LC-OCD analysis was used to provide insight into the DOC composition of the SBR effluents, coagulated effluents and membrane permeates. Based upon multiple signals, the LC-OCD analysis reports dissolved organic carbon in terms of biopolymers, humic substances, building blocks, LMW acids and LMW neutrals (Huber et al., 2011) The biopolymer concentrations reported by the LC-OCD analysis were then divided into polysaccharide and protein components assuming all of the DON in the biopolymers was bound in proteinaceous matter and employing a typical C:N mass ratio of 3 for proteins (Huber et al., 2011).

7.2.4 Membrane fouling analysis

Three resistance-based fouling indices, based on the resistance-in-series model (Nguyen et al., 2011) were employed to quantify the evolution of fouling in the filtration tests and thereby support a comparison of the various filtration conditions. The total resistance values ($R_{t,i}$) reflected the sum of intrinsic membrane, hydraulically reversible and irreversible resistances in cycle i. Hydraulically reversible resistance values ($R_{rev,i}$) quantified the resistance that accumulated during a cycle and which was recovered during physical cleaning between cycles. Hydraulically irreversible resistance values ($R_{irr,i}$) were determined as the resistance that accumulated during a cycle which was not

removed by physical cleaning. A detailed description of the calculations employed can be found in Chapter 5.

The combined fouling models established by Bolton et al. (2006) were fit to the experimental data to transform the transient responses of TMP observed in the filtration tests into a fixed number of fouling rate parameters that could be compared between tests conditions. The combined fouling models included cake-complete, cake-intermediate, complete-standard, intermediate-standard and cake-standard models with K_c, K_b, K_i and K_s as the fitted parameters to quantify cake fouling, complete blocking, intermediate blocking and standard blocking, respectively. The normalized TMP values (P/P_0) over time from the duplicate runs were simultaneously used in the model fitting. The best fit was determined by minimizing the sum of squared residuals (SSR) where the residual was equal to the difference between measured data and model prediction.

7.3 Results and discussion

This study sought to evaluate the performance of pre-coagulation and ultrafiltration when treating the effluents from SBRs operated at different temperatures. The performance of the pre-coagulation with respect to conventional water quality parameters was initially assessed to evaluate the efficiency of coagulation for the various coagulant doses and the different effluents. The DOC fractions, as determined by LC-OCD, were then examined to characterize how the combination of SBR operating condition and coagulant dosage impacted DOC fractions that are associated with membrane fouling. The quantitative relationship between fouling and DOC fractions removal was studied by linear regression. The results from the ultrafiltration tests were employed to estimate fouling indices that provided insights into the effect of pre-coagulation on fouling of tertiary membranes.

7.3.1 Effect of alum on water quality

Pre-coagulation was conducted over a range of alum dosages (0, 0.05, 0.1, 0.2, 0.5 and 1.0 mM) to the SBR effluents to assist with identifying the preferred dosage for each effluent. Since a real wastewater was employed, the characteristics of the raw wastewater were assessed at the time each alum dosage was evaluated, and it was found the raw wastewater properties were consistent over the tested period. Therefore, the influence of changes in raw wastewater properties on SBR effluent and coagulated effluent were deemed to be minimal and did not influence the findings of the study. The mean and standard deviations of the water qualities in duplicated pre-coagulation tests were employed for comparison. In all cases, the standard deviations were consistently less than 17% of the corresponding means indicating good reproducibility of the tests.

The conventional water quality measures in the raw and coagulated secondary effluents are illustrated in Figure 7-1 as a function of alum dose. Effluent pH is typically regulated and it can impact the solubility of precipitates, hence the pH of the effluents before and after coagulation was compared. It was observed that before coagulation the pH of the effluents from the two SBRs ranged from 7 to 7.5. With increasing alum dose, the pH decreased to values as low as 6 with an alum dosage of 1 mM. The acceptable pH range indicated by the membrane provider is 5–10. Therefore, within the tested dosages the drop in pH values was not expected to affect their operating performance although a pH of 6 is typically considered low for discharge to receiving waters.

The soluble carbon-related metrics including sCOD and UV_{254} were evaluated since soluble components have been demonstrated to be major foulants in tertiary fouling (Yang et al., 2021). For the effluent from the SBR operated at 20 ℃, the removal of sCOD increased from 1 to 30% as alum dosage increased from 0.05 to 1 mM with maximal removal achieved at a dosage of 1 mM. The corresponding removals of sCOD for the effluent from the SBR operated at 8 ℃ ranged from 1 to 40%. In comparison, the removal of the UV_{254} response was also similar for the effluents from both SBR temperatures and reached 40% when the alum dosage was 1.0 mM. Although the removal efficiencies were similar for both effluents, the concentrations of sCOD and UV_{254} after coagulation (Figure 7-1) were higher for the effluent from the SBR operated at 8 ℃ as the initial concentrations before coagulation were higher. Hence, with same dosage of alum the removal of sCOD and UV_{254} were similar while the remained sCOD and UV_{254} were greater for the SBR operated low temperature and it was anticipated that this may induce higher fouling in subsequent membrane treatment.

The particulate metrics including turbidity and SS were examined as they could also be indicative of fouling of the membranes in the subsequent filtration tests. The turbidity in coagulated effluents increased with alum dose with increases of 441% and 771% observed at the highest dosage for the effluents from the SBRs operated at 20 ℃ and 8 ℃ respectively (Figure 7-1). Increases in alum addition also resulted in substantial concentrations of SS with 612% and 400% increases for the effluents from SBRs operated at 20 and 8 ℃, respectively. The trends of turbidity and SS were in alignment with the observations when ferrate (0–0.2 mM) was used as coagulant for membrane fouling mitigation in reclaimed water treatment (Liu et al., 2018). The formation of aluminum hydroxide precipitate, and the incorporation of organics into the precipitate flocs has been reported to contribute to solids generation (Gao et al., 2011; Yu et al., 2013). Hence increasing alum doses resulted in higher loading of particulates to the membranes which might affect the fouling potential.

The removal of TP by coagulation was assessed since alum is often used for phosphorus control in addition to fouling mitigation. UF membranes typically only remove a small amount of phosphorus

(Rosenberger et al., 2006), therefore the permeate concentration of TP was anticipated to largely depend on alum dosage. It was observed that the concentration of TP before coagulation ranged from 2–3 mg/L for the effluents from the two SBRs with the higher concentrations in the 8 ℃ effluent. It was found that an alum dosage of 0.2 and 0.5 mM was required for the effluents from SBRs operated at 8 and 20 ℃ to achieve a permeate TP value of 0.1 mg/L which is a typical design objective in a water resource recovery facility in Ontario, Canada (Abu-Obaid et al., 2020). This dosage will be compared with the dosage that required for the fouling mitigation in section 7.3.3.

It was anticipated that the response of conventional water quality measures could provide insight into how pre-coagulation would affect the filtration test outcomes. The values of sCOD and UV_{254} consistently decreased (>35%) (Figure 7-1) as the dosage increased. The fouling of tertiary membranes has been reported to be associated with soluble foulants (Chen et al., 2020) and therefore it was expected that the removal of these soluble component removal would result in a reduction in membrane fouling. However, prior studies (Abu-Obaid et al., 2020) have indicated that that the presence of specific DOC fractions are better indicators of fouling. Hence, the DOC fractions reported by LC-OCD in the SBR effluents and coagulated effluents were also examined for the various combinations of SBR temperature and coagulant dose.

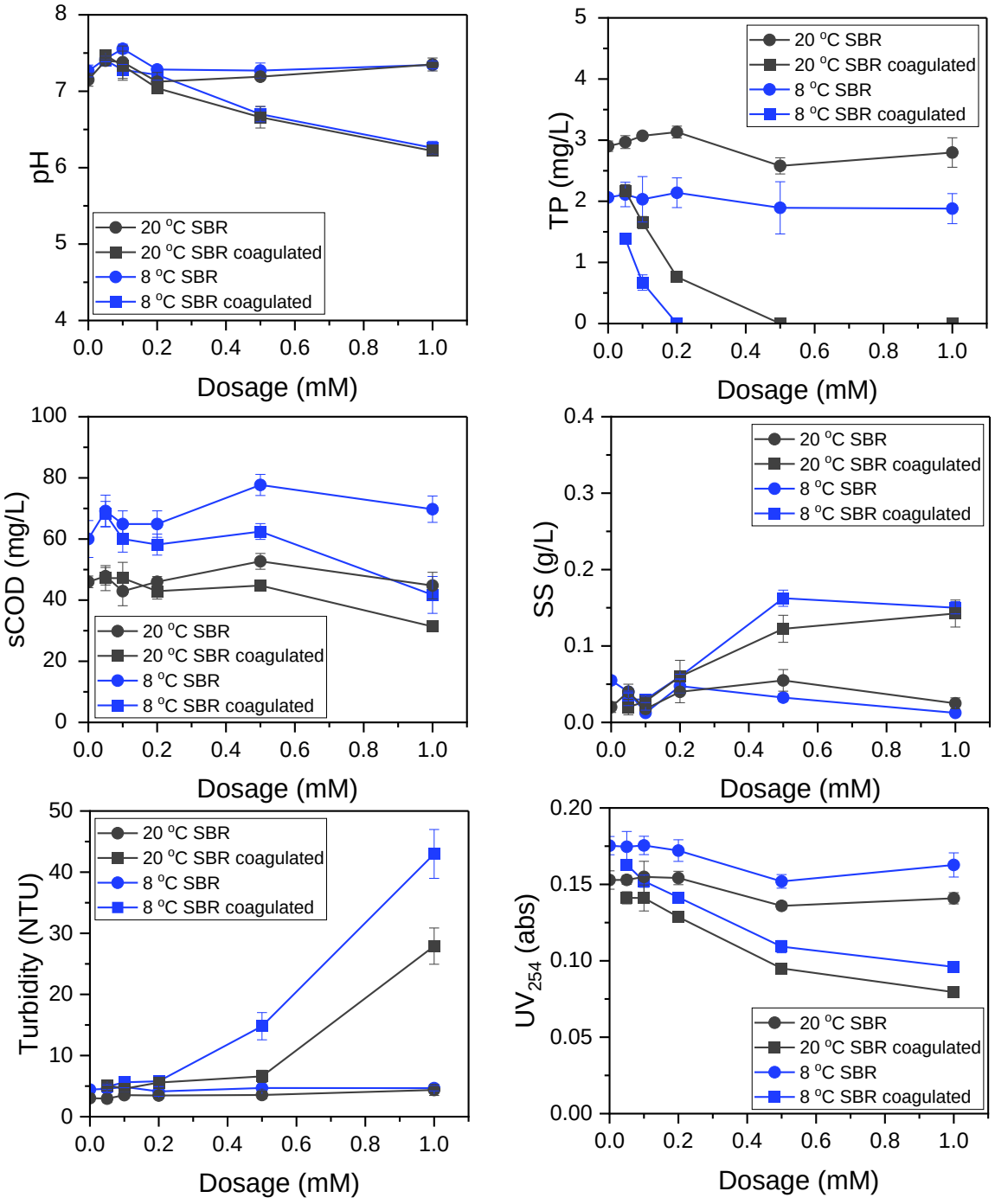

Figure 7-1. Conventional characteristics (mean ± standard deviation) of SBR effluent and coagulated effluent.

7.3.2 Effect of alum dosage on removal of DOC and DOC fractions

The concentrations of DOC and DOC fractions present in the raw effluents from the SBRs operated at 8 and 20 ℃ were initially compared in Table 7-1 to assess the effluent properties before pre-coagulation. It was observed that the concentration of DOC was 42% higher in the effluent from the SBR operated at 8 ℃ than that of 20 ℃. The higher DOC concentrations can be attributed to higher high MW and low MW organics generated at low SBR temperatures. However, the concentrations of intermediate MW organics were not significantly different at the two SBR temperatures and was expected not to affect the coagulation efficiency (Tao et al., 2022). Hence, analysis of the performance of pre-coagulation focused on the total DOC, high and low MW organics concentration which were significantly different in the effluents from the SBR operated at 8 and 20 ℃. The means and standard deviations of removal efficiencies of total DOC and the two DOC fractions by pre-coagulation are presented in Figure 2. The standard deviations were less than 20% of the corresponding mean values indicating good reproducibility of the duplicated coagulation tests.

Table 7-1. Effluent concentrations of DOC and DOC fractions in the SBRs operated at 8 and 20 ℃.

SBR temperature (℃)	DOC (mg/L)	DOC fractions (mg/L)			
		High MW		Intermediate MW	Low MW
		polysaccharide	protein		
8	14.9±1	2.04±0.15	0.78±0.02	4.0±0.20	4.75±0.13
20	10.5±1	0.69±0.08	0.30±0.04	4.1±0.23	3.07±0.12

The effect of alum dosage on the removal of total organics was assessed by DOC removal. It was observed that for the effluent from the SBR operated at 20 ℃ low-intermediate doses (0.05–0.20 mM) resulted in DOC removal efficiencies that were less than 20%. As dosage increased to 0.5 mM, the removal efficiency significantly increased and reached 37±2% with no significant improvement as dosage further increased to 1.0 mM. The trend of removal efficiency for the effluent from the SBR operated at 8 ℃ was similar to that of the 20 ℃ effluent with removals in the range of 6–38% as the dosage increased to 0.5 mM. Dosages higher than 0.5 mM did not appear to lead to any additional benefit with respect to DOC. The DOC removal efficiencies by pre-coagulation were consistent with a previous study treating algae-laden water in which 25.6% of DOC was removed by 0.5 mM of

$FeCl_3$ when the DOC content in raw water was around 15.5 mg/L (He et al., 2021). However, the DOC concentrations remaining in the coagulated effluents were higher for the SBR operated at 8 ℃ due to higher initial concentrations in SBR effluent (Table 7-1), and it was anticipated that this might result in differences in fouling evolution.

High MW organics, that consist of polysaccharides and proteins, have been reported to cause more severe membrane fouling than other DOC fractions (Chen et al., 2021). The removal efficiency of high MW organics through pre-coagulation is illustrated in Figure 2. It was observed that for the effluent from the SBR operated at 20 ℃, the removal efficiency consistently increased to 90% at the dosage of 1.0 mM. A similar trend was observed for the effluent from the SBR operated at 8 ℃, however the removal efficiency only reached 80% at the dosage of 1.0 mM. The results indicate that alum dosage achieved different removals of high MW organics for the two SBR temperatures with lower efficiencies for the SBR operated at the low temperature. This was attributed to the increased concentrations of high MW organics in the effluent from the SBR operated at low temperature which required a higher dosage of coagulant to neutralize charges between particles (Lee et al., 2009).

Polysaccharides and proteins have been reported to impact membrane fouling differently (Ferrer-Polonio et al., 2018) and therefore their removals were assessed separately (Figure 7-2). From the plots a three-step pattern in the removal efficiency of polysaccharides can be observed for the effluent from the SBR operated at 20 ℃. When alum dosages were in the ranges of 0.05, 0.1–0.2, and 0.5–1.0 mM, the corresponding removal efficiencies were 2%, 34–45%, and 80–90%, respectively. For the effluent from the SBR operated at 8 ℃, the removal efficiency of polysaccharides was 4±1% at the dosage of 0.05 mM and then consistently increased to 84±3% at the dosage of 1.0 mM. This stepwise response of the organic removal efficiencies by coagulation has been reported by Lee et al. (2009) and Yu et al. (2013), and was attributed to changes in zeta potential with dosage. At low coagulant dosages, the alum-flocs were negatively charged and the removal of organics increased significantly as dosage increased; however when the charge of alum-flocs reversed the removals only slightly increased with dosage (Yu et al., 2013).

The removal of proteins was assessed in Chapter 5 that despite the strength of the correlation between membrane fouling and proteins has been reported to be less than that of polysaccharides. Compared to polysaccharides, the removal efficiency of proteins increased proportionately to alum dose for both SBRs effluents, and ultimately reached 90±5% and 78±5% for the SBRs operated at 20

and 8 ℃, respectively. It was noted that even at the very low level of alum dosage the removal of proteins reached approximate 20% for the effluents from both SBRs, which was much higher than that of polysaccharides. This was likely due to the reactions between alum and amino acids functional groups in the proteins (Arunkumar et al., 2019; Chen et al., 2021). The difference in fouling potential of the residual polysaccharides and proteins will be subsequently compared.

Low MW organics have been reported to contribute to membrane pore blocking (Guo et al., 2014) and hence the impact of pre-coagulation on their removal from the SBR effluents was analyzed (Figure 7-2). No specific trend was observed for the low MW organics removal as dosage increased. For the effluent from the SBR operated at 20 ℃, the average removal was 48%. The corresponding value for the SBR operated at 8 ℃ was 30%. Hence it was expected that the mitigation by coagulation on pore blocking might be less efficient due to the relatively low removal of low MW organics.

The removals of high and low MW organics were compared for the two SBR temperature conditions to obtain insights into the fouling mitigation mechanisms. It was found that the highest removal of low MW organics was relatively lower (30–48%) than that of the high MW organics (80–90%) regardless of SBR temperature. This was consistent with previous research which demonstrated that higher MW fractions of DOC can be more effectively removed by coagulation-flocculation process compared to lower MW organics (Wang et al., 2017; Yu et al., 2014). The selective removal of high MW organics might have been due to their large amount of different functional groups, allowing an enhanced interaction with metal hydroxide precipitates (Haberkamp et al., 2007). In addition, less removal of LMW organics can be explained by their high charge densities to be neutralized by coagulant. The greater removal of high MW organics might result in substantial decrease in cake fouling which was subsequently discussed.

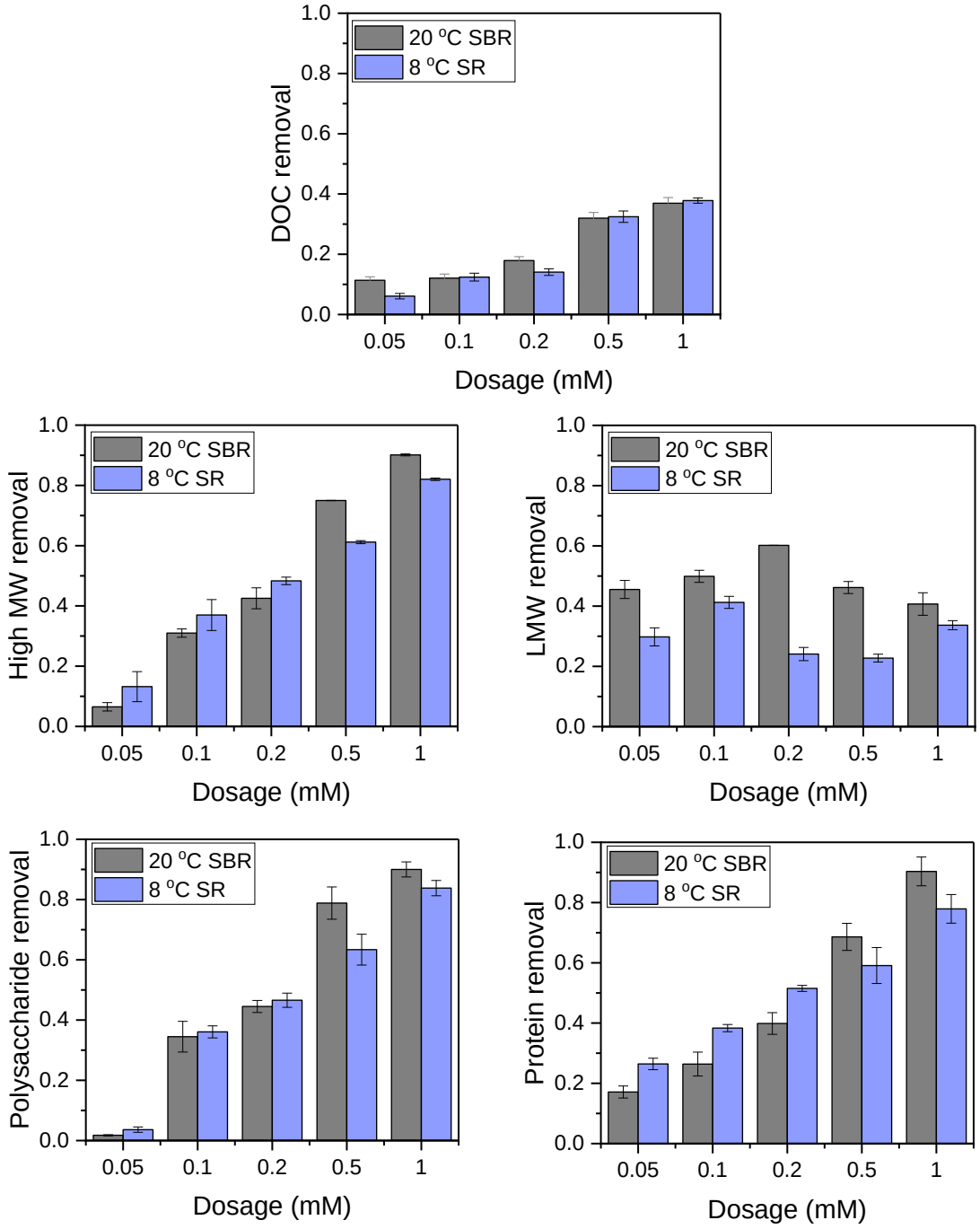

Figure 7-2. DOC and DOC fraction removals (mean ± standard deviation) at different alum dosages.

7.3.3 Impacts of pre-coagulation on membrane fouling

The impact of coagulation on fouling control was assessed by examining the responses of total, hydraulically reversible and irreversible resistances ($R_{t,i}$, $R_{rev,i}$ and $R_{irr,i}$). The mean and standard deviations of the membrane resistances in duplicate tests were computed for the different conditions. In all cases, the standard deviations were consistently less than 20% of the corresponding means indicating good reproducibility of the filtration tests. The slopes of linear regressions of the membrane resistances versus cycle number were used to facilitate an assessment of the impact of coagulation on the development of each resistance in the filtrations. The regression equations where the slopes were significantly different from 0 are presented in Figure 7-3. The initial values of membrane resistances and the slopes of the regression affected by dosages were compared to access the initial status as well as their change rates.

Values of $R_{t,i}$ were initially examined to assess the effect of dosage on the trends in the combined resistances over the multiple filtration cycles. The effluent from the SBR operated at 20 ℃ was assessed as a reference condition. It was observed that the initial values of $R_{t,i}$ decreased by 15% as dosage increased to 1.0 mM indicating moderate mitigation on total fouling by pre-coagulation. In addition to modest decrease in initial $R_{t,i}$ values, the slopes of the regressions decreased by 47% ($P<0.05$) as alum dosage increased from 0 to 0.05 mM. However, the slopes were not significantly different from 0 for higher alum dosages, indicating no accumulation of $R_{t,i}$ over the multiple filtration cycles. The results indicate that pre-coagulation not only reduced the values of $R_{t,i}$ but also led to slower increase in $R_{t,i}$ over the multiple filtration cycles.

The trends of $R_{t,i}$ for the SBR operated at 8 ℃ were analyzed to assess if the effects of dosage was different for the SBRs operated at low temperature. It was noted that without coagulation the values of $R_{t,i}$ were substantially higher for the SBR operated at 8 ℃ than that of 20 ℃. The greater $R_{t,i}$ in the effluent from the SBR operated at low temperature was due to a higher content of high and low MW organics (Table 7-1) that were previously demonstrated in Chapter 5 to be responsible for total membrane resistance. Similar to the observations for 20 ℃ SBR, the initial values of $R_{t,i}$ also decreased modestly (24%; $P<0.05$) when alum dosage increased from 0 to 1.0 mM. The slopes for the SBR operated at 8 ℃ decreased by 85% as dosage increased to 0.10 mM and then the values of $R_{t,i}$ were relatively constant over the multiple filtration cycles for higher dosages. By comparing with the data for the SBR operated at 20 ℃, the reduction in initial $R_{t,i}$ values and slopes by pre-coagulation

were both greater for the SBR operated at 8 ℃; however, the $R_{t,i}$ values after coagulation were still higher for low temperature SBR. Hence, it was concluded that while the efficiency of pre-coagulation was higher for the low temperature SBR, the extent of fouling at the lower temperature was still higher due to the higher organics remained after coagulation.

The response of $R_{rev,i}$ were evaluated to obtain insights into the impact of alum coagulation on hydraulically reversible fouling. For the SBR operated at 20 ℃, the slopes of the regressions were not significantly different from 0 in all cases. This indicates a relatively stable process that a certain amount of foulants attaching and detaching from membrane surfaces repeatedly over the multiple filtration cycle. Hence the means of $R_{rev,i}$ values were compared to assess the impact of dosage. It was found that when alum dosage increased from 0 to 0.5 mM, the means of the $R_{rev,i}$ values decreased by 90% and no additional benefit was observed at higher alum dosage. The results indicate that a dosage of 0.5 mM achieved the maximum improvement for the SBR operated at 20 ℃ in terms of the control of hydraulically reversible fouling.

The impact of dosage on hydraulically reversible fouling mitigation was then evaluated for the effluent from the SBR operated at 8 ℃. With this effluent the slope of the regression for $R_{rev,i}$ was significantly from 0 without coagulation (2.8×10^{9} m^{-1}/cycle), which suggests that an increased accumulation of organics attached on the membrane surfaces with time despite the use of back pulsing and air scouring at the end of each cycle. The difference in this response when compared to the 20 ℃ effluent was attributed to higher concentrations of high MW organics in the effluent from the SBR operated at 8 ℃. The slopes of the regressions declined to 0 at a dosage of 0.10 mM indicating a change in the interaction between the hydraulically reversible foulants and membranes over this dose range. For the higher dosages the means over all of the cycles were computed and found to decrease progressively to a value of 88% at a dosage of 1.0 mM. The results indicate that pre-coagulation can efficiently reduce hydraulically reversible resistance with greater dosages required to achieve equivalent reduction in $R_{rev,i}$ values for low temperature SBR when compared to the higher temperature effluent.

Values of $R_{irr,i}$ were then assessed to study how pre-coagulation impacted the development of hydraulically irreversible fouling (Figure 7-3). It was observed that the trend of $R_{irr,i}$ over the multiple filtration cycles were similar to that of $R_{t,i}$, which indicated that the increase in $R_{t,i}$ was mainly contributed by the increase in $R_{irr,i}$ over the multiple filtration cycles. In addition, different from $R_{rev,i}$,

initial values of $R_{irr,i}$ did not significantly change with dosage. This was likely due to the low efficiency of coagulation for removal of low MW organics. In contrast, the slopes of the regression decreased as dosage increased. For the SBR operated at 20 ℃, the slopes of the regressions decreased progressively with dosage until an 81% reduction in slope was attained at 0.2 mM after which the slopes were not significantly different from zero. The decreased development rates of hydraulically irreversible fouling may have been due to the increased formation of flocs at higher doses that led to a thicker cake layer which would trap the low MW organics from directly blocking membrane pores. It was concluded that a preferred dosage for hydraulically irreversible fouling control was 0.2 mM for the effluent from SBR operated at 20 ℃ as higher doses did not result in lower $R_{irr,i}$ values .

The response of $R_{irr,i}$ at the SBR temperature of 8 ℃ was compared to that of 20 ℃. It was found that the slopes progressively decreased to a reduction of 90% when the dosage increased to 0.2 mM after which the slopes were zero. Moreover, despite the $R_{irr,i}$ was constant, for dosage of 0.5 and 1.0 mM, the means of the $R_{irr,i}$ values for the SBR operated at 8 ℃ were 40% higher than those of 20 ℃. Hence, the hydraulically irreversible fouling could be held constant at a dosage of 0.2 mM for both temperatures however, $R_{irr,i}$ values remained higher for the SBR operated at low temperature. Additional increments in dosage above 0.2 mM did not substantial reduce hydraulically irreversible fouling and hence this dosage represented an upper limit on the extent to which this response could be improved with alum for all temperatures.

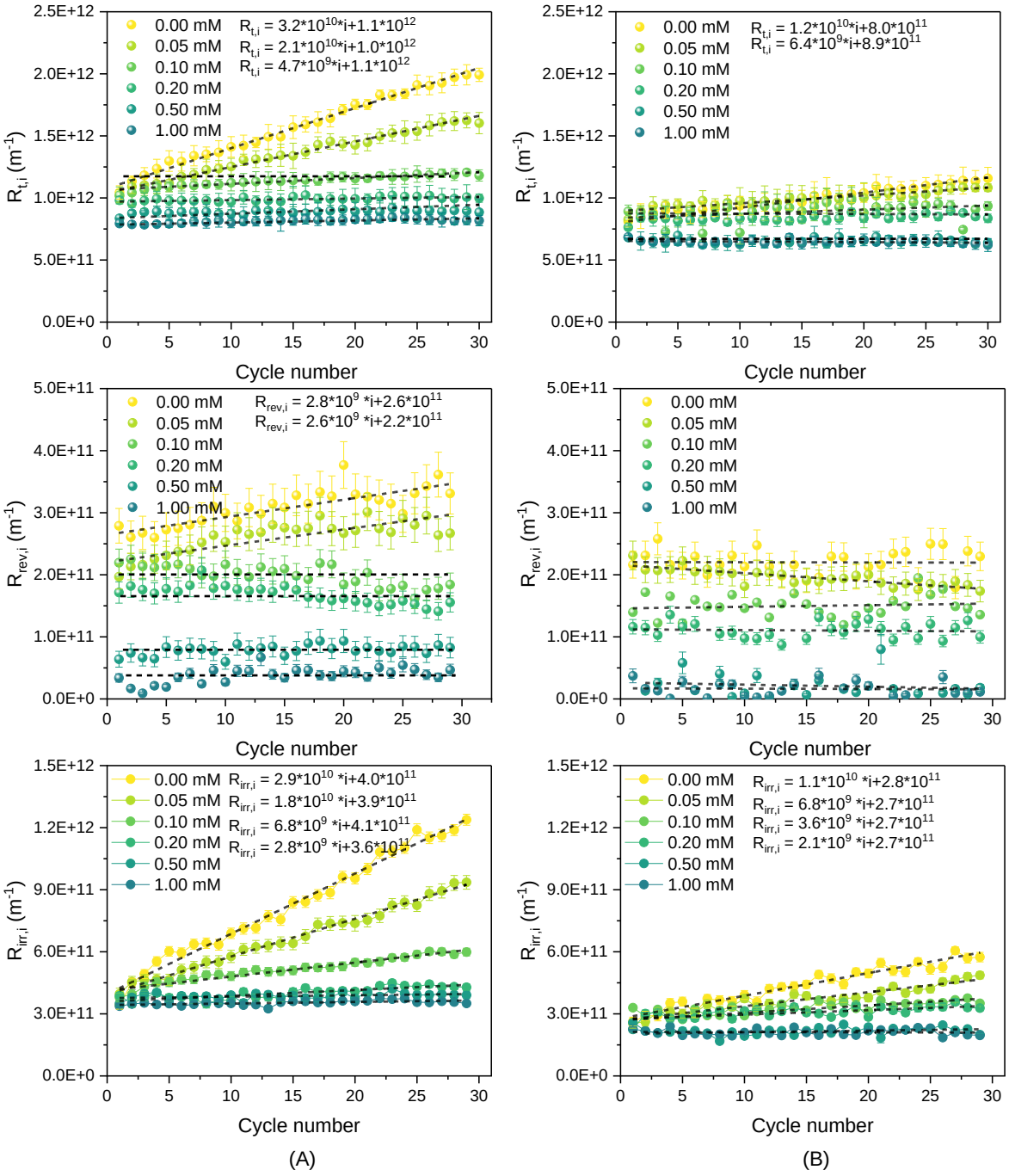

Figure 7-3. Membrane fouling indices (mean ± standard deviation) vs alum dose for effluents from SBRs operated at (A) 8 ℃ and (B) 20 ℃.

7.3.4 Fouling mitigation mechanisms

The filtration tests generated transient data on TMP development over multiple filtration cycles. The combined fouling models described by Bolton et al. (2006) were therefore employed to translate the transient data into a fixed number of fitted model parameters that could be compared with the effect of coagulation dosage. In the model fitting exercise, the combined cake-intermediate pore blocking model was found to provide the best fit of the data with the lowest value of SSE (<0.7) and r^2 >0.8, indicating cake and intermediate blocking were the major contributors to membrane fouling. Hence, only the parameters (mean ± standard error) estimated for the combined cake-intermediate pore blocking model are presented (Figure 7-4) and discussed.

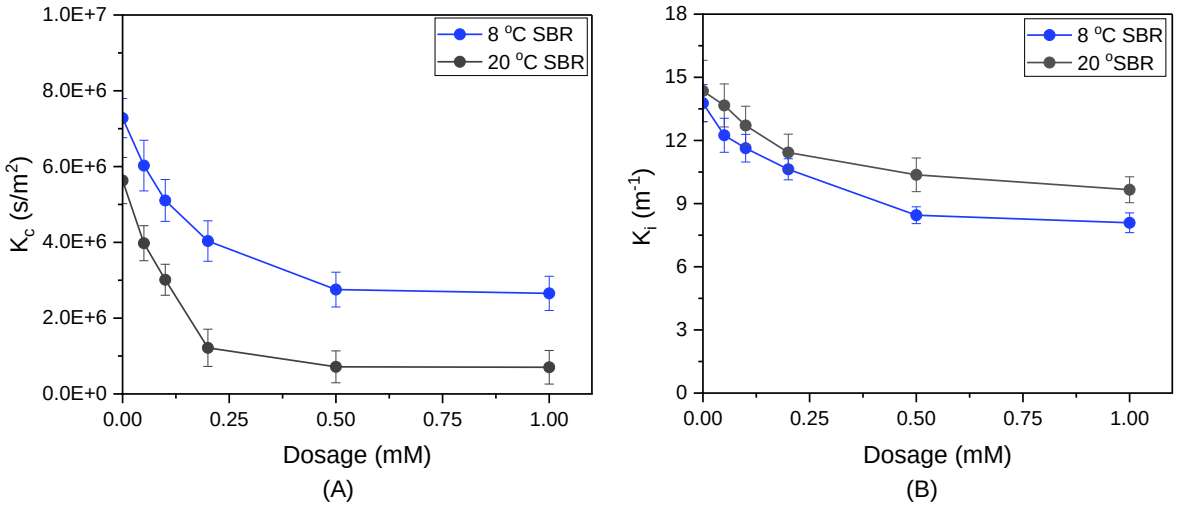

Figure 7-4. Fitted model parameters (mean ± standard error) (A) K_c and (B) K_i under different dosages.

The impact of alum dosage on the extent of cake fouling was evaluated by comparing the fitted K_c values. It was observed from Figure 7-4 that the values of K_c were consistently higher for the SBR operated at 8 °C due to greater concentrations of high MW organics after pre-coagulation. For the effluent from the SBR operated at 20 °C, the values of K_c presented a two-stage development with alum dosage. When alum dosage increased from 0 to 0.5 mM the values of K_c progressively decreased to a value that was 75% less than the undosed case and then remained constant for higher

doses. The trend of K_c values with dosage for the effluent from the SBR operated at 8 ℃ was similar with a 56% decrease in K_c values over the same range of dosing. The increased concentration of SS and the effective decrease of high MW organics after pre-coagulation has been reported to facilitate the formation of a more porous cake layer which presented less fouling propensity (Liu et al., 2018). Hence it was concluded that there is an alum dosage (0.5 mM) above which there is no further improvement in K_c values irrespective of SBR temperature. The dosage of 0.5 mM can also meet common requirements for TP control which that previously discussed in Section 7.3.1.

Linear regression was conducted between K_c values and removal efficiencies of high and low MW organics to quantitatively assess their relationship using the data with different dosages (Figure 7-5). The regression was conducted separately for the SBRs operated at 8 (Figure 7-5A) and 20 ℃ (Figure 7-5B) as the initial concentrations were different for the two cases. As illustrated, K_c values negatively correlated with the removal efficiency of high MW organics for both SBRs operated at 8 ($r^2 = 0.94$) and 20 ℃ ($r^2 = 0.85$). However, no correlation was observed between K_c and the removal of low MW organics regardless of SBR temperature ($P>0.05$). The results indicate that the reduction in cake fouling as dosage increased was attributed to the removal of high MW organics. This was consistent with the observations by Haberkamp et al. (2007). In addition, the linear regression between K_c values and polysaccharides and proteins were also analyzed (data not shown) and it was found the K_c values were best correlated with removal of polysaccharides. The results indicate that polysaccharides removals have the greatest impact on the rate of cake fouling, and are consistent with previous studies in MBRs operated at low temperature (van den Brink et al., 2011).

The impact of alum dosage on intermediate pore blocking was evaluated by examining the fitted K_i values (Figure 7-4). When dosage increased to 0.5 mM, the values of K_i decreased by 39% for the SBR operated at 20 ℃ and did not further decrease for higher doses. The trend for the SBR operated at 8 ℃ was similar to 20 ℃ with a corresponding decrease of 33% at a dosage of 0.5 mM with no further change for higher doses. The K_i values for the SBR operated at 8 ℃ were consistently higher than those of 20 ℃ and there was no indication that increasing the alum dosage would reduce the K_i values for the 8 ℃ effluent to match those of the 20 ℃ effluent.

The relationship between K_i values and the removal efficiencies of high and low MW organics was analyzed separately for the two SBR temperatures. It was observed from Figure 7-5 the values of K_i were only negatively correlated with the removal of high MW organics for both SBRs operated at 8

(r^2 = 0.97) and 20 ℃ (r^2 = 0.96). The decrease in pore blocking may have been due to the decrease in low MW organics but may also have resulted from the increased development of a cake layer from the increased floc production that then entrapped the low MW organics and prevented them from blocking the membrane pores (Naim et al., 2014). In the present study the latter case accounted more for the reduction of K_i because only a small amount of low MW organics were removed by pre-coagulation. Moreover, it was observed that the decreases in K_i (33–39%) by coagulation were much lower than those of K_c (56–75%). This was likely due to the lower removal of low MW organics by coagulation. To sum up, the fouling mitigation by pre-coagulation with alum was mainly attributed to the removal on high MW organic. The lower concentrations of high MW organics directly resulted in less cake fouling and the formed flocs likely led to a greater cake layer that led to reduced pore blocking.

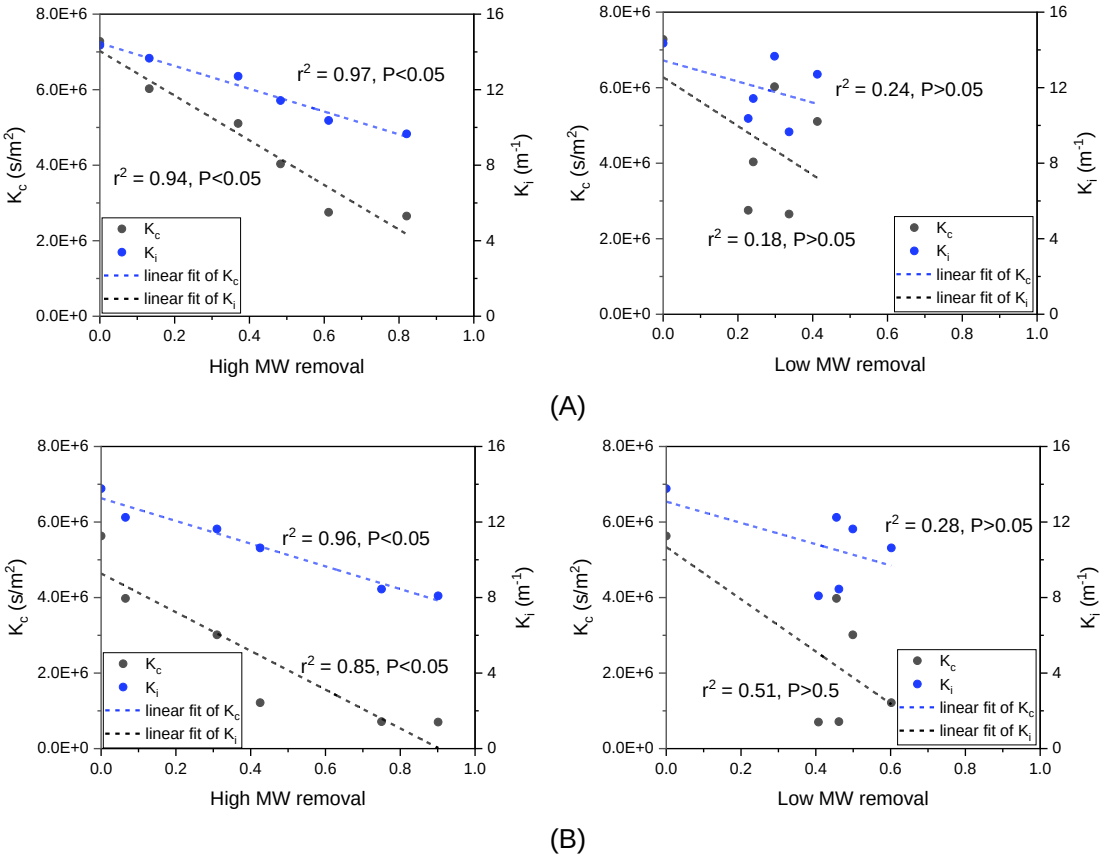

Figure 7-5. Linear regression between fitted parameters and DOC fractions removal for SBRs operated at (A) 8 ℃ and (B) 20 ℃.

7.4 Conclusions

Pre-coagulation with alum was employed prior to UF membranes to treat secondary effluents from SBRs operated at low temperature (8 ℃) to investigate its efficiency on fouling mitigation when compared against operation at 20 ℃ as a reference condition. Performance in DOC fractions removal and fouling mitigation were compared over a dosage range of 0–1.0 mM. The results showed that the removal efficiency for high MW organics can reach 90% whereas for low MW organics the removal efficiency was less than 60% as dosage increased to 1.0 mM. Dosages of 0.5 and 1.0 mM effectively controlled the increase of hydraulically reversible resistance over the multiple filtration cycles for the effluents from the SBR operated at 20 and 8 ℃, respectively. Moreover, the hydraulically irreversible resistance was controlled at a dosage of 0.5 mM for the effluents from SBRs operated at 20 and 8 ℃. However, the values of total, hydraulically reversible and irreversible resistance after coagulation were consistently higher for the SBR operated at 8 ℃ and this was due to higher residual high and low MW organics in the effluents. The addition of alum resulted in 56–75% decrease in cake fouling and 33–39% decrease in intermediate blocking for the two SBRs, which was attributed to reduced removal of low MW organics by coagulation. Such results provide a design reference when pre-coagulation is employed to mitigate fouling of tertiary membranes under low temperature conditions.

Chapter 8
Conclusions and Recommendations

8.1 Conclusions

The major objective of this research was to investigate the effects of low temperature and high flow in secondary treatment on fouling of tertiary membrane with the goal of supporting fouling mitigation strategies.

The linkage between biological processes and SMP formation as a function of secondary temperature was investigated through a combination of bioprocess modelling and SMP characterization. The use of LC-OCD analysis revealed that temperature (8, 14 and 20 ℃) significantly affected the SMP composition with much higher concentrations of polysaccharides and proteins as temperature decreased. Lower temperatures led to greater UAP and BAP concentrations and yields with a greater impact on BAP values. UAP and BAP yields were estimated as the ratios of the observed generation rates to the rates of substrate utilization and endogenous decay respectively, which both declined as temperature increased. A strong correlation was observed between temperature and BAP/UAP yields whereas the generation of BAP was more temperature sensitive than UAP. Such process modelling can be employed to assist with the optimization of the design and operation of membrane processes when treating wastewaters under challenging conditions like low temperature.

A comprehensive assessment of the effects of temperature on hydraulically irreversible membrane permeability in tertiary ultrafiltration of municipal wastewater was conducted. Reduced SBR and filtration temperatures impacted hydraulically irreversible permeability by changing SMP characteristics, water viscosity, membrane intrinsic resistance, and membrane-foulants interactions. The water viscosity and intrinsic membrane resistance were observed to be responsible for 20–29% of the total decrease in hydraulically irreversible permeability. These declines established the upper limit to which fouling mitigation strategies could enhance hydraulically irreversible permeabilities at low temperature. Moreover, narrowed membrane pore size retained more organic matter and further decreased hydraulically irreversible permeability. The approach in differentiating the effects of temperature on secondary treatment and filtration processes provides insights into hydraulically

irreversible fouling development and the results from the present study can be employed to understand the limits of tertiary fouling control under challenging conditions.

The impact of SBR temperature and filtration temperature on general fouling of tertiary membranes was also assessed. When SBR temperature decreased from 20 to 14 and 8 ℃, the increase in total membrane resistances was 27%, 45% and 82% over the multiple filtration cycles, respectively. Reduction in filtration temperature further induced 122% and 55% increases in total membrane resistances compared to the filtration temperature of 20 ℃ with the effluents from the SBRs operated at 8 and 14 ℃, respectively, which can be contributed by both increased hydraulically reversible and irreversible resistances. Correlation analysis revealed that the fouling of tertiary membranes was governed by high and low MW organics which were generated to a greater extent at lower SBR temperatures. Moreover, the generation of BAP was more sensitive to SBR temperature and presented higher fouling potential. Cake fouling and intermediate pore blocking were dominant fouling mechanisms and they intensified as SBR temperature decreased from 20 to 8 ℃. The outcomes provide insights into the combined effects of temperature on biological and filtration processes that influence the fouling behavior of tertiary membranes and can be employed to assist with the design of fouling mitigation measures in cold climates.

The effect of secondary treatment HRT (10, 15 and 20 h) on SMP generation and subsequent fouling of tertiary membranes was assessed at two secondary operating and filtration temperatures (8 and 20 ℃). Reducing HRT from 20 to 10 h resulted in a substantial increase in high and low MW organics for both SBR effluents. The results of SMP modelling demonstrated that a reduction in HRT induced decreased UAP yields and the influence was greater at the low SBR temperature. However, the BAP yields were relatively stable with HRT and the values were higher at the low SBR temperature. Reducing HRT from 20 to 10 h induced a moderate increase in total membrane resistance (26–38%) for SBRs operated at both temperatures. The increase in hydraulically reversible resistance was greater for the SBR operated at 20 ℃ (454%) than 8 ℃ (52%) due to the higher increase in high MW organics. In contrast, the greater increase in hydraulically irreversible fouling was observed for the SBR operated at 8 ℃ with the greater increase in low MW organics. A multiple linear regression analyses indicated that the contribution of filtration temperature to membrane resistances was dominant and this was followed in importance by SBR temperature and HRT. The comprehensive analysis provides insights into the interaction effects of secondary and tertiary

operations on fouling development and the results can be employed to understand the limits of tertiary fouling control under challenging conditions.

The effect of coagulation with different doses of alum (0–1.0 mM) on fouling of tertiary membranes was studied at a secondary operating temperature of 8 and 20 ℃ to investigate its efficiency in fouling mitigation. The removal efficiency for high MW organics reached as high as 90% whereas for low MW organics the removal efficiency was less than 60% when the dosage increased to 1.0 mM. The preferred dosage to mitigate hydraulically reversible and irreversible fouling was 1.0 and 0.2 mM for the SBR operated at 8 ℃ while the corresponding value for the SBR operated at 20 ℃ was 0.5 and 0.2 mM, respectively. At the preferred dosage, the values of the three membrane resistances were still higher for the SBR operated at 8 ℃ due to the higher concentrations of DOC fractions remained in the coagulated effluent. The addition of alum resulted in 56–75% decrease in cake fouling and 33–39% decrease in intermediate blocking for the two SBRs, which was attributed to reduced removal of low MW organics by coagulation. The potential of pre-coagulation in membrane fouling alleviation and effluent quality improvement can be limited at the low temperature and high flow operating of secondary treatment.

8.2 Recommendations

Based on the findings from this research, several recommendations are made for future research related to fouling of tertiary membranes under cold climates:

- The concentrations and yields of BAP and UAP were determined by mass balance approach and activated sludge modelling based on previous reported ratios of the components. An experimental measurement of the BAP and UAP production with the effect of secondary operating parameters would help to confirm the accuracy of the modelling approach.
- The bench scale membrane set-up used in the present study was different from the membrane cassette used in the real operation where the packing density is quite high and fibers are packed horizontally. A test with full scale membrane modules would help to validate the results generated from lab-scale membranes.

- The fouling indices results indicate that the increased total, hydraulically reversible and irreversible resistances were contributed by increased concentrations of high and low MW organics under low secondary operating temperature and short HRTs. Hence the fouling mitigation approach can be designed to removal or modify high and low MW organics before UF.
- The filtration temperature of UF has been proved to significantly impact fouling degree and the influence was even greater than those of secondary temperature and HRT. Considering it would not be economically feasible to raise the effluent temperature, in cold filtration operating conditions further strategies need to be explored to offset or mitigate the fouling enhanced by filtration temperature.
- The present study showed the limit of low temperature on pre-coagulation efficiency. The performance of other pretreatment strategies needs to be further investigated under cold temperature conditions.

References

Abu-Obaid, S., Bérubé, P., & Parker, W. J. (2020). Characterization of performance of full-scale tertiary membranes under stressed operating conditions. *Water Science and Technology*, 571–584. https://doi.org/10.2166/wst.2020.140

APHA, 2005. Standard Methods for the Examination ofWater andWastewater. twentieth ed. American Public Health Association, American Water Works Association, Water Environmental Federation, Washington, USA.

Akhondi, E., Wicaksana, F., & Fane, A. G. (2014). Evaluation of fouling deposition, fouling reversibility and energy consumption of submerged hollow fiber membrane systems with periodic backwash. *Journal of Membrane Science*, *452*, 319–331. https://doi.org/10.1016/j.memsci.2013.10.031

Alresheedi, M. T., & Basu, O. D. (2019). Effects of feed water temperature on irreversible fouling of ceramic ultrafiltration membranes. *Journal of Water Process Engineering*, *31*(July). https://doi.org/10.1016/j.jwpe.2019.100883

Aly, S. A., Anderson, W. B., & Huck, P. M. (2021). In-line coagulation assessment for ultrafiltration fouling reduction to treat secondary effluent for water reuse. *Water Science and Technology*, *83*(2), 284–296. https://doi.org/10.2166/wst.2020.571

Aquino, S. F., & Stuckey, D. C. (2008). Integrated model of the production of soluble microbial products (SMP) and extracellular polymeric substances (EPS) in anaerobic chemostats during transient conditions. *Biochemical Engineering Journal*, *38*(2), 138–146. https://doi.org/10.1016/j.bej.2007.06.010

Arunkumar, P., Sadish Kumar, V., Saran, S., Bindun, H., & Devipriya, S. P. (2019). Isolation of active coagulant protein from the seeds of Strychnos potatorum–a potential water treatment agent. *Environmental Technology (United Kingdom)*, *40*(12), 1624–1632. https://doi.org/10.1080/09593330.2018.1427798

Ayache, C., Pidou, M., Croué, J. P., Labanowski, J., Poussade, Y., Tazi-Pain, A., Keller, J., & Gernjak, W. (2013). Impact of effluent organic matter on low-pressure membrane fouling in tertiary treatment. *Water Research*, *47*(8), 2633–2642. https://doi.org/10.1016/j.watres.2013.01.043

Bang, W. H., Jung, Y., Park, J. W., Lee, S., & Maeng, S. K. (2019). Effects of hydraulic loading rate and organic load on the performance of a pilot-scale hybrid VF-HF constructed wetland in treating secondary effluent. *Chemosphere*, *218*, 232–240. https://doi.org/10.1016/j.chemosphere.2018.11.110

Barker, D. J., & Stuckey, D. C. (1999). *a Review of Soluble Microbial Products (Smp) in Wastewater Treatment Systems*. *33*(14).

Belfort, G., Davis, R. H., & Zydney, A. L. (1994). Behavior of suspensions and macromolecular solution in cross flow microfiltration: A Review. *Journal of Membrane Science*, *96*, 1–58.

Bessiere, Y., Jefferson, B., Goslan, E., & Bacchin, P. (2009). Effect of hydrophilic/hydrophobic fractions of natural organic matter on irreversible fouling of membranes. *Desalination*, *249*(1),

182–187. https://doi.org/10.1016/j.desal.2008.12.047

Boerlage, S. F. E., Kennedy, M. D., Aniye, M. P., Abogrean, E., Tarawneh, Z. S., & Schippers, J. C. (2003). The MFI-UF as a water quality test and monitor. *Journal of Membrane Science*, *211*(2), 271–289. https://doi.org/10.1016/S0376-7388(02)00427-1

Bolton, G., LaCasse, D., & Kuriyel, R. (2006). Combined models of membrane fouling: Development and application to microfiltration and ultrafiltration of biological fluids. *Journal of Membrane Science*, *277*(1–2), 75–84. https://doi.org/10.1016/j.memsci.2004.12.053

Cai, Q. Q., Wu, M. Y., Li, R., Deng, S. H., Lee, B. C. Y., Ong, S. L., & Hu, J. Y. (2020). Potential of combined advanced oxidation – Biological process for cost-effective organic matters removal in reverse osmosis concentrate produced from industrial wastewater reclamation: Screening of AOP pre-treatment technologies. *Chemical Engineering Journal*, *389*(November 2019). https://doi.org/10.1016/j.cej.2019.123419

Chen, F., Peldszus, S., Peiris, R. H., Ruhl, A. S., Mehrez, R., Jekel, M., Legge, R. L., & Huck, P. M. (2014). Pilot-scale investigation of drinking water ultrafiltration membrane fouling rates using advanced data analysis techniques. *Water Research*, *48*(1), 508–518. https://doi.org/10.1016/j.watres.2013.10.007

Chen, W., Westerhoff, P., Leenheer, J. A., & Booksh, K. (2003). Fluorescence Excitation-Emission Matrix Regional Integration to Quantify Spectra for Dissolved Organic Matter. *Environmental Science and Technology*, *37*(24), 5701–5710. https://doi.org/10.1021/es034354c

Chen, Z., Yang, B., Wen, Q., & Chen, C. (2020). Evaluation of enhanced coagulation combined with densadeg-ultrafiltration process in treating secondary effluent: Organic micro-pollutants removal, genotoxicity reduction, and membrane fouling alleviation. *Journal of Hazardous Materials*, *396*(March), 122697. https://doi.org/10.1016/j.jhazmat.2020.122697

Chen, Z., Yang, B., Wen, Q., & Tang, Y. (2021). Application of potassium ferrate combined with poly-aluminum chloride for mitigating ultrafiltration (UF) membrane fouling in secondary effluent: Comparison of oxidant dosing strategies. *Chemosphere*, *274*, 129862. https://doi.org/10.1016/j.chemosphere.2021.129862

Choi, B. G., Cho, J., Song, K. G., & Maeng, S. K. (2013). Correlation between effluent organic matter characteristics and membrane fouling in a membrane bioreactor using advanced organic matter characterization tools. *Desalination*, *309*, 74–83. https://doi.org/10.1016/j.desal.2012.09.018

Chu, H., Zhao, F., Tan, X., Yang, L., Zhou, X., Zhao, J., & Zhang, Y. (2016). The impact of temperature on membrane fouling in algae harvesting. *Algal Research*, *16*, 458–464. https://doi.org/10.1016/j.algal.2016.04.012

Corsino, S. F., de Oliveira, T. S., Di Trapani, D., Torregrossa, M., & Viviani, G. (2020). Simultaneous sludge minimization, biological phosphorous removal and membrane fouling mitigation in a novel plant layout for MBR. *Journal of Environmental Management*, *259*(October 2019), 109826. https://doi.org/10.1016/j.jenvman.2019.109826

Cui, L., Goodwin, C., Gao, W., & Liao, B. (2017). Effect of cold water temperature on membrane structure and properties. *Journal of Membrane Science*, *540*(February), 19–26. https://doi.org/10.1016/j.memsci.2017.06.037

Deng, L., Ngo, H. H., Guo, W., & Zhang, H. (2019). Pre-coagulation coupled with sponge-membrane filtration for organic matter removal and membrane fouling control during drinking water treatment. *Water Research*, *157*, 155–166. https://doi.org/10.1016/j.watres.2019.03.052

Ding, A., Wang, J., Lin, D., Tang, X., Cheng, X., Li, G., Ren, N., & Liang, H. (2017). In situ coagulation versus pre-coagulation for gravity-driven membrane bioreactor during decentralized sewage treatment: Permeability stabilization, fouling layer formation and biological activity. *Water Research*, *126*, 197–207. https://doi.org/10.1016/j.watres.2017.09.027

Drews, A. (2010). Membrane fouling in membrane bioreactors-Characterisation, contradictions, cause and cures. *Journal of Membrane Science*, *363*(1–2), 1–28. https://doi.org/10.1016/j.memsci.2010.06.046

Duyar, A., Ciftcioglu, V., Cirik, K., Civelekoglu, G., & Uruş, S. (2021). Treatment of landfill leachate using single-stage anoxic moving bed biofilm reactor and aerobic membrane reactor. *Science of the Total Environment*, *776*. https://doi.org/10.1016/j.scitotenv.2021.145919

Feng, L., Wang, W., Feng, R., Zhao, S., Dong, H., Sun, S., Gao, B., & Yue, Q. (2015). Coagulation performance and membrane fouling of different aluminum species during coagulation/ultrafiltration combined process. *Chemical Engineering Journal*, *262*, 1161–1167. https://doi.org/10.1016/j.cej.2014.10.078

Ferrer-Polonio, E., White, K., Mendoza-Roca, J. A., & Bes-Piá, A. (2018). The role of the operating parameters of SBR systems on the SMP production and on membrane fouling reduction. *Journal of Environmental Management*, *228*(September), 205–212. https://doi.org/10.1016/j.jenvman.2018.09.036

Filloux, E., Gallard, H., & Croue, J. P. (2012). Identification of effluent organic matter fractions responsible for low-pressure membrane fouling. *Water Research*, *46*(17), 5531–5540. https://doi.org/10.1016/j.watres.2012.07.034

Fu, C., Yue, X., Shi, X., Ng, K. K., & Ng, H. Y. (2017). Membrane fouling between a membrane bioreactor and a moving bed membrane bioreactor: Effects of solids retention time. *Chemical Engineering Journal*, *309*, 397–408. https://doi.org/10.1016/j.cej.2016.10.076

Gao, W. J., Qu, X., Leung, K. T., & Liao, B. Q. (2012). Influence of temperature and temperature shock on sludge properties, cake layer structure, and membrane fouling in a submerged anaerobic membrane bioreactor. *Journal of Membrane Science*, *421–422*, 131–144. https://doi.org/10.1016/j.memsci.2012.07.003

Gao, W., Liang, H., Ma, J., Han, M., Chen, Z. lin, Han, Z. shuang, & Li, G. bai. (2011). Membrane fouling control in ultrafiltration technology for drinking water production: A review. *Desalination*, *272*(1–3), 1–8. https://doi.org/10.1016/j.desal.2011.01.051

Guo, J., Liu, H., Liu, J., & Wang, L. (2014). Ultrafiltration performance of EfOM and NOM under different MWCO membranes: Comparison with fluorescence spectroscopy and gel filtration chromatography. *Desalination*, *344*, 129–136. https://doi.org/10.1016/j.desal.2014.03.006

Guo, W., Ngo, H. H., & Li, J. (2012). A mini-review on membrane fouling. *Bioresource Technology*, *122*, 27–34. https://doi.org/10.1016/j.biortech.2012.04.089

Gupta, K., & Chellam, S. (2020). Contributions of surface and pore deposition to (ir)reversible fouling during constant flux microfiltration of secondary municipal wastewater effluent. *Journal*

of Membrane Science, *610*(January), 118231. https://doi.org/10.1016/j.memsci.2020.118231

Gurung, K., Ncibi, M. C., & Sillanpää, M. (2017). Assessing membrane fouling and the performance of pilot-scale membrane bioreactor (MBR) to treat real municipal wastewater during winter season in Nordic regions. *Science of the Total Environment*, *579*, 1289–1297. https://doi.org/10.1016/j.scitotenv.2016.11.122

Haberkamp, J., Ruhl, A. S., Ernst, M., & Jekel, M. (2007). Impact of coagulation and adsorption on DOC fractions of secondary effluent and resulting fouling behaviour in ultrafiltration. *Water Research*, *41*(17), 3794–3802. https://doi.org/10.1016/j.watres.2007.05.029

Hao, S., Ren, S., Zhou, N., Chen, H., Usman, M., He, C., Shi, Q., Luo, G., & Zhang, S. (2020). Molecular composition of hydrothermal liquefaction wastewater from sewage sludge and its transformation during anaerobic digestion. *Journal of Hazardous Materials*, *383*(August 2019), 121163. https://doi.org/10.1016/j.jhazmat.2019.121163

He, H. Y., Qiu, W., Liu, Y. L., Yu, H. R., Wang, L., & Ma, J. (2021). Effect of ferrate pre-oxidation on algae-laden water ultrafiltration: Attenuating membrane fouling and decreasing formation potential of disinfection byproducts. *Water Research*, *190*, 116690. https://doi.org/10.1016/j.watres.2020.116690

Henderson, R. K., Subhi, N., Antony, A., Khan, S. J., Murphy, K. R., Leslie, G. L., Chen, V., Stuetz, R. M., & Le-Clech, P. (2011). Evaluation of effluent organic matter fouling in ultrafiltration treatment using advanced organic characterisation techniques. *Journal of Membrane Science*, *382*(1–2), 50–59. https://doi.org/10.1016/j.memsci.2011.07.041

Holloway, T. G., Williams, J. B., Ouelhadj, D., & Cleasby, B. (2021). Process stress, stability and resilience in wastewater treatment processes: A novel conceptual methodology. *Journal of Cleaner Production*, *282*, 124434. https://doi.org/10.1016/j.jclepro.2020.124434

Hu, H., Shi, Y., Liao, K., Ma, H., Xu, K., & Ren, H. (2019). Effect of temperature on the characterization of soluble microbial products in activated sludge system with special emphasis on dissolved organic nitrogen. *Water Research*, *162*, 87–94. https://doi.org/10.1016/j.watres.2019.06.034

Huang, W., Wang, L., Zhou, W., Lv, W., Hu, M., Chu, H., & Dong, B. (2017). Effects of combined ozone and PAC pretreatment on ultrafiltration membrane fouling control and mechanisms. *Journal of Membrane Science*, *533*(December 2016), 378–389. https://doi.org/10.1016/j.memsci.2017.03.044

Huang, Z., Ong, S. L., & Ng, H. Y. (2011). Submerged anaerobic membrane bioreactor for low-strength wastewater treatment: Effect of HRT and SRT on treatment performance and membrane fouling. *Water Research*, *45*(2), 705–713. https://doi.org/10.1016/j.watres.2010.08.035

Huber, S. A., Balz, A., Abert, M., & Pronk, W. (2011). Characterisation of aquatic humic and non-humic matter with size-exclusion chromatography - organic carbon detection - organic nitrogen detection (LC-OCD-OND). *Water Research*, *45*(2), 879–885. https://doi.org/10.1016/j.watres.2010.09.023

Iorhemen, O. T., Hamza, R. A., & Tay, J. H. (2016). Membrane bioreactor (Mbr) technology for wastewater treatment and reclamation: Membrane fouling. *Membranes*, *6*(2), 13–16.

https://doi.org/10.3390/membranes6020033

Iorhemen, O. T., Hamza, R. A., Zaghloul, M. S., & Tay, J. H. (2019). Aerobic granular sludge membrane bioreactor (AGMBR): Extracellular polymeric substances (EPS) analysis. *Water Research*, *156*, 305–314. https://doi.org/10.1016/j.watres.2019.03.020

Iversen, V., Mehrez, R., Horng, R. Y., Chen, C. H., Meng, F., Drews, A., Lesjean, B., Ernst, M., Jekel, M., & Kraume, M. (2009). Fouling mitigation through flocculants and adsorbents addition in membrane bioreactors: Comparing lab and pilot studies. *Journal of Membrane Science*, *345*(1–2), 21–30. https://doi.org/10.1016/j.memsci.2009.08.014

Jarusutthirak, C., & Amy, G. (2007). Understanding soluble microbial products (SMP) as a component of effluent organic matter (EfOM). *Water Research*, *41*(12), 2787–2793. https://doi.org/10.1016/j.watres.2007.03.005

Jiang, Q., Ngo, H. H., Nghiem, L. D., Hai, F. I., Price, W. E., Zhang, J., Liang, S., Deng, L., & Guo, W. (2018). Effect of hydraulic retention time on the performance of a hybrid moving bed biofilm reactor-membrane bioreactor system for micropollutants removal from municipal wastewater. *Bioresource Technology*, *247*(September 2017), 1228–1232. https://doi.org/10.1016/j.biortech.2017.09.114

Jiang, T., Kennedy, M. D., Schepper, V. De, Nam, S. N., Nopens, I., Vanrolleghem, P. A., & Amy, G. (2010). Characterization of soluble microbial products and their fouling impacts in membrane bioreactors. *Environmental Science and Technology*, *44*(17), 6642–6648. https://doi.org/10.1021/es100442g

Jiang, T., Myngheer, S., De Pauw, D. J. W., Spanjers, H., Nopens, I., Kennedy, M. D., Amy, G., & Vanrolleghem, P. A. (2008). Modelling the production and degradation of soluble microbial products (SMP) in membrane bioreactors (MBR). *Water Research*, *42*(20), 4955–4964. https://doi.org/10.1016/j.watres.2008.09.037

Johir, M. A. H., Vigneswaran, S., Sathasivan, A., Kandasamy, J., & Chang, C. Y. (2012). Effect of organic loading rate on organic matter and foulant characteristics in membrane bio-reactor. *Bioresource Technology*, *113*, 154–160. https://doi.org/10.1016/j.biortech.2011.12.002

Jutaporn, P., Cory, R. M., Singer, P. C., & Coronell, O. (2021). Efficacy of selected pretreatment processes in the mitigation of low-pressure membrane fouling and its correlation to their removal of microbial DOM. *Chemosphere*, *277*, 130284. https://doi.org/10.1016/j.chemosphere.2021.130284

Kakuda, T., Iwasaki, H., & Kimura, K. (2020). Fouling potential of lipopolysaccharides released at low temperatures in MBRs. *Water Science and Technology*, *81*(3), 529–534. https://doi.org/10.2166/WST.2020.131

Kimura, K., Kakuda, T., & Iwasaki, H. (2019). Membrane fouling caused by lipopolysaccharides: A suggestion for alternative model polysaccharides for MBR fouling research. *Separation and Purification Technology*, *223*(April), 224–233. https://doi.org/10.1016/j.seppur.2019.04.059

Kimura, K., & Kume, K. (2020). Irreversible fouling in hollow-fiber PVDF MF/UF membranes filtering surface water: Effects of precoagulation and identification of the foulant. *Journal of Membrane Science*, *602*(February), 117975. https://doi.org/10.1016/j.memsci.2020.117975

Kimura, K., Ogyu, R., Miyoshi, T., & Watanabe, Y. (2015). Transition of major components in

irreversible fouling of MBRs treating municipal wastewater. *Separation and Purification Technology*, *142*, 326–331. https://doi.org/10.1016/j.seppur.2014.12.030

Kimura, K., & Oki, Y. (2017). Efficient control of membrane fouling in MF by removal of biopolymers: Comparison of various pretreatments. *Water Research*, *115*, 172–179. https://doi.org/10.1016/j.watres.2017.02.033

Kimura, K., Shikato, K., Oki, Y., Kume, K., & Huber, S. A. (2018). Surface water biopolymer fractionation for fouling mitigation in low-pressure membranes. *Journal of Membrane Science*, *554*(November 2017), 83–89. https://doi.org/10.1016/j.memsci.2018.02.024

Kimura, K., Tanaka, K., & Watanabe, Y. (2014). Microfiltration of different surface waters with/without coagulation: Clear correlations between membrane fouling and hydrophilic biopolymers. *Water Research*, *49*, 434–443. https://doi.org/10.1016/j.watres.2013.10.030

Krzeminski, P., Iglesias-Obelleiro, A., Madebo, G., Garrido, J. M., van der Graaf, J. H. J. M., & van Lier, J. B. (2012). Impact of temperature on raw wastewater composition and activated sludge filterability in full-scale MBR systems for municipal sewage treatment. *Journal of Membrane Science*, *423–424*, 348–361. https://doi.org/10.1016/j.memsci.2012.08.032

Krzeminski, Pawel, Leverette, L., Malamis, S., & Katsou, E. (2017). Membrane bioreactors – A review on recent developments in energy reduction, fouling control, novel configurations, LCA and market prospects. *Journal of Membrane Science*, *527*(December 2016), 207–227. https://doi.org/10.1016/j.memsci.2016.12.010

Kunacheva, C., & Stuckey, D. C. (2014). Analytical methods for soluble microbial products (SMP) and extracellular polymers (ECP) in wastewater treatment systems: A review. *Water Research*, *61*, 1–18. https://doi.org/10.1016/j.watres.2014.04.044

Lee, B. B., Choo, K. H., Chang, D., & Choi, S. J. (2009). Optimizing the coagulant dose to control membrane fouling in combined coagulation/ultrafiltration systems for textile wastewater reclamation. *Chemical Engineering Journal*, *155*(1–2), 101–107. https://doi.org/10.1016/j.cej.2009.07.014

Lin, H., Zhang, M., Wang, F., Meng, F., Liao, B. Q., Hong, H., Chen, J., & Gao, W. (2014). A critical review of extracellular polymeric substances (EPSs) in membrane bioreactors: Characteristics, roles in membrane fouling and control strategies. *Journal of Membrane Science*, *460*, 110–125. https://doi.org/10.1016/j.memsci.2014.02.034

Lishman, L. A., Legge, R. L., & Farquhar, G. J. (2000). Temperature effects on wastewater treatment under aerobic and anoxic conditions. *Water Research*, *34*(8), 2263–2276. https://doi.org/10.1016/S0043-1354(99)00393-0

Liu, Jing, He, K., Tang, S., Wang, T., & Zhang, Z. (2019). A comparative study of ferrous, ferric and ferrate pretreatment for ceramic membrane fouling alleviation in reclaimed water treatment. *Separation and Purification Technology*, *217*(January), 118–127. https://doi.org/10.1016/j.seppur.2019.01.040

Liu, Jing, He, K., Zhang, J., Li, C., & Zhang, Z. (2019). Coupling ferrate pretreatment and in-situ ozonation/ceramic membrane filtration for wastewater reclamation: Water quality and membrane fouling. *Journal of Membrane Science*, *590*(June), 117310. https://doi.org/10.1016/j.memsci.2019.117310

Liu, Jing, Zhang, Z., Liu, Z., & Zhang, X. (2018). Integration of ferrate (VI) pretreatment and ceramic membrane reactor for membrane fouling mitigation in reclaimed water treatment. *Journal of Membrane Science*, *552*(December 2017), 315–325. https://doi.org/10.1016/j.memsci.2018.02.031

Liu, Junxia, Yang, E., Huang, T., Wang, Z., & Dong, B. (2020). Correlation of chemically irreversible fouling with organic constituents of feed water during membrane filtration. *Colloids and Surfaces A: Physicochemical and Engineering Aspects*, *597*(March), 124790. https://doi.org/10.1016/j.colsurfa.2020.124790

Liu, T., Chen, Z. L., Yu, W. Z., Shen, J. M., & Gregory, J. (2011). Effect of two-stage coagulant addition on coagulation-ultrafiltration process for treatment of humic-rich water. *Water Research*, *45*(14), 4260–4268. https://doi.org/10.1016/j.watres.2011.05.037

Liu, T., Lian, Y., Graham, N., Yu, W., Rooney, D., & Sun, K. (2017). Application of polyacrylamide flocculation with and without alum coagulation for mitigating ultrafiltration membrane fouling: Role of floc structure and bacterial activity. *Chemical Engineering Journal*, *307*, 41–48. https://doi.org/10.1016/j.cej.2016.08.063

Liu, X., Yin, H., Zhao, J., Guo, Z., Liu, Z., & Sang, Y. (2021). Understanding the coagulation mechanism and floc properties induced by ferrate(VI) and FeCl3: population balance modeling. *Water Science and Technology*, 1–12. https://doi.org/10.2166/wst.2021.150

Ly, Q. V., Nghiem, L. D., Sibag, M., Maqbool, T., & Hur, J. (2018). Effects of COD/N ratio on soluble microbial products in effluent from sequencing batch reactors and subsequent membrane fouling. *Water Research*, *134*, 13–21. https://doi.org/10.1016/j.watres.2018.01.024

Ma, C., Yu, S., Shi, W., Heijman, S. G. J., & Rietveld, L. C. (2013). Effect of different temperatures on performance and membrane fouling in high concentration PAC-MBR system treating micro-polluted surface water. *Bioresource Technology*, *141*, 19–24. https://doi.org/10.1016/j.biortech.2013.02.025

Ma, Z., Wen, X., Zhao, F., Xia, Y., Huang, X., Waite, D., & Guan, J. (2013). Effect of temperature variation on membrane fouling and microbial community structure in membrane bioreactor. *Bioresource Technology*, *133*, 462–468. https://doi.org/10.1016/j.biortech.2013.01.023

Maqbool, T., Cho, J., & Hur, J. (2017). Dynamic changes of dissolved organic matter in membrane bioreactors at different organic loading rates: Evidence from spectroscopic and chromatographic methods. *Bioresource Technology*, *234*, 131–139. https://doi.org/10.1016/j.biortech.2017.03.035

Matilainen, A., Gjessing, E. T., Lahtinen, T., Hed, L., Bhatnagar, A., & Sillanpää, M. (2011). An overview of the methods used in the characterisation of natural organic matter (NOM) in relation to drinking water treatment. *Chemosphere*, *83*(11), 1431–1442. https://doi.org/10.1016/j.chemosphere.2011.01.018

Meng, F., Chae, S. R., Drews, A., Kraume, M., Shin, H. S., & Yang, F. (2009). Recent advances in membrane bioreactors (MBRs): Membrane fouling and membrane material. *Water Research*, *43*(6), 1489–1512. https://doi.org/10.1016/j.watres.2008.12.044

Meng, F., Shi, B., Yang, F., & Zhang, H. (2007). Effect of hydraulic retention time on membrane fouling and biomass characteristics in submerged membrane bioreactors. *Bioprocess and Biosystems Engineering*, *30*(5), 359–367. https://doi.org/10.1007/s00449-007-0132-1

Meng, F., Zhang, S., Oh, Y., Zhou, Z., Shin, H. S., & Chae, S. R. (2017). Fouling in membrane bioreactors: An updated review Fangang. *Water Research*, *114*, 151–180. https://doi.org/10.1016/j.watres.2017.02.006

Menniti, A., & Morgenroth, E. (2010). Mechanisms of SMP production in membrane bioreactors: Choosing an appropriate mathematical model structure. *Water Research*, *44*(18), 5240–5251. https://doi.org/10.1016/j.watres.2010.06.040

Michael-Kordatou, I., Michael, C., Duan, X., He, X., Dionysiou, D. D., Mills, M. A., & Fatta-Kassinos, D. (2015). Dissolved effluent organic matter: Characteristics and potential implications in wastewater treatment and reuse applications. *Water Research*, *77*, 213–248. https://doi.org/10.1016/j.watres.2015.03.011

Miyoshi, T., Tsuyuhara, T., Ogyu, R., Kimura, K., & Watanabe, Y. (2009). Seasonal variation in membrane fouling in membrane bioreactors (MBRs) treating municipal wastewater. *Water Research*, *43*(20), 5109–5118. https://doi.org/10.1016/j.watres.2009.08.035

Metcalf, Eddy, 2003. Wastewater Engineering: Treatment and Reuse. 4th ed. McGraw- Hill, New York

Melcer, H., Dold, P.L., Jones, R.M., Bye, C.M., Takacs, I., Stensel, H.D., Wilson, A.W., Sun, P., Bury, S., 2003. Methods for wastewater characterization in activated sludge model- ing. WERF Final Report, Project 99-WWF-3. Water Environment Research Founda- tion, Alexandria, VA

Nachaiyasit, S., & Stuckey, D. C. (1997). Effect of Low Temperatures on the Performance of an Anaerobic Baffled Reactor (ABR). *Journal of Chemical Technology & Biotechnology*, *69*(2), 276–284. https://doi.org/10.1002/(sici)1097-4660(199706)69:2<276::aid-jctb711>3.3.co;2-k

Naim, R., Epsztein, R., Felder, A., Heyer, M., Heijnen, M., & Gitis, V. (2014). Rethinking the role of in-line coagulation in tertiary membrane filtration of municipal effluents. *Separation and Purification Technology*, *125*, 11–20. https://doi.org/10.1016/j.seppur.2014.01.036

Namkung, E., & Rittmann, B. E. (1986). Soluble microbial products (SMP) formation kinetics by biofilms. *Water Research*, *20*(6), 795–806. https://doi.org/10.1016/0043-1354(86)90106-5

Nguyen, A. H., Tobiason, J. E., & Howe, K. J. (2011). Fouling indices for low pressure hollow fiber membrane performance assessment. *Water Research*, *45*(8), 2627–2637. https://doi.org/10.1016/j.watres.2011.02.020

Ni, B. J., Fang, F., Xie, W. M., Xu, J., & Yu, H. Q. (2012). Formation of distinct soluble microbial products by activated sludge: Kinetic analysis and quantitative determination. *Environmental Science and Technology*, *46*(3), 1667–1674. https://doi.org/10.1021/es202756d

Ni, B. J., Rittmann, B. E., & Yu, H. Q. (2011). Soluble microbial products and their implications in mixed culture biotechnology. *Trends in Biotechnology*, *29*(9), 454–463. https://doi.org/10.1016/j.tibtech.2011.04.006

Ozgun, H., Tao, Y., Ersahin, M. E., Zhou, Z., Gimenez, J. B., Spanjers, H., & van Lier, J. B. (2015). Impact of temperature on feed-flow characteristics and filtration performance of an upflow anaerobic sludge blanket coupled ultrafiltration membrane treating municipal wastewater. *Water Research*, *83*, 71–83. https://doi.org/10.1016/j.watres.2015.06.035

Paul, P. (2011). Investigation of a MBR membrane fouling model based on time series analysis

system identification methods. *Desalination and Water Treatment*, *35*(1–3), 92–100. https://doi.org/DOI 10.5004/dwt.2011.3135

Peiris, R. H., Jaklewicz, M., Budman, H., Legge, R. L., & Moresoli, C. (2013). Assessing the role of feed water constituents in irreversible membrane fouling of pilot-scale ultrafiltration drinking water treatment systems. *Water Research*, *47*(10), 3364–3374. https://doi.org/10.1016/j.watres.2013.03.015

Peiris, Ramila H., Hallé, C., Budman, H., Moresoli, C., Peldszus, S., Huck, P. M., & Legge, R. L. (2010). Identifying fouling events in a membrane-based drinking water treatment process using principal component analysis of fluorescence excitation-emission matrices. *Water Research*, *44*(1), 185–194. https://doi.org/10.1016/j.watres.2009.09.036

Peleato, N. M., Legge, R. L., & Andrews, R. C. (2017). Characterization of UF foulants and fouling mechanisms when applying low in-line coagulant pre-treatment. *Water Research*, *126*, 1–11. https://doi.org/10.1016/j.watres.2017.08.064

Poojamnong, K., Tungsudjawong, K., Khongnakorn, W., & Jutaporn, P. (2020). Characterization of reversible and irreversible foulants in membrane bioreactor (MBR) for eucalyptus pulp and paper mill wastewater treatment using fluorescence regional integration. *Journal of Environmental Chemical Engineering*, *8*(5), 104231. https://doi.org/10.1016/j.jece.2020.104231

Pramanik, B. K., Roddick, F. A., & Fan, L. (2016). Long-term operation of biological activated carbon pre-treatment for microfiltration of secondary effluent: Correlation between the organic foulants and fouling potential. *Water Research*, *90*, 405–414. https://doi.org/10.1016/j.watres.2015.12.041

Qu, F., Yang, Z., Li, X., Yu, H., Pan, Z., Fan, G., He, J., & Rong, H. (2021). Membrane fouling control by UV/persulfate in tertiary wastewater treatment with ultrafiltration: A comparison with UV/hydroperoxide and role of free radicals. *Separation and Purification Technology*, *257*(August 2020), 117877. https://doi.org/10.1016/j.seppur.2020.117877

Rabuni, M. F., Nik Sulaiman, N. M., Aroua, M. K., Yern Chee, C., & Awanis Hashim, N. (2015). Impact of in situ physical and chemical cleaning on PVDF membrane properties and performances. *Chemical Engineering Science*, *122*, 426–435. https://doi.org/10.1016/j.ces.2014.09.053

Riley, S. M., Ahoor, D. C., Regnery, J., & Cath, T. Y. (2018). Tracking oil and gas wastewater-derived organic matter in a hybrid biofilter membrane treatment system: A multi-analytical approach. *Science of the Total Environment*, *613–614*, 208–217. https://doi.org/10.1016/j.scitotenv.2017.09.031

Robles, A., Ruano, M. V., Ribes, J., & Ferrer, J. (2013). Factors that affect the permeability of commercial hollow-fibre membranes in a submerged anaerobic MBR (HF-SAnMBR) system. *Water Research*, *47*(3), 1277–1288. https://doi.org/10.1016/j.watres.2012.11.055

Rosenberger, S., Laabs, C., Lesjean, B., Gnirss, R., Amy, G., Jekel, M., & Schrotter, J. C. (2006). Impact of colloidal and soluble organic material on membrane performance in membrane bioreactors for municipal wastewater treatment. *Water Research*, *40*(4), 710–720. https://doi.org/10.1016/j.watres.2005.11.028

Salazar-Peláez, M. L., Morgan-Sagastume, J. M., & Noyola, A. (2011). Influence of hydraulic

retention time on fouling in a UASB coupled with an external ultrafiltration membrane treating synthetic municipal wastewater. *Desalination*, *277*(1–3), 164–170. https://doi.org/10.1016/j.desal.2011.04.021

Sánchez, A., Garrido, J. M., & Méndez, R. (2011). Tertiary membrane filtration of an industrial wastewater using granular or flocculent biomass sequencing batch reactors. *Journal of Membrane Science*, *382*(1–2), 316–322. https://doi.org/10.1016/j.memsci.2011.08.027

Shang, R., Vuong, F., Hu, J., Li, S., Kemperman, A. J. B., Nijmeijer, K., Cornelissen, E. R., Heijman, S. G. J., & Rietveld, L. C. (2015). Hydraulically irreversible fouling on ceramic MF/UF membranes: Comparison of fouling indices, foulant composition and irreversible pore narrowing. *Separation and Purification Technology*, *147*, 303–310. https://doi.org/10.1016/j.seppur.2015.04.039

Sharma, R. R., Agrawal, R., & Chellam, S. (2003). Temperature effects on sieving characteristics of thin-film composite nanofiltration membranes: Pore size distributions and transport parameters. *Journal of Membrane Science*, *223*(1–2), 69–87. https://doi.org/10.1016/S0376-7388(03)00310-7

Shen, X., Gao, B., Huang, X., Bu, F., Yue, Q., Li, R., & Jin, B. (2017). Effect of the dosage ratio and the viscosity of PAC/PDMDAAC on coagulation performance and membrane fouling in a hybrid coagulation-ultrafiltration process. *Chemosphere*, *173*, 288–298. https://doi.org/10.1016/j.chemosphere.2017.01.074

Shi, Y., Huang, J., Zeng, G., Gu, Y., Hu, Y., Tang, B., Zhou, J., Yang, Y., & Shi, L. (2018). Evaluation of soluble microbial products (SMP) on membrane fouling in membrane bioreactors (MBRs) at the fractional and overall level: a review. *Reviews in Environmental Science and Biotechnology*, *17*(1), 71–85. https://doi.org/10.1007/s11157-017-9455-9

Shon, H. K., Vigneswaran, S., & Snyder, S. A. (2006). Effluent organic matter (EfOM) in wastewater: Constituents, effects, and treatment. *Critical Reviews in Environmental Science and Technology*, *36*(4), 327–374. https://doi.org/10.1080/10643380600580011

Soh, Y. N. A., Kunacheva, C., Webster, R. D., & Stuckey, D. C. (2020). Identification of the production and biotransformational changes of soluble microbial products (SMP) in wastewater treatment processes: A short review. *Chemosphere*, *251*, 126391. https://doi.org/10.1016/j.chemosphere.2020.126391

Steinhauer, T., Hanély, S., Bogendörfer, K., & Kulozik, U. (2015). Temperature dependent membrane fouling during filtration of whey and whey proteins. *Journal of Membrane Science*, *492*, 364–370. https://doi.org/10.1016/j.memsci.2015.05.053

Sun, F., Sun, B., Li, Q., Deng, X., Hu, J., & Wu, W. (2014). Pilot-scale nitrogen removal from leachate by ex situ nitrification and in situ denitrification in a landfill bioreactor. *Chemosphere*, *101*, 77–85. https://doi.org/10.1016/j.chemosphere.2013.12.030

Sun, J., Xiao, K., Mo, Y., Liang, P., Shen, Y., Zhu, N., & Huang, X. (2014). Seasonal characteristics of supernatant organics and its effect on membrane fouling in a full-scale membrane bioreactor. *Journal of Membrane Science*, *453*, 168–174. https://doi.org/10.1016/j.memsci.2013.11.003

Taimur Khan, M. M., Takizawa, S., Lewandowski, Z., Habibur Rahman, M., Komatsu, K., Nelson, S. E., Kurisu, F., Camper, A. K., Katayama, H., & Ohgaki, S. (2013). Combined effects of EPS

and HRT enhanced biofouling on a submerged and hybrid PAC-MF membrane bioreactor. *Water Research*, *47*(2), 747–757. https://doi.org/10.1016/j.watres.2012.10.048

Tao, C., Parker, W., & Bérubé, P. (2021). Characterization and modelling of soluble microbial products in activated sludge systems treating municipal wastewater with special emphasis on temperature effect. *Science of the Total Environment*, *779*, 146471. https://doi.org/10.1016/j.scitotenv.2021.146471

Tao, C., Parker, W., & Pierre, B. (2022). Assessing the role of cold temperatures on irreversible membrane permeability of tertiary ultrafiltration treating municipal wastewater. *Separation and Purification Technology*, *278*(June 2021). https://doi.org/10.1016/j.seppur.2021.119556

Teng, J., Shen, L., Xu, Y., Chen, Y., Wu, X. L., He, Y., Chen, J., & Lin, H. (2020). Effects of molecular weight distribution of soluble microbial products (SMPs) on membrane fouling in a membrane bioreactor (MBR): Novel mechanistic insights. *Chemosphere*, *248*, 126013. https://doi.org/10.1016/j.chemosphere.2020.126013

Tian, Y., Chen, L., & Jiang, T. (2011). Characterization and modeling of the soluble microbial products in membrane bioreactor. *Separation and Purification Technology*, *76*(3), 316–324. https://doi.org/10.1016/j.seppur.2010.10.022

Tian, Y., Chen, L., Zhang, S., Cao, C., & Zhang, S. (2011). Correlating membrane fouling with sludge characteristics in membrane bioreactors: An especial interest in EPS and sludge morphology analysis. *Bioresource Technology*, *102*(19), 8820–8827. https://doi.org/10.1016/j.biortech.2011.07.010

Tian, Y., Chen, L., Zhang, S., & Zhang, S. (2011). A systematic study of soluble microbial products and their fouling impacts in membrane bioreactors. *Chemical Engineering Journal*, *168*(3), 1093–1102. https://doi.org/10.1016/j.cej.2011.01.090

Tian, Y., & Su, X. (2012). Relation between the stability of activated sludge flocs and membrane fouling in MBR: Under different SRTs. *Bioresource Technology*, *118*, 477–482. https://doi.org/10.1016/j.biortech.2012.05.072

van den Brink, P., Satpradit, O. A., van Bentem, A., Zwijnenburg, A., Temmink, H., & van Loosdrecht, M. (2011). Effect of temperature shocks on membrane fouling in membrane bioreactors. *Water Research*, *45*(15), 4491–4500. https://doi.org/10.1016/j.watres.2011.05.046

Vera, L., González, E., Díaz, O., Sánchez, R., Bohorque, R., & Rodríguez-Sevilla, J. (2015). Fouling analysis of a tertiary submerged membrane bioreactor operated in dead-end mode at high-fluxes. *Journal of Membrane Science*, *493*, 8–18. https://doi.org/10.1016/j.memsci.2015.06.014

Wang, D., Guo, F., Wu, Y., Li, Z., & Wu, G. (2018). Technical, economic and environmental assessment of coagulation/filtration tertiary treatment processes in full-scale wastewater treatment plants. *Journal of Cleaner Production*, *170*, 1185–1194. https://doi.org/10.1016/j.jclepro.2017.09.231

Wang, H., Park, M., Liang, H., Wu, S., Lopez, I. J., Ji, W., Li, G., & Snyder, S. A. (2017). Reducing ultrafiltration membrane fouling during potable water reuse using pre-ozonation. *Water Research*, *125*, 42–51. https://doi.org/10.1016/j.watres.2017.08.030

Wang, M., & Chen, Y. (2018). Generation and characterization of DOM in wastewater treatment processes. *Chemosphere*, *201*, 96–109. https://doi.org/10.1016/j.chemosphere.2018.02.124

Wang, Y., Fortunato, L., Jeong, S., & Leiknes, T. O. (2017). Gravity-driven membrane system for secondary wastewater effluent treatment: Filtration performance and fouling characterization. *Separation and Purification Technology*, *184*, 26–33. https://doi.org/10.1016/j.seppur.2017.04.027

Wang, Zhenbei, Nan, J., Yao, M., Yang, Y., & Zhang, X. (2017). Insight into the combined coagulation-ultrafiltration process: The role of Al species of polyaluminum chlorides. *Journal of Membrane Science*, *529*(October 2016), 80–86. https://doi.org/10.1016/j.memsci.2017.01.061

Wang, Zhi-ping, & Zhang, T. (2010). Characterization of soluble microbial products (SMP) under stressful conditions. *Water Research*, *44*(18), 5499–5509. https://doi.org/10.1016/j.watres.2010.06.067

Wang, Zhiwei, Wu, Z., & Tang, S. (2010). Impact of temperature seasonal change on sludge characteristics and membrane fouling in a submerged membrane bioreactor. *Separation Science and Technology*, *45*(7), 920–927. https://doi.org/10.1080/01496391003656974

Watanabe, R., Nie, Y., Wakahara, S., Komori, D., & Li, Y. Y. (2017). Investigation on the response of anaerobic membrane bioreactor to temperature decrease from 25 °C to 10 °C in sewage treatment. *Bioresource Technology*, *243*, 747–754. https://doi.org/10.1016/j.biortech.2017.07.001

Weishaar, J. L., Aiken, G. R., Bergamaschi, B. A., Fram, M. S., Fujii, R., & Mopper, K. (2003). Evaluation of specific ultraviolet absorbance as an indicator of the chemical composition and reactivity of dissolved organic carbon. *Environmental Science and Technology*, *37*(20), 4702–4708. https://doi.org/10.1021/es030360x

Xie, W. M., Ni, B. J., Sheng, G. P., Seviour, T., & Yu, H. Q. (2016). Quantification and kinetic characterization of soluble microbial products from municipal wastewater treatment plants. *Water Research*, *88*, 703–710. https://doi.org/10.1016/j.watres.2015.10.065

Xu, J., Sheng, G. P., Luo, H. W., Fang, F., Li, W. W., Zeng, R. J., Tong, Z. H., & Yu, H. Q. (2011). Evaluating the influence of process parameters on soluble microbial products formation using response surface methodology coupled with grey relational analysis. *Water Research*, *45*(2), 674–680. https://doi.org/10.1016/j.watres.2010.08.032

Yamamura, H., Okimoto, K., Kimura, K., & Watanabe, Y. (2014). Hydrophilic fraction of natural organic matter causing irreversible fouling of microfiltration and ultrafiltration membranes. *Water Research*, *54*, 123–136. https://doi.org/10.1016/j.watres.2014.01.024

Yang, J., Monnot, M., Eljaddi, T., Ercolei, L., Simonian, L., & Moulin, P. (2021). Ultrafiltration as tertiary treatment for municipal wastewater reuse. *Separation and Purification Technology*, *272*(May 2020), 118921. https://doi.org/10.1016/j.seppur.2021.118921

Yang, T., Xiong, H., Liu, F., Yang, Q., Xu, B., & Zhan, C. (2019). Effect of UV/TiO2 pretreatment on fouling alleviation and mechanisms of fouling development in a cross-flow filtration process using a ceramic UF membrane. *Chemical Engineering Journal*, *358*(October 2018), 1583–1593. https://doi.org/10.1016/j.cej.2018.10.149

Yang, W., Cicek, N., & Ilg, J. (2006). State-of-the-art of membrane bioreactors: Worldwide research and commercial applications in North America. *Journal of Membrane Science*, *270*(1–2), 201–211. https://doi.org/10.1016/j.memsci.2005.07.010

Yang, X., Li, D., Yu, Z., Meng, Y., Zheng, X., Zhao, S., & Meng, F. (2021). Biochemical characteristics and membrane fouling behaviors of soluble microbial products during the lifecycle of Escherichia coli. *Water Research*, *192*, 116835. https://doi.org/10.1016/j.watres.2021.116835

Yu, H., Li, X., Chang, H., Zhou, Z., Zhang, T., Yang, Y., Li, G., Ji, H., Cai, C., & Liang, H. (2020). Performance of hollow fiber ultrafiltration membrane in a full-scale drinking water treatment plant in China: A systematic evaluation during 7-year operation. *Journal of Membrane Science*, *613*(April), 118469. https://doi.org/10.1016/j.memsci.2020.118469

Yu, W. Z., Liu, H. J., Xu, L., Qu, J. H., & Graham, N. (2013). The pre-treatment of submerged ultrafiltration membrane by coagulation-Effect of polyacrylamide as a coagulant aid. *Journal of Membrane Science*, *446*, 50–58. https://doi.org/10.1016/j.memsci.2013.06.012

Yu, Wen zheng, Graham, N., Liu, H. juan, & Qu, J. hui. (2013). Comparison of FeCl3 and alum pre-treatment on UF membrane fouling. *Chemical Engineering Journal*, *234*, 158–165. https://doi.org/10.1016/j.cej.2013.08.105

Yu, Wenzheng, & Graham, N. J. D. (2015). Application of Fe(II)/K2MnO4 as a pre-treatment for controlling UF membrane fouling in drinking water treatment. *Journal of Membrane Science*, *473*, 283–291. https://doi.org/10.1016/j.memsci.2014.08.060

Yu, Wenzheng, Graham, N. J. D., & Fowler, G. D. (2016). Coagulation and oxidation for controlling ultrafiltration membrane fouling in drinking water treatment: Application of ozone at low dose in submerged membrane tank. *Water Research*, *95*, 1–10. https://doi.org/10.1016/j.watres.2016.02.063

Yu, Wenzheng, Graham, N., & Liu, T. (2019). Prevention of UF membrane fouling in drinking water treatment by addition of H 2 O 2 during membrane backwashing. *Water Research*, *149*, 394–405. https://doi.org/10.1016/j.watres.2018.11.006

Yu, Wenzheng, Xu, L., Qu, J., & Graham, N. (2014). Investigation of pre-coagulation and powder activate carbon adsorption on ultrafiltration membrane fouling. *Journal of Membrane Science*, *459*, 157–168. https://doi.org/10.1016/j.memsci.2014.02.005

Yu, Wenzheng, Yang, Y., & Graham, N. (2016). Evaluation of ferrate as a coagulant aid/oxidant pretreatment for mitigating submerged ultrafiltration membrane fouling in drinking water treatment. *Chemical Engineering Journal*, *298*, 234–242. https://doi.org/10.1016/j.cej.2016.03.080

Yu, Wenzheng, Zhang, D., & Graham, N. J. D. (2017). Membrane fouling by extracellular polymeric substances after ozone pre-treatment: Variation of nano-particles size. *Water Research*, *120*, 146–155. https://doi.org/10.1016/j.watres.2017.04.080

Zhan, M., Gwak, G., Kim, D. I., Park, K., & Hong, S. (2020). Quantitative analysis of the irreversible membrane fouling of forward osmosis during wastewater reclamation: Correlation with the modified fouling index. *Journal of Membrane Science*, *597*(December 2019), 117757. https://doi.org/10.1016/j.memsci.2019.117757

Zhao, B., Wang, D., Li, T., Chow, C. W. K., & Huang, C. (2010). Influence of floc structure on coagulation-microfiltration performance: Effect of Al speciation characteristics of PACls. *Separation and Purification Technology*, *72*(1), 22–27.

https://doi.org/10.1016/j.seppur.2009.12.023

Zhao, F., Chu, H., Zhang, Y., Jiang, S., Yu, Z., Zhou, X., & Zhao, J. (2017). Increasing the vibration frequency to mitigate reversible and irreversible membrane fouling using an axial vibration membrane in microalgae harvesting. *Journal of Membrane Science*, *529*(July 2016), 215–223. https://doi.org/10.1016/j.memsci.2017.01.039

Zhao, Y., Fang, Y., Jin, Y., Huang, J., Ma, X., He, K., He, Z., Wang, F., & Zhao, H. (2015). Microbial community and removal of nitrogen via the addition of a carrier in a pilot-scale duckweed-based wastewater treatment system. *Bioresource Technology*, *179*, 549–558. https://doi.org/10.1016/j.biortech.2014.12.037

Appendix A

Supplementary Data for Chapter 3

Table A1. Wastewater fractionation.

Modelled parameter	Symbol	Equation*
Fraction of non-biodegradable soluble COD	f_{si}	$\boldsymbol{f_{si} = \frac{sCOD_{EFF}}{COD_{T,INF}}}$
Fraction of non-biodegradable particulate COD	f_{xi}	$\boldsymbol{X_{VSS} = \frac{QCOD_{T,INF}\Theta_c}{f_{CV}}\left\{\frac{(1-f_{si}-f_{xi})Y_{HET}}{1+b_H\Theta_c}(1 + fb_H\Theta_c) + f_{xi}\right\}}$
Concentration of biodegradable COD in influent	S_0	$\boldsymbol{S_0 = (1 - f_{si} - f_{xi})COD_{T,INF}}$
Concentration of non-biodegradable particulate COD in influent	$X_{i,0}$	$\boldsymbol{X_{i,0} = f_{xi}COD_{T,INF}}$

*Where $sCOD_{EFF}$ is effluent soluble COD concentration (mg/L), $COD_{T,INF}$ is influent total COD concentration (mg/L), X_{VSS} is mixed liquor VSS concentration (mg VSS/L), Q is influent flow rate (L/d), Θ_C is sludge age (d), V is reactor volume (L), Y_{HET} is heterotroph yield coefficient, b_H is steady state theory endogenous decay rate (1/d), f is steady state theory endogenous residue fraction and f_{CV} is mixed liquor solids COD/VSS ratio.

Table A2. Activated sludge process model.

Modelled parameter	Symbol	Equation*
Effluent biodegradable soluble COD	S	$\boldsymbol{S} = \frac{\boldsymbol{K_S}(\mathbf{1} + \boldsymbol{k_d}\Theta_c)}{\Theta_c(\boldsymbol{Yk} - \boldsymbol{k_d}) - \mathbf{1}}$
Biomass VSS	$X_{VSS,bio}$	$\boldsymbol{X_{VSS,bio}} = \frac{\Theta_c}{\Theta}\left[\frac{\boldsymbol{Y}(\boldsymbol{S_0} - \boldsymbol{S})}{\mathbf{1} + \boldsymbol{k_d}\Theta_c}\right]$
Biomass and endogenous decay associated solids wastes daily	$P_{X,VSS,bio}$	$\boldsymbol{P_{x,VSS,bio}} = \boldsymbol{Q}[\frac{\boldsymbol{Y}(\boldsymbol{S} - \boldsymbol{S_0})}{\mathbf{1} + \boldsymbol{k_d}\Theta_c}] + [\frac{\boldsymbol{k_d f_d Q Y}(\boldsymbol{S_0} - \boldsymbol{S})\Theta_c}{\mathbf{1} + \boldsymbol{k_d}\Theta_c}]$
Total solids wasted daily	$P_{X,VSS}$	$\boldsymbol{P_{x,VSS}} = \boldsymbol{Q}[\frac{\boldsymbol{Y}(\boldsymbol{S} - \boldsymbol{S_0})}{\mathbf{1} + \boldsymbol{k_d}\Theta_c}] + [\frac{\boldsymbol{k_d f_d Q Y}(\boldsymbol{S_0} - \boldsymbol{S})\Theta_c}{\mathbf{1} + \boldsymbol{k_d}\Theta_c}] + \boldsymbol{Q X_{i,0}}$
Mixed liquor VSS concentration	X_{VSS}	$\boldsymbol{X_{VSS,bio}} = \frac{\Theta_c}{\Theta}\left[\frac{\boldsymbol{Y}(\boldsymbol{S_0} - \boldsymbol{S})}{\mathbf{1} + \boldsymbol{k_d}\Theta_c}\right]$

*Where K_S is half-velocity constant (mg bCOD/L), k_d is specific endogenous decay coefficient (d^{-1}), S_0 is influent biodegradable COD (mg/L), Θ is hydraulic retention time (d), f_d is fraction of biomass that remains as cell debris and $X_{i,0}$ is influent non-biodegradable particulate COD (mg/L).

Table A3. Biokinetic parameters for wastewater fractionation and activated sludge process model.

Symbol	Name	Value	Unit
Y_{HET}	heterotroph yield coefficient	0.67	mg COD/mg COD
b_H	steady state theory endogenous decay rate	0.24	1/d
f	steady state theory endogenous residue fraction	0.20	mg VSS/mg VSS
f_{CV}	mixed liquor solids COD/VSS ratio	1.48	mg COD/mg VSS
k	maximum specific substrate utilization rate	4 (at 20°C)	1/d
K_s	half-velocity constant	60	mg bCOD/L
k_d	specific endogenous decay coefficient	0.1(at 20°C)	1/d
f_d	fraction of biomass that remains as cell debris	0.15	-

Table A4. Results of wastewater fractionation.

Temperature (°C)	$COD_{T,INF}$ (mg/L)	f_{si}	f_{xi}	S_0 (mg/L)	$X_{i,0}$ (mg/L)
20	506	0.075	0.21	361	106
14	506	0.093	0.22	348	111
8	480	0.098	0.24	318	115

Appendix B

Supplementary Data for Chapter 4

Figure B1. Statistics of linear fit (a. polysaccharide; b. protein; c. humic-like substances; and d. LMW organics).

a.

Notes

Input Data

Masked Data - Values Excluded from Computations

Bad Data (missing values) -- Values that are invalid and thus not used in computations

Parameters

		Value	Standard Error	t-Value	Prob>|t|
rate	Intercept	0.07489	0.0137	5.46773	9.38126E-4
	Slope	1.2394E-4	1.63247E-5	7.59217	1.27108E-4

Slope is significantly different from zero (See ANOVA Table).

Standard Error was scaled with square root of reduced Chi-Sqr.

Statistics

	rate
Number of Points	9
Degrees of Freedom	7
Residual Sum of Squares	0.00288
Pearson's r	0.9443
R-Square (COD)	0.89171
Adj. R-Square	0.87624

Summary

	Intercept		Slope		Statistics
	Value	Standard Error	Value	Standard Error	Adj. R-Square
rate	0.07489	0.0137	1.2394E-4	1.63247E-5	0.87624

ANOVA

		DF	Sum of Squares	Mean Square	F Value	Prob>F
rate	Model	1	0.02374	0.02374	57.64108	1.27108E-4
	Error	7	0.00288	4.11936E-4		
	Total	8	0.02663			

At the 0.05 level, the slope is significantly different from zero.

\

b.

Notes

Input Data

Masked Data - Values Excluded from Computations

Bad Data (missing values) -- Values that are invalid and thus not used in computations

Parameters

		Value	Standard Error	t-Value	Prob>|t|
rate	Intercept	0.05171	0.04346	1.19002	0.27283
	Slope	3.28748E-4	1.18841E-4	2.76627	0.02784

Slope is significantly different from zero (See ANOVA Table).

Standard Error was scaled with square root of reduced Chi-Sqr.

Statistics

	rate
Number of Points	9
Degrees of Freedom	7
Residual Sum of Squares	0.01272
Pearson's r	0.72267
R-Square (COD)	0.52226
Adj. R-Square	0.45401

Summary

	Intercept		Slope		Statistics
	Value	Standard Error	Value	Standard Error	Adj. R-Square
rate	0.05171	0.04346	3.28748E-4	1.18841E-4	0.45401

ANOVA

		DF	Sum of Squares	Mean Square	F Value	Prob>F
rate	Model	1	0.01391	0.01391	7.65227	0.02784
	Error	7	0.01272	0.00182		
	Total	8	0.02663			

At the 0.05 level, the slope is significantly different from zero.

c.

Notes

Input Data

Masked Data - Values Excluded from Computations

Bad Data (missing values) -- Values that are invalid and thus not used in computations

Parameters

		Value	Standard Error	t-Value	Prob>|t|
rate	Intercept	0.019	0.30003	0.06333	0.95127
	Slope	3.11273E-5	6.36853E-5	0.48877	0.63995

Slope is NOT significantly different from zero (See ANOVA Table).

Standard Error was scaled with square root of reduced Chi-Sqr.

Statistics

	rate
Number of Points	9
Degrees of Freedom	7
Residual Sum of Squares	0.02575
Pearson's r	0.18166
R-Square (COD)	0.033
Adj. R-Square	-0.10514

Summary

	Intercept		Slope		Statistics
	Value	Standard Error	Value	Standard Error	Adj. R-Square
rate	0.019	0.30003	3.11273E-5	6.36853E-5	-0.10514

ANOVA

		DF	Sum of Squares	Mean Square	F Value	Prob>F
rate	Model	1	8.7876E-4	8.7876E-4	0.23889	0.63995
	Error	7	0.02575	0.00368		
	Total	8	0.02663			

At the 0.05 level, the slope is NOT significantly different from zero.

d.

+ *Notes*
+ *Input Data*
+ *Masked Data - Values Excluded from Computations*
+ *Bad Data (missing values) -- Values that are invalid and thus not used in computations*
- *Parameters*

		Value	Standard Error	t-Value	Prob>|t|
rate	Intercept	-0.0546	0.03049	-1.79063	0.11647
	Slope	6.61013E-5	8.92611E-6	7.40539	1.4874E-4

Slope is significantly different from zero (See ANOVA Table).
Standard Error was scaled with square root of reduced Chi-Sqr.

- *Statistics*

	rate
Number of Points	9
Degrees of Freedom	7
Residual Sum of Squares	0.00301
Pearson's r	0.9417
R-Square (COD)	0.8868
Adj. R-Square	0.87063

- *Summary*

	Intercept		Slope		Statistics
	Value	Standard Error	Value	Standard Error	Adj. R-Square
rate	-0.0546	0.03049	6.61013E-5	8.92611E-6	0.87063

- *ANOVA*

		DF	Sum of Squares	Mean Square	F Value	Prob>F
rate	Model	1	0.02361	0.02361	54.83974	1.4874E-4
	Error	7	0.00301	4.30597E-4		
	Total	8	0.02663			

At the 0.05 level, the slope is significantly different from zero.

Appendix C

Supplementary Data for Chapter 5

Figure C1. Results of flux step test.

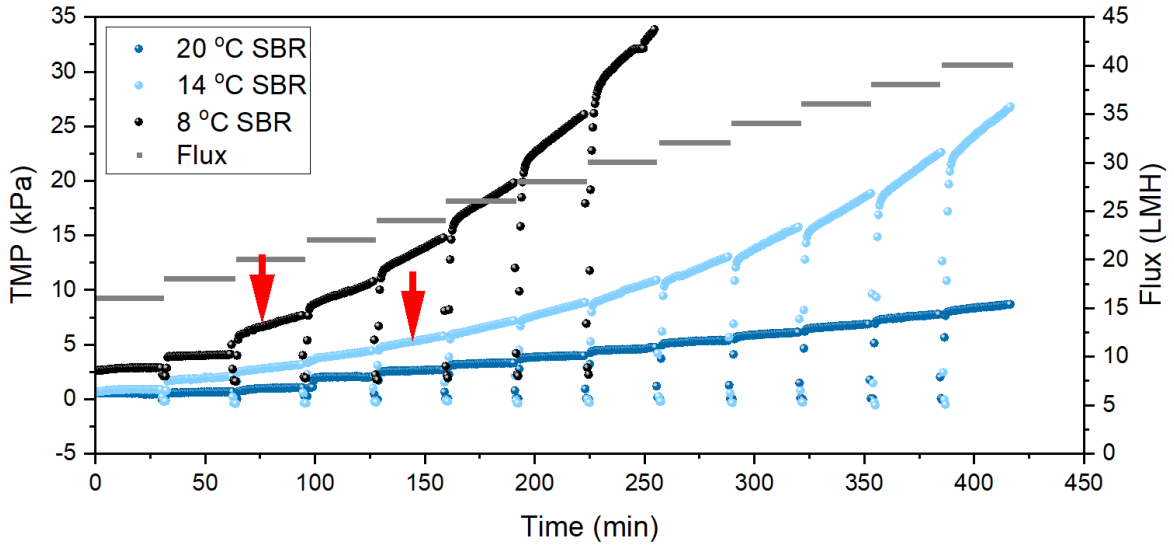

Appendix D

Supplementary Data for Chapter 6

Table D1. Statistics of multiple linear regression between R_t and operating conditions.

Descriptive Statistics

	Mean	Std. Deviation	N
Rt	1726192629629	960946241189	27
HRT	15.00	4.16	27
SBRT	12.00	5.76	27
FT	16.00	5.76	27

SBRT: SBR temperature; FT: filtration temperature

Model Summary

Model	R	R Square	Adjusted R Square	Std. Error of the Estimate
1	.995	.990	.989	102910735461

Coefficients

Model		Unstandardized Coefficients		Standardized Coefficients		
		B	Std. Error	Beta	t	Sig.
1	(Constant)	5036090388888	95325825486		52	.000
	HRT	-39303611111	4851258593	-.170	-8	.000
	SBRT	-57004435185	4042715494	-.342	-14	.000
	FT	-127268148148	4042715494	-.763	-31	.000

Table D2. Statistics of multiple linear regression between R_{rev} and operating conditions.

Descriptive Statistics

	Mean	Std. Deviation	N
Rrev	480843185185	316593717663	27
HRT	15	4.16	27
SBRT	12	5.76	27
FT	16	5.76	27

Model Summary

Model	R	R Square	Adjusted R Square	Std. Error of the Estimate
1	.977[a]	.954	.948	72006867911

Coefficients

Model		Unstandardized Coefficients		Standardized Coefficients		
		B	Std. Error	Beta	t	Sig.
1	(Constant)	1685468870370	66699689722		25	.000
	HRT	-25327744444	3394436306	-.333	-7	.000
	SBRT	-26480027777	2828696921	-.482	-9	.000
	FT	-31684324074	2828696921	-.577	-11	.000

Table D3. Statistics of multiple linear regression between R_{irr} and operating conditions.

Descriptive Statistics

	Mean	Std. Deviation	N
Rirr	697292618518	506354607299	27
HRT	15	4	27
SBRT	12	5	27
FT	16	5	27

Model Summary

Model	R	R Square	Adjusted R Square	Std. Error of the Estimate
1	.992[a]	.984	.982	67489290511

Coefficients

Model		Unstandardized Coefficients		Standardized Coefficients		
		B	Std. Error	Beta	t	Sig.
1	(Constant)	2345978072222	62515074843		37	.000
	HRT	-13842136666	3181475665	-.114	-4	.000
	SBRT	-30579660185	2651229721	-.348	-11	.000
	FT	-67131092592	2651229721	-.764	-25	.000

Appendix E

Supplementary Data for Chapter 7

Figure E1. Statistics of linear fit (a. 8 ℃ SBR and b. 20 ℃ SBR).

a.

High MW Vs K_c

Notes

Input Data

Input X Data Source	Input Y Data Source	Range
[Book1]Sheet1!C"high MW"	[Book1]Sheet1!A"Kc"	[1*:6*]

Masked Data - Values Excluded from Computations

Bad Data (missing values) -- Values that are invalid and thus not used in computations

Parameters

		Value	Standard Error	t-Value	Prob>|t|
Kc	Intercept	7023606.51846	333795.40377	21.04165	3.01523E-5
	Slope	-5911519.94858	682598.38819	-8.66032	9.7806E-4

Slope is significantly different from zero (See ANOVA Table).
Standard Error was scaled with square root of reduced Chi-Sqr.

Statistics

	Kc
Number of Points	6
Degrees of Freedom	4
Residual Sum of Squares	8.59386E11
Pearson's r	-0.97436
R-Square (COD)	0.94937
Adj. R-Square	0.93671

Summary

	Intercept		Slope		Statistics
	Value	Standard Error	Value	Standard Error	Adj. R-Square
Kc	7023606.51846	333795.40377	-5911519.94858	682598.38819	0.93671

ANOVA

		DF	Sum of Squares	Mean Square	F Value	Prob>F
Kc	Model	1	1.61137E13	1.61137E13	75.00113	9.7806E-4
	Error	4	8.59386E11	2.14847E11		
	Total	5	1.69731E13			

At the 0.05 level, the slope is significantly different from zero.

High MW Vs K_i

Notes

Input Data

Input X Data Source	Input Y Data Source	Range
[Book1]Sheet1!C"high MW"	[Book1]Sheet1!B"Ki"	[1*:6*]

Masked Data - Values Excluded from Computations

Bad Data (missing values) -- Values that are invalid and thus not used in computations

Parameters

		Value	Standard Error	t-Value	Prob>|t|
Ki	Intercept	14.46393	0.23867	60.6032	4.43998E-7
	Slope	-6.04141	0.48806	-12.37835	2.44815E-4

Slope is significantly different from zero (See ANOVA Table).
Standard Error was scaled with square root of reduced Chi-Sqr.

Statistics

	Ki
Number of Points	6
Degrees of Freedom	4
Residual Sum of Squares	0.43935
Pearson's r	-0.9872
R-Square (COD)	0.97456
Adj. R-Square	0.9682

Summary

	Intercept		Slope		Statistics
	Value	Standard Error	Value	Standard Error	Adj. R-Square
Ki	14.46393	0.23867	-6.04141	0.48806	0.9682

ANOVA

		DF	Sum of Squares	Mean Square	F Value	Prob>F
Ki	Model	1	16.82963	16.82963	153.22343	2.44815E-4
	Error	4	0.43935	0.10984		
	Total	5	17.26898			

At the 0.05 level, the slope is significantly different from zero.

LMW Vs K_c

Notes

Input Data

Masked Data - Values Excluded from Computations

Bad Data (missing values) -- Values that are invalid and thus not used in computations

Parameters

		Value	Standard Error	t-Value	Prob>|t|
Ki	Intercept	13.44204	1.69351	7.9374	0.00136
	Slope	-5.58915	5.97457	-0.93549	0.4025

Slope is NOT significantly different from zero (See ANOVA Table).
Standard Error was scaled with square root of reduced Chi-Sqr.

Statistics

	Ki
Number of Points	6
Degrees of Freedom	4
Residual Sum of Squares	14.16901
Pearson's r	-0.42369
R-Square (COD)	0.17951
Adj. R-Square	-0.02561

Summary

	Intercept		Slope		Statistics
	Value	Standard Error	Value	Standard Error	Adj. R-Square
Ki	13.44204	1.69351	-5.58915	5.97457	-0.02561

ANOVA

		DF	Sum of Squares	Mean Square	F Value	Prob>F
Ki	Model	1	3.09997	3.09997	0.87514	0.4025
	Error	4	14.16901	3.54225		
	Total	5	17.26898			

At the 0.05 level, the slope is NOT significantly different from zero.

LMW Vs K_i

Notes

Input Data

Masked Data - Values Excluded from Computations

Bad Data (missing values) -- Values that are invalid and thus not used in computations

Parameters

		Value	Standard Error	t-Value	Prob>|t|
Kc	Intercept	6276749.66067	1610745.07402	3.8968	0.01759
	Slope	-6470827.07026	5682599.92784	-1.13871	0.31839

Slope is NOT significantly different from zero (See ANOVA Table).
Standard Error was scaled with square root of reduced Chi-Sqr.

Statistics

	Kc
Number of Points	6
Degrees of Freedom	4
Residual Sum of Squares	1.2818E13
Pearson's r	-0.49478
R-Square (COD)	0.24481
Adj. R-Square	0.05601

Summary

	Intercept		Slope		Statistics
	Value	Standard Error	Value	Standard Error	Adj. R-Square
Kc	6276749.66067	1610745.07402	-6470827.07026	5682599.92784	0.05601

ANOVA

		DF	Sum of Squares	Mean Square	F Value	Prob>F
Kc	Model	1	4.15514E12	4.15514E12	1.29666	0.31839
	Error	4	1.2818E13	3.2045E12		
	Total	5	1.69731E13			

At the 0.05 level, the slope is NOT significantly different from zero.

b.

High MW Vs K_c

Notes

Input Data

Input X Data Source	Input Y Data Source	Range
[Book2]Sheet1!C"high MW"	[Book2]Sheet1!A"Kc"	[1*:6*]

Masked Data - Values Excluded from Computations

Bad Data (missing values) -- Values that are invalid and thus not used in computations

Parameters

		Value	Standard Error	t-Value	Prob>|t|
Kc	Intercept	4637289.54459	572644.79296	8.09802	0.00126
	Slope	-5126296.1547	1090101.64306	-4.70259	0.00929

Slope is significantly different from zero (See ANOVA Table).
Standard Error was scaled with square root of reduced Chi-Sqr.

Statistics

	Kc
Number of Points	6
Degrees of Freedom	4
Residual Sum of Squares	3.10927E12
Pearson's r	-0.92023
R-Square (COD)	0.84683
Adj. R-Square	0.80853

Summary

	Intercept		Slope		Statistics
	Value	Standard Error	Value	Standard Error	Adj. R-Square
Kc	4637289.54459	572644.79296	-5126296.1547	1090101.64306	0.80853

ANOVA

		DF	Sum of Squares	Mean Square	F Value	Prob>F
Kc	Model	1	1.71898E13	1.71898E13	22.11431	0.00929
	Error	4	3.10927E12	7.77318E11		
	Total	5	2.02991E13			

At the 0.05 level, the slope is significantly different from zero.

High MW Vs K_i

Notes

Input Data

Input X Data Source	Input Y Data Source	Range
[Book2]Sheet1!C"high MW"	[Book2]Sheet1!B"Ki"	[1*:6*]

Masked Data - Values Excluded from Computations

Bad Data (missing values) -- Values that are invalid and thus not used in computations

Parameters

		Value	Standard Error	t-Value	Prob>|t|
Ki	Intercept	13.25999	0.30148	43.98324	1.59774E-6
	Slope	-6.0132	0.5739	-10.47774	4.68983E-4

Slope is significantly different from zero (See ANOVA Table).
Standard Error was scaled with square root of reduced Chi-Sqr.

Statistics

	Ki
Number of Points	6
Degrees of Freedom	4
Residual Sum of Squares	0.86179
Pearson's r	-0.98227
R-Square (COD)	0.96485
Adj. R-Square	0.95606

Summary

	Intercept		Slope		Statistics
	Value	Standard Error	Value	Standard Error	Adj. R-Square
Ki	13.25999	0.30148	-6.0132	0.5739	0.95606

ANOVA

		DF	Sum of Squares	Mean Square	F Value	Prob>F
Ki	Model	1	23.65241	23.65241	109.78311	4.68983E-4
	Error	4	0.86179	0.21545		
	Total	5	24.5142			

At the 0.05 level, the slope is significantly different from zero.

LMW Vs K_c

Notes

Input Data

Input X Data Source	Input Y Data Source	Range
[Book2]Sheet1!D"low MW"	[Book2]Sheet1!A"Kc"	[1*:6*]

Masked Data - Values Excluded from Computations

Bad Data (missing values) -- Values that are invalid and thus not used in computations

Parameters

		Value	Standard Error	t-Value	Prob>|t|
Kc	Intercept	5337293.42321	1507880.38108	3.5396	0.02402
	Slope	-6914271.04661	3375298.48849	-2.04849	0.10988

Slope is NOT significantly different from zero (See ANOVA Table).
Standard Error was scaled with square root of reduced Chi-Sqr.

Statistics

	Kc
Number of Points	6
Degrees of Freedom	4
Residual Sum of Squares	9.90646E12
Pearson's r	-0.71552
R-Square (COD)	0.51198
Adj. R-Square	0.38997

Summary

	Intercept		Slope		Statistics
	Value	Standard Error	Value	Standard Error	Adj. R-Square
Kc	5337293.42321	1507880.38108	-6914271.04661	3375298.48849	0.38997

ANOVA

		DF	Sum of Squares	Mean Square	F Value	Prob>F
Kc	Model	1	1.03927E13	1.03927E13	4.19632	0.10988
	Error	4	9.90646E12	2.47661E12		
	Total	5	2.02991E13			

At the 0.05 level, the slope is NOT significantly different from zero.

LMW Vs K_i

Notes

Input Data

Input X Data Source	Input Y Data Source	Range
[Book2]Sheet1!D"low MW"	[Book2]Sheet1!B"Ki"	[1*:6*]

Masked Data - Values Excluded from Computations

Bad Data (missing values) -- Values that are invalid and thus not used in computations

Parameters

		Value	Standard Error	t-Value	Prob>|t|
Ki	Intercept	13.07986	2.01076	6.50493	0.00288
	Slope	-5.63317	4.50097	-1.25155	0.27893

Slope is NOT significantly different from zero (See ANOVA Table).
Standard Error was scaled with square root of reduced Chi-Sqr.

Statistics

	Ki
Number of Points	6
Degrees of Freedom	4
Residual Sum of Squares	17.61593
Pearson's r	-0.53047
R-Square (COD)	0.2814
Adj. R-Square	0.10175

Summary

	Intercept		Slope		Statistics
	Value	Standard Error	Value	Standard Error	Adj. R-Square
Ki	13.07986	2.01076	-5.63317	4.50097	0.10175

ANOVA

		DF	Sum of Squares	Mean Square	F Value	Prob>F
Ki	Model	1	6.89826	6.89826	1.56637	0.27893
	Error	4	17.61593	4.40398		
	Total	5	24.5142			

At the 0.05 level, the slope is NOT significantly different from zero.